CXCR4 MAINTAINS A UNIQUE BONE MARROW B-1A POPULATION AND REGULATES ATHEROPROTECTIVE IGM PRODUCTION

Aditi Upadhye
Okemos, Michigan

B.Sc. Biochemistry, Michigan State University, 2013

A Dissertation presented to the Graduate Faculty of the University of Virginia in Candidacy for the Degree of Doctor of Philosophy

Department of Microbiology, Immunology, and Cancer Biology

University of Virginia
December, 2019

_____	_____
Coleen McNamara, MD	Loren Erickson, PhD
_____	_____
Timothy P. Bender, PhD	Kodi Ravichandran, PhD
_____	
Gary Owens, PhD	

Abstract

Atherosclerosis is a chronic inflammatory disease of the artery wall that leads to the development of cardiovascular disease (CVD) and its sequelae, which remain the leading cause of death worldwide. The development of CVD varies significantly among individuals with similar traditional risk factors, suggesting that CVD could be further prevented by additional strategies. The completion of the Canakinumab anti-inflammatory thrombosis outcome study (CANTOS) has given validation to the inflammatory hypothesis that reducing inflammation reduces the risk of CVD independent of lipid-lowering therapies, and immunomodulatory therapy holds promise for improving CVD prevention.

B cells have emerged as important immune cells that regulate atherosclerosis in a subset-specific manner. B-1 cells have a known atheroprotective function that is mediated by production of anti-inflammatory IgM antibodies that recognize oxidation specific epitopes (OSE), which accumulate in atherosclerosis. Bone marrow B-1 cells contribute significantly to circulating IgM titers at homeostasis, yet the mechanisms regulating B-1 cell localization to the bone marrow are undetermined. Moreover, factors that regulate anti-OSE IgM production by the putative human B-1 cell subset, and its atheroprotective role in human CVD remain unexplored.

The C-X-C motif chemokine receptor CXCR4 regulates cell trafficking and localization and is broadly expressed on both immune and non-immune cell populations. Genome-wide association studies and murine experimental models have implicated CXCR4 in CVD, yet results have been conflicting due to its broad expression and the relative lack of cell type-specific studies.

In this dissertation, I present evidence demonstrating a role for CXCR4 in regulating B-1 cell production of atheroprotective IgM antibody, and characterize a deeper heterogeneity present in human and murine B-1 cell populations. I present my work in murine models showing that CXCR4 regulated B-1 cell localization to the bone marrow and circulating amount of anti-OSE IgM, and in a human CVD cohort that B-1 CXCR4 expression associated with reduced coronary artery plaque burden and a protected plaque phenotype. Murine studies utilized a B cell-specific CXCR4 knockout mouse model, which revealed fewer B-1a cells and IgM antibody-secreting cells in the bone marrow in the absence of CXCR4. Conversely, retroviral-mediated overexpression of CXCR4 *in vivo* increased B-1a localization to the bone marrow and associated with increased circulating anti-OSE IgM. Mechanistically, we found that CXCR4 mediated trafficking of circulating peripheral B-1a cells to the bone marrow and regulated bone marrow B-1a cell survival. I additionally examine niche-specific heterogeneity in murine B-1 cell populations, and provide novel characterization of the immunoglobulin repertoire of aged hyperlipidemic $ApoE^{-/-}$ mice, which reveals greater IgM repertoire diversity expressed by bone marrow B-1a cells compared to peritoneal B-1a cells. Finally, analysis of a human CVD cohort demonstrates that CXCR4 expression on the putative human B-1 subset associates with increased circulating anti-OSE IgM antibodies and decreased coronary artery disease. Thus, the evidence presented here supports the hypothesis that the bone marrow B-1a pool uniquely contributes to the pool of available atheroprotective IgM antibodies, and its maintenance is governed by CXCR4, a novel marker associating with protection in human CVD.

Acknowledgments and Dedication

It has been an honor to be a graduate student at the University of Virginia. The lessons I have learned here have been countless and foundational. Foremost, I would like to thank Coleen McNamara for her guidance and support. Coleen has been an incredible mentor, and I thank her for encouraging me to keep following the science when things don't make sense, and for always encouraging me to keep an open mind. Her patience, persevering mindset, and optimism have made graduate school so enjoyable, and are qualities I aspire to apply myself, both inside and outside of lab.

One of the biggest lessons I've learned at UVA is that science works better as a team sport, and I am incredibly grateful to the other members of the McNamara lab who have given much effort, insight, and support for this work. Prasad Srikakulapu has been a great friend and colleague. I thank him for being a trusty coworker when working late nights on long experiments, and for always being there to bounce ideas back and forth. Melissa Marshall has been essential to my success and a great friend. Tori Osinski, Hema Kothari, and Chantel McSkimming have made coming into work so fun and I thank them for their scientific insights, friendship, and support. Anh Nguyen and Jeff Sturek have been wonderful colleagues to learn from and have always given sound advice. Jim Garmey keeps the lab running and I thank him for his help throughout my time here. I'd also like to thank Heather Perry who showed me the ropes and set a great example when I first rotated through the lab, and for providing advice along the way.

I am also thankful for the assistance I received from other members of the UVA community. Tim Bender has been an invaluable co-mentor and I thank him for his scientific help as well as his helpful advice and willingness to chat about career and future plans. The other members of my committee, Loren Erickson, Kodi Ravichandran,

and Gary Owens, provided excellent advice about my projects and helped me to focus on the big picture. The technical assistance provided by Joanne Lannigan, Mike Solga, Claude Chew, and Lesa Campbell at the UVA Flow Cytometry Core was essential for the success of my experiments. I would also like to thank our collaborators at UCSD and Western Michigan University, in particular Drs. Joseph Witztum, Ayelet Gönen, Sabrina Hendrikx, Sotirios Tsimikas, Nichol Holodick and Thomas Rothstein for their scientific contributions and advice.

I want to give a special thanks to friends and family, in and out of Charlottesville, who have been a wonderful support system throughout my time here. In particular, Mihir Upadhye, Amrita Pawar, Fiza Irfan, and Samantha Wallace have been there to lend an ear, given helpful advice when times have been rough, and have been there to celebrate the good times as well. To my best animal friends, Magic, Wiggles, and Lallie boo, I could not have done this without you.

Finally, I would like to dedicate this to my parents, Devendra and Manasi Upadhye, who have been unfailingly supportive since day one. They taught me perseverance, resilience, and to always give your best to what you do, and I owe my success in graduate school to the example they set for me. I thank them from the bottom of my heart.

Table of Contents

List of Figures

List of Tables

List of Abbreviations

$ApoE^{-/-}$	Apolipoprotein E knockout mouse
ASC	Antibody secreting cell
ATLO	Adventitial tertiary lymphoid organ
BCR	B cell receptor
BM	Bone marrow
BrdU	Bromodeoxyuridine
CDR-H3	Immunoglobulin heavy chain complementarity determining region 3
CXCR4	Chemokine receptor 4
$CXCR4^{BKO}ApoE^{-/-}$	B cell-specific CXCR4 knockout mouse
$CXCR4^{WT}ApoE^{-/-}$	Wild- type littermate control to $CXCR4^{BKO}ApoE^{-/-}$ mouse
CuOx-LDL	Copper-oxidized low density lipoprotein
CVD	Cardiovascular disease
DAMPs	Damage associated molecular patterns
E06/T15	BCR/IgM idiotype specific for phosphorylcholine
ELISA	Enzyme linked immunosorbent assay
FACS	Fluorescence activated cell sorting
FALC	Fat associated lymphoid cluster
FDC	Follicular dendritic cell
GM-CSF	Granulocyte/macrophage colony stimulating factor
HDL	High density lipoprotein
IFN-γ	Interferon gamma
Ig	Immunoglobulin
IgH V	Variable region of the immunoglobulin heavy chain

IL	Interleukin
LDL	Low density lipoprotein
LPS	Lipopolysaccharide
MDA-LDL	Malondialdehyde-modified LDL
MZ	Marginal zone
N-additions	Non-template encoded nucleotide additions
OSE	Oxidation-specific epitope
oxLDL	oxidized LDL
PAMPs	Pathogen associated molecular patterns
PBMC	Peripheral blood mononuclear cells
PC	Phosphorylcholine
PtC	Phosphatidylcholine
PerC	Peritoneal cavity
PPS	Pneumococcal polysaccharide
PVAT	Perivascular adipose tissue
$Rag1^{-/-}ApoE^{-/-}$	Mouse deficient in ApoE and Recombination activating gene 1
RLU	Relative light units
$sIgM^{-/-}ApoE^{-/-}$	Mouse deficient in ApoE and secreted IgM
SNP	Single nucleotide polymorphism
TD	T cell-dependent
T_{FH}	T follicular helper cell
Th1	T helper 1 cell
TLR	Toll like receptor
TI-1/2	T cell-independent type I or type II response
VDJ	Variable-Diversity-Junctional genes

VSMC	Vascular smooth muscle cell
WD	Western diet

Chapter 1

Introduction

Impact and Pathogenesis of Atherosclerosis

Cardiovascular disease (CVD) remains the leading cause of death worldwide, responsible for 31% of all global deaths in 2013[1], and projected to account for >23.6 million annual global deaths by the year 2030[2]**.** Additionally, more than any other diagnosis, CVD imposes the greatest economic burden on the healthcare system; CVD diagnoses and treatment resulted in $199.2 billion in direct healthcare costs in the US from 2013 to 2014, accounting for 14% of total health expenditures in that year[2]. The primary cause of CVD is atherosclerosis, a chronic inflammatory disease involving accumulation of oxidized lipids within the artery wall and progressive lesion formation that can over time result in arterial stenosis, ischemia, and downstream adverse events [3-5]. Atherosclerosis is initiated by accumulation and subsequent oxidative modification of low-density lipoprotein (LDL) within the subendothelial space of the artery wall, resulting in early lesions termed “fatty streaks”. These oxidized lipids are pro-inflammatory and result in endothelial cell dysfunction, a consequence of which is increased adhesion molecule expression and circulating leukocyte recruitment into the vascular wall. Within the subintimal space, recruited monocytes and other immune cells secrete pro-inflammatory cytokines and chemokines that further contribute to increased immune cell entry into the nascent lesion. Monocytes differentiate into macrophages upon scavenging oxidized LDL, eventually becoming lipid-laden foam cells. As disease progresses, infiltrating immune cells, buildup of dying cells, and phenotypically switched smooth muscle cells, among other mediators, contribute to formation of the atherosclerotic plaque consisting of a lipid-rich necrotic core stabilized by a collagen-rich fibrous cap. In late stages of disease, plaques can become destabilized by erosion of the fibrous cap. Rupture of the lesion and exposure of necrotic core material to thrombotic

factors in the circulation can potentiate clot formation and adverse clinical events including heart attacks and strokes.

While overall mortality attributable to CVD has been on the decline in the US since 1980 due to medical therapies and lifestyle changes[2], this decline is reaching a plateau, suggesting that the standard forms of therapy available may need to be supplemented with other effective strategies to lower risk and burden. The completion of the Canakinumab anti-inflammatory thrombosis outcome study[6] has both given validation to the inflammatory hypothesis that reducing inflammation reduces the risk of cardiovascular disease independent of standard lipid lowering therapies, and also underscored the importance of developing targeted immune strategies to avoid untoward consequences of altering the immune system on a systemic level. The contribution of innate and adaptive immunity to atherosclerosis development is well established, and immune modulation can tip the balance of pro- or anti-inflammatory effects resulting in progression or attenuation of atherosclerosis.

B cells in atherosclerosis

A wealth of murine studies over the last several years have demonstrated that the role of B cells in atherosclerosis is subset specific (**Figure 1**)[7-9]. Several subsets of B cells exist in mice, and can broadly be defined into B-1 and B-2 subsets that are so-called due to the timing of their development; B-1 cell subsets arise earlier in ontogeny primarily within the fetal liver and persist through self-renewal, while B-2 cells arise later and are continuously generated *de novo* by progenitors in adult bone marrow[10]. Functionally, B-1 cells participate in T cell-independent responses leading to the generation of primarily IgM isotype antibodies. B-2 cells consist of follicular B cells and marginal zone (MZ) B cells. Follicular B-2 cells participate in the germinal center (GC)

reaction through cognate interaction with T cells, resulting in the generation of long-lived recirculating memory B cells or plasma cells and high-affinity class-switched antibodies. Marginal zone (MZ) B cells are a non-circulating population in mice that reside within the marginal zone of the spleen and are uniquely positioned to encounter blood-borne pathogens, participate in T cell-independent IgM production, and rapidly process and present antigen to T cells. A third broad subset of B cells, regulatory B cells, are defined primarily through their secretion of the anti-inflammatory cytokine IL-10 and can be derived from B-1 or B-2 subsets. B cell subsets are developmentally, functionally, and phenotypically distinct, with unique subset-specific contributions to atherosclerosis development.

While B cells are found in low numbers in atherosclerotic lesions themselves, they are found abundantly within the perivascular adipose tissue and arterial adventitia, and B cell antibodies are detected in plaques themselves. Importantly, prior work demonstrates that loss or gain of peripheral B cell subsets does impact atherogenesis. Early studies examining B cell-deficient $LDLR^{-/-}$ mice or splenectomized $ApoE^{-/-}$ mice that resulted in increased atherosclerosis indicated a protective role for B cells[11,12]. However, selective follicular B-2 cell depletion with anti-CD20 monoclonal antibody administration or through BAFFR deficiency was associated with reduced atherosclerotic lesion area, fewer T cells and macrophages in atherosclerotic lesions, and reduced proinflammatory cytokine expression[13-16]. Importantly, these studies appeared to selectively preserve either B-1 cells or B-1-derived IgM antibodies, suggesting an atherogenic role for B-2 cells. In support of this, adoptive transfer of CD22+ splenic B-2 cells into lymphocyte-deficient $Rag2^{-/-}ApoE^{-/-}$ or B cell-deficient μMT $ApoE^{-/-}$ mice resulted in increased lesion area and lesional macrophage content[15].

However, the role of B-2 cell derived IgG antibodies in atherosclerosis development remains unclear and is likely dependent on multiple factors. Several studies have suggested a protective role for IgG antibodies following immunization with oxidized LDL (oxLDL)[17,18], in which induction of anti-oxLDL IgG titers associated with reduced atherosclerotic lesion development. Moreover, anti-oxLDL IgG antibodies were demonstrated to enhance LDL clearance through immune complex formation in humanized mice[19], and passive administration of recombinant anti-MDA-LDL IgG1 into hypercholesterolemic mice inhibited lesion formation[20]. In contrast, studies in human CVD patients have demonstrated a positive association between circulating amount of IgG against oxidation specific epitopes and increased coronary artery disease and risk of CVD events[21,22], though these correlations lose significance when multivariate analyses are performed. The role for IgG in atherosclerosis is further complicated by different IgG isotypes that have varying affinities for Fcγ receptors, which can be activating or inhibitory. Recently, the B cell-specific role of the inhibitory FcγRIIb was demonstrated to be cell- and sex-specific, differentially regulating proatherogenic IgG-mediated GC B cell responses and atheroprotective IgM-mediated B-1 cell responses in male versus female mice[23]. Overall, the role for B-2 cells in atherosclerosis remains incompletely resolved, as their roles in non-B immune cell modulation versus generation of a humoral response may lead to opposing effects on atherosclerosis.

The role of IgE isotype antibodies in atherosclerosis has also received recent attention. IgE is involved in allergic responses and its binding to FcεRI receptor on perivascular mast cells can result in pro-inflammatory histamine and cytokine release that potentiate atherosclerosis[24-26]. Recently, Tsiantoulas and colleagues discovered that LDLR$^{-/-}$ mice deficient for secretory IgM (sIgM$^{-/-}$) had increased IgE and increased

atherosclerosis, and that delivery of neutralizing IgE conferred atheroprotection and reduced the frequency of activated mast cells in perivascular regions of atherosclerotic plaques[27]. Consistent with these murine findings, increased plasma IgE is also associated with CVD in humans[28 29 30 31,32].

The role of marginal zone and regulatory B cells in atherosclerosis has been less widely investigated, though recent studies have highlighted their importance. Marginal zone (MZ) B cells were recently demonstrated to limit atherosclerosis through restricting splenic T follicular helper (T_{FH}) accumulation in an ATF3-dependent manner, suppressing T_{FH} cell motility in a PDL1-dependent manner, and altering T_{FH} differentiation[33]. Regulatory B cells, defined primarily through their secretion of the anti-inflammatory cytokine IL-10, can be derived from B-1 or B-2 subsets. The role of regulatory B cells in atherosclerosis is conflicted. One study demonstrated a protective role for lymph node-derived IL-10-producing B2 cells in a perivascular carotid collar model of atherosclerosis development [34]. Additionally, decreased regulatory B cell number in the aortas of L-selectin-deficient mice was associated with less serum and aortic IL-10 and increased atherosclerosis [35]. In contrast, another study utilizing chimeric $LDLR^{-/-}$ mice with B cell-specific deficiency of IL-10 demonstrated no differences in plaque size or composition in a high fat diet-induced model of atherosclerosis[36].

B-1 cells, on the other hand, have a known protective role in atherosclerosis that is mediated primarily by IgM antibody production. Murine B-1 cells can be divided into distinct B-1a and B-1b subsets based on expression of the surface marker CD5 (B-1a being $CD5^{+}$), and both subsets secrete IgM against oxidation-specific epitopes (OSE) and protect against atherosclerosis after adoptive transfer into immunodeficient recipient hosts[37,38]. However, one unique subset of B-1a-derived cells, termed innate response activator (IRA) B cells, produce GM-CSF and can promote atherosclerosis development

through promoting the expansion of dendritic cells and the inflammatory IFN-γ producing T helper 1 (Th1) cell subset[39]. But in general, B-1a and B-1b cells and their secreted IgM are protective against atherosclerosis development.

Figure 1. B cell-derived antibodies in atherosclerosis. B cells have subset-specific roles in atherosclerosis. Peripheral antibody production occurs primarily in the spleen and bone marrow. IgM-secreting B-1 cells in the bone marrow and spleen contribute significantly to plasma IgM titers. Plasma cells in the bone marrow also produce IgM and IgG antibodies. In the spleen, follicular B-2 cells present antigens to T follicular helper cells (T_{FH}) via MHCII, and provide co-stimulatory signaling through CD40-CD40L interaction. This can lead germinal center (GC) reactions in which B cells undergo affinity maturation and isotype switching to generate high-affinity IgG or IgE antibodies. B-2 cells can differentiate into long lived plasma cells that reside in the bone marrow. Additionally, FcγRIIb has been shown to inhibit GC-derived IgG production in B-2 cells. In response to hypercholesterolemia, marginal zone (MZ) B cells upregulate PD-L1 which interacts with PD-1 on T_{FH} cells to suppress T_{FH} differentiation, thus limiting pro-inflammatory T_{FH}/B-2 cell interactions. During atherosclerosis, LDL accumulation and oxidative modification into oxLDL is pro-inflammatory and results in recruitment of monocytes and other immune cells into the subendothelial space of the artery wall. IgM, IgG, and IgE antibodies made peripherally or locally in the perivascular adipose tissue (PVAT) and adventitial tertiary lymphoid organs (ATLO) enters the lesion with immunomodulatory effects. IgM binds oxLDL and prevents its binding through scavenger receptors (SR) on monocytes and macrophages in the lesion, thus preventing pro-inflammatory cytokine secretion and foam cell formation. IgG binding to Fcγ receptors (FcγR) and IgE binding to FcεRI on macrophages can also result in proinflammatory cytokine production. T_{FH} and B-2 interactions in ATLO can result in IgG and IgE antibodies that are pro-inflammatory. IgE can bind FcεRI present on mast cells, resulting in release of pro-inflammatory cytokines including IL-6 and IFN-g.

Figure 1.

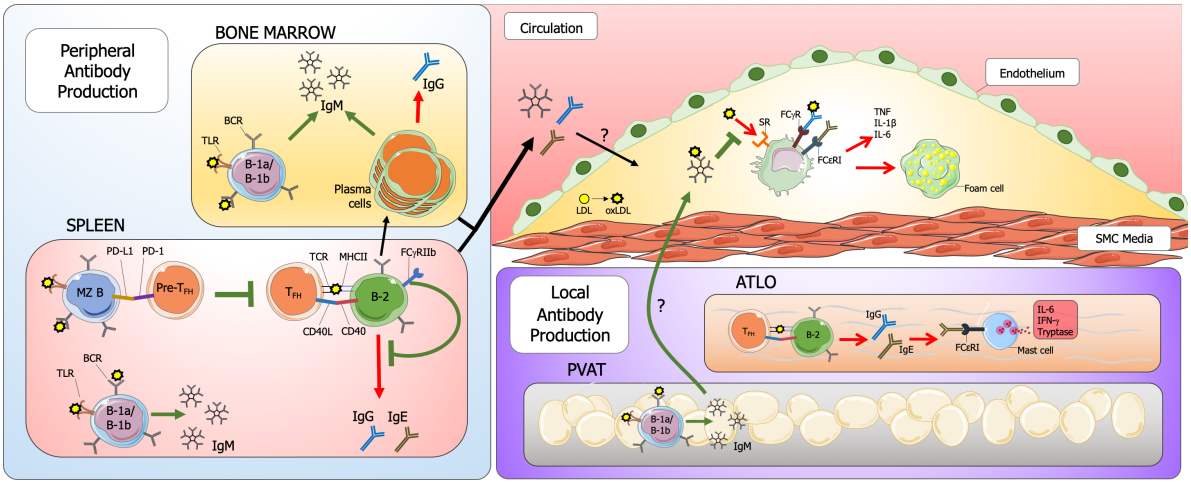
Peripheral Antibody Production
BONE MARROW
IgM
IgG
BCR
TLR
B-1a/ B-1b
Plasma cells
SPLEEN
PD-L1
PD-1
MZ B
Pre-TFH
TFH
TCR
MHCII
FCγRIIb
B-2
CD40L
CD40
BCR
TLR
B-1a/ B-1b
IgM
IgG
IgE
Circulation
Endothelium
SR
FCγR
TNF
IL-1β
IL-6
FCεRI
Foam cell
LDL
oxLDL
SMC Media
Local Antibody Production
ATLO
TFH
B-2
IgG
IgE
FCεRI
IL-6
IFN-γ
Tryptase
Mast cell
PVAT
B-1a/ B-1b
IgM

B-1 cells produce anti-OSE IgM antibodies in a T cell-independent manner

B-1 cells serve to protect against atherosclerosis primarily through their production of IgM antibodies. Studies using IgM allotype chimeric mice have demonstrated that ~80% of steady-state IgM is B-1 derived[40]. Importantly, B-1 cells are the main B cell subset contributing to the production of natural antibodies, a subset of primarily IgM isotype antibodies that form in the absence of any exogenous antigen exposure [41-45], and are thus present even in germ-free mice fed an antigen-free diet[46]. The repertoire of natural IgM antibodies consists primarily of germline VDJ gene segments with a propensity for autoreactive specificities[47-49]. Natural IgM antibodies undergo limited somatic hypermutation and contain few non-template-encoded N-nucleotide insertions, resulting in antibodies that are low affinity and polyreactive. In addition to natural IgM, B-1 cells can also be induced to secrete antigen-specific immune IgM in response to exogenous pathogens.

In contrast to follicular B-2 cells of the adaptive immune response, which are strongly selected against self-reactivity and produce high affinity, class-switched antibodies in a T cell-dependent manner, B-1a and B-1b cells instead participate in type 1 and type 2 T cell-independent (TI) responses. In the TI type 1 response, signals independent of the BCR, including stimulation of pattern recognition receptors (PRR) like toll-like receptors (TLR) or cytokine receptors, induces the secretion of polyclonal IgM antibodies. In the TI type 2 response, extensive BCR crosslinking to multivalent antigens, like the capsular polysaccharides of gram-negative bacteria, overrides the requirement of T cell help for production of antigen-specific immune antibodies. Studies using pneumococcal polysaccharide (PPS) immunization initially supported a simple division of labor model in which B-1a cells were responsible for natural IgM production while B-1b cells were responsible for generating PPS-specific immune IgM, memory

responses, and long-lasting immunity to pathogen challenge[50,51]. However, alternative infection models utilizing *Francisella tularensis* immunization[52,53] demonstrated that B-1a cells, too, can generate pathogen-specific IgM antibody and long-term immunity. Therefore, it is clear that the B-1 cell IgM response likely depends on a diversity of factors, including the antigen itself. It has been proposed that the differences between natural IgM-secreting B-1 cells versus antigen-induced IgM-secreting B-1 cells may arise from differences in B-1 ontogeny, microenvironmental niche, and responsiveness to self-antigens versus foreign antigens, as elegantly reviewed by Baumgarth and colleagues[41].

Notably, a significant proportion (~30%) of B-1 derived natural IgM antibodies recognize oxidation specific epitopes (OSE)[54], including phosphocholine (PC) and malondialdehyde (MDA). Interestingly, these epitopes are commonly conserved on both pathogen-associated molecular patterns (PAMPs) on invading pathogens, and the damage-associated molecular patterns (DAMPs) on neo-self epitopes that arise endogenously in health and disease. For example, the prototypic natural antibody, T15, recognizes the PC head group present as the immunodominant epitope on the cell wall of *S. pneumoniae*, the cell membrane of apoptotic cells, and on oxidized phospholipids present in atherosclerotic lesions[55]. Analysis of hybridomas derived from splenic B cells of hypercholesterolemic ApoE$^{-/-}$ mice demonstrated that there are abundant IgM antibodies specific for various epitopes of oxidized LDL (oxLDL) *in vivo* and that they localize to atherosclerotic lesions[54,56,57]. Moreover, sequencing of the antigen-binding CDR3 region of one clone, E06, demonstrated 100% similarity in the V_L and V_H regions to T15[58]. Because B-1 cells are thought to undergo positive selection for their autoreactivity [59,60], it has been argued that the self-antigens that form the B-1 repertoire are “evolutionarily conserved templates” providing antibody specificities for both damaging self and pathogen-related epitopes[47].

Natural anti-OSE IgM is atheroprotective

The functions of natural IgM antibodies include providing the first line of defense against exogenous pathogens[40,51-53,61-63], providing a housekeeping role through enhancing apoptotic cell clearance via the complement protein C1q[64-66], and performing an immunoregulatory role by inhibiting proinflammatory pathways induced by OSE[58,67,68]. As dying cells, OSE, and a proinflammatory milieu are all involved in the pathogenesis of atherosclerosis, there are several ways by which IgM might serve to protect against atherosclerosis.

In support of this, LDLR$^{-/-}$ mice deficient for secreted IgM (sIgM$^{-/-}$) have increased atherosclerosis[69], and delivery of polyclonal IgM during the last 4 weeks of a 29-week Western diet feed reduces lesion area[70]. Strategies to increase IgM production have also been shown to mitigate atherosclerosis development. Immunization with phosphatidyl serine-coated liposomes, apoptotic cells, or PPS was demonstrated to increase IgM titers to OSE, increase IgM-secreting B-1 cell number, and curb lesion development[71-73]. Mechanistically, anti-OSE IgM has been shown to block oxLDL uptake by macrophages *in vitro*[71], suggesting that it may inhibit foam cell formation *in vivo*. In support of this, transgenic mice overexpressing E06-scFv, the antigen-binding portion of the IgM antibody identical to T15 that recognizes PC, have decreased oxLDL uptake by peritoneal cavity (PerC) macrophages, reduced inflammatory phenotype in both PerC and aortic macrophages, and reduced atherosclerotic lesion and necrotic core area[74]. Overexpression of IK17-scFv, which recognizes MDA epitopes, is also able to reduce lipid accumulation in PerC macrophages and decrease atherosclerosis[75]. These studies using scFv antibodies suggest that anti-OSE antibodies mediate atheroprotection primarily through sequestering OSE and blocking its ability to induce inflammation in

macrophages. However, whether endogenous anti-OSE IgM might subsequently facilitate OSE clearance through binding receptors via its Fc portion remains unclear. Studies comparing atherosclerosis in C1q-deficient and sIgM-deficient mice suggest that the protective effects of IgM in atherosclerosis are partially independent of the classical complement pathway and apoptotic cell clearance[69]. This also aligns with studies in which mice given $sIgM^{-/-}$ B-1a cells had similar lesional apoptotic cell content as mice given $sIgM^{+/+}$ B-1a cells[37]. Whether the Fcμ or Fcα/μ receptors have a role in anti-OSE IgM-mediated atheroprotection is unexplored.

Importantly, IgM secretion is the primary mechanism of B-1-mediated atheroprotection, as adoptive transfer of sIgM-deficient B-1a cells fails to protect from atherosclerosis, unlike transfer of sIgM-sufficient B-1a cells[37]. As B-1-derived anti-OSE IgM has been demonstrated to be atheroprotective, it is important to understand the factors that regulate its production, as this may provide new therapeutic targets for atherosclerosis prevention.

Niche-specific differences in B-1 IgM antibody production

In mice, B-1 cells are present at highest frequency (~40% of all lymphocytes) in the serosal (peritoneal and pleural) cavities, while smaller frequencies are seen in the spleen, bone marrow (BM), intestinal lamina propria, and lymph nodes[47]. In addition to lymphoid organs, IgM-secreting B-1 cells are also present in adipose tissues, including omental fat and the perivascular adipose tissue (PVAT), which surrounds the aorta and other major vessels [76,77]. Importantly, while B-1 frequency is high in the peritoneal cavity, constitutive IgM antibody production by PerC B-1 cells occurs at a very low level during steady state[78], though activation by innate stimuli can induce their proliferation, rapid migration to other sites, and differentiation into antibody secreting cells[79-81].

In contrast, B1 cells in lymphoid organs such as the spleen and bone marrow secrete greater amounts of IgM on a per cell basis constitutively and are the primary contributors to steady-state IgM titers[81-84]. Baumgarth and colleagues have further demonstrated that sorted bone marrow IgM-secreting cells produce more IgM on a per cell basis than splenic IgM-secreting cells *in vitro*[82]. Additionally, studies from our lab demonstrate that the highest B1:B2 cell ratio is present in PVAT and omental fat, compared to spleen, bone marrow, and PerC, suggesting that these adipose tissues may also significantly contribute to circulating IgM levels (as shown in reference[77] and unpublished data).

IgM-secreting B-1 cells also accumulate within artery tertiary lymphoid organs (ATLOs) that form in the adventitia in aged ApoE$^{-/-}$ mice[85,86]. Studies by Habenicht and colleagues demonstrate that lymphotoxin-β receptor signaling induces smooth muscle cell expression of CXCL13 and CCL21, lymphorganogenic chemokines that result in progressive immune cell aggregation and eventual formation of ATLOs that contain high endothelial venules, B cell follicles and germinal centers, T cell zones, and other immune cells[87]. Interestingly, most B-1 cells within ATLOs are B-1b cells, a majority of which produce the anti-inflammatory cytokine IL-10[85].

As B-1 cell IgM production appears to be heterogeneous and niche-specific (**Figure 2**), it becomes important from a therapeutic standpoint to understand the factors that regulate their localization to sites of high antibody production. The differences in IgM antibody production by B cells from different locations could be due to intrinsic properties of those B-1 cells, or extrinsic factors that inhibit or activate B-1 antibody production. Current studies demonstrate that multiple factors contribute to B-1 cell heterogeneity, including 1) the microenvironment within a specific niche and 2) intrinsic factors such as the B-1 cell antibody repertoire, ontogeny, and intracellular signaling molecules.

Figure 2. Niche-specific B-1 cell heterogeneity. B-1 cells from distinct anatomical regions display functional heterogeneity in IgM antibody production, arising from both extrinsic microenvironmental factors and intrinsic differences. Peritoneal cavity (PerC) B-1 cells secrete less IgM constitutively compared to B-1 cells from spleen, bone marrow, perivascular adipose tissue (PVAT), and adventitial tertiary lymphoid organs (ATLO). In the PerC, PC-1 expression distinguishes B-1a cells with high capacity to produce IgM (PC-1^{lo}), from those with low capacity to produce IgM (PC-1^{hi}). The Src family kinase Lck also maintains the hyporesponsiveness of PerC B-1a cells. Additional heterogeneity in the PerC B-1 population is evidenced by distinct immunoglobulin heavy chain (IgH) repertoires expressed by PerC B-1a vs B-1b cells, with PerC B-1a cells expressing more germline sequences that lack N-additions and a preference for V_H11/V_H12 family gene segments. In contrast, splenic B-1a cells produce more IgM constitutively in a manner dependent on the transcription factor IRF4, and the splenic B-1a IgH repertoire contains more N-additions and greater VDJ gene segment diversity. The transcription factor Id3 inhibits B-1b cell number and consequently IgM antibody production. Bone marrow (BM) B-1 cells also produce more IgM constitutively compared to PerC B-1 cells, and IL-5 has been shown to maintain the BM IgM-secreting cell population. The PVAT contains type 2 innate lymphoid cells (ILC-2) that secrete IL-5 in response to IL-33. Whether ILC-2 derived IL-5 is responsible for maintaining the high constitutive IgM production that occurs in PVAT is unknown. ATLO contain an abundance of IL-10 producing B-1b cells. B-1 cell trafficking between these compartments relies on adhesion molecules. The chemokine receptor CXCR5 mediates B-1 cell trafficking between the spleen and the PerC. CXCR4 mediates B-1 cell migration to the bone marrow. CCR6 and L-selectin mediate B-1 localization to the PVAT and aorta.

Figure 2.

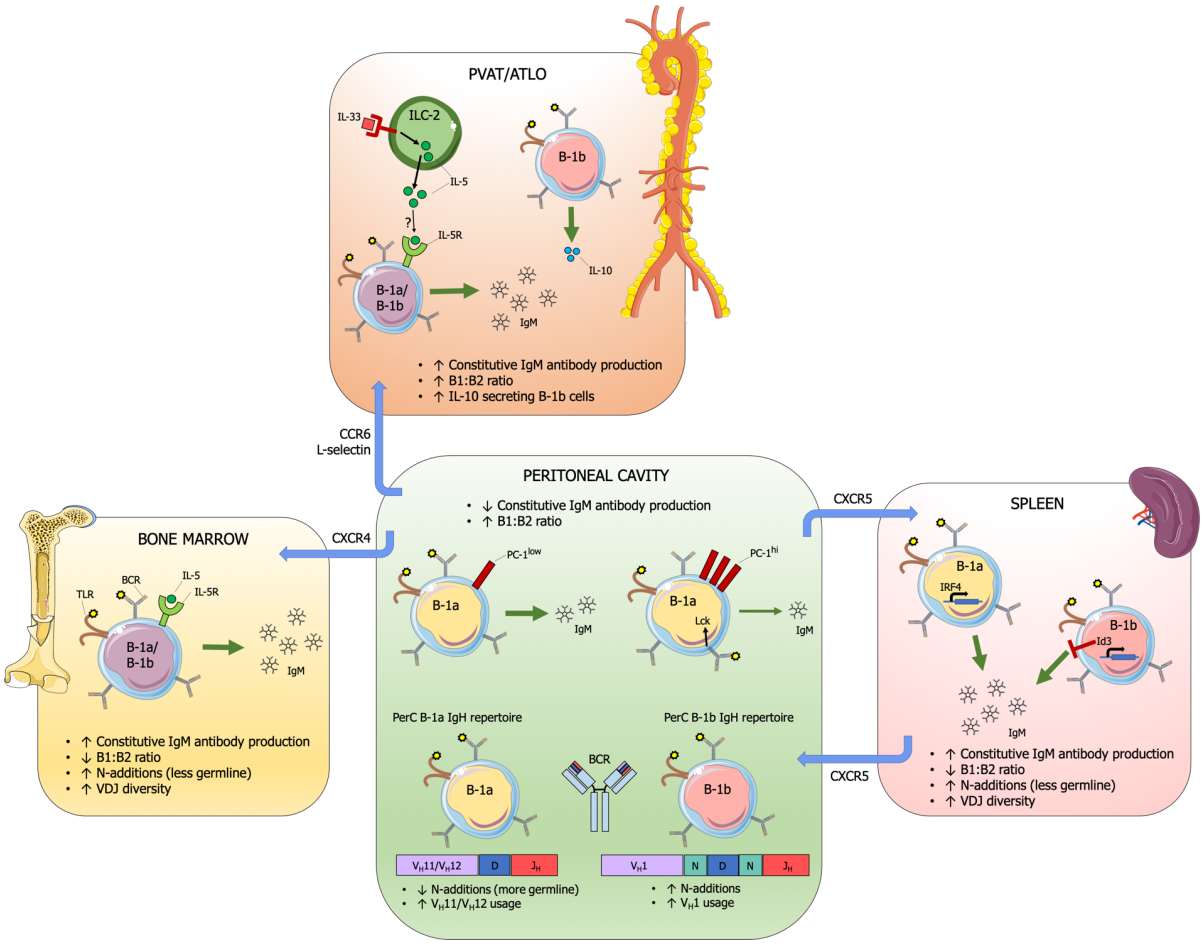
PVAT/ATLO
IL-33
ILC-2
IL-5
?
IL-5R
B-1b
IL-10
B-1a/
B-1b
IgM
• ↑ Constitutive IgM antibody production
• ↑ B1:B2 ratio
• ↑ IL-10 secreting B-1b cells
CCR6
L-selectin
PERITONEAL CAVITY
• ↓ Constitutive IgM antibody production
• ↑ B1:B2 ratio
CXCR4
CXCR5
BONE MARROW
TLR
BCR
IL-5
IL-5R
B-1a/
B-1b
IgM
• ↑ Constitutive IgM antibody production
• ↓ B1:B2 ratio
• ↑ N-additions (less germline)
• ↑ VDJ diversity
PC-1low
B-1a
IgM
PC-1hi
B-1a
Lck
IgM
PerC B-1a IgH repertoire
PerC B-1b IgH repertoire
B-1a
BCR
B-1b
VH11/VH12
D
JH
VH1
N
D
N
JH
• ↓ N-additions (more germline)
• ↑ VH11/VH12 usage
• ↑ N-additions
• ↑ VH1 usage
CXCR5
SPLEEN
B-1a
IRF4
B-1b
Id3
IgM
• ↑ Constitutive IgM antibody production
• ↓ B1:B2 ratio
• ↑ N-additions (less germline)
• ↑ VDJ diversity

Extrinsic mechanisms contributing to B-1 cell heterogeneity

In support of B cell-extrinsic mechanisms contributing to B-1 cell functional heterogeneity, Chace and colleagues reported that release of prostaglandin E2 by peritoneal macrophages inhibited LPS-induced IgM production by peritoneal B1 cells *in vitro*, suggesting that PerC macrophages may be partially responsible for the low IgM-producing capacity of PerC B-1 cells *in vivo*[88]. As certain cytokines have also been shown to be important for maintaining B-1 cell homeostasis and IgM production, differential cytokine concentration or availability within distinct niches could likely impact IgM production within a niche. For example, interleukin (IL)-5 has a critical role in maintaining peritoneal B-1a cell survival and proliferation, and consequently antibody production [89,90]. IgM production by bone marrow B cells was also demonstrated to be enhanced by IL-5 *in vitro* [91]. Moreover, IL-5-deficient bone marrow chimeras have decreased T15/E06 IgM titers in response to Western diet feeding and increased atherosclerosis[92]. IL-10 has also been demonstrated to be important for B-1 cell function, operating in synergy with CXCL12 signaling to mediate B-1 cell proliferation, survival, and retention within the peritoneal cavity[93]. In the NZB/W mouse model of lupus, the combined actions of IL-10 and CXCL12 were demonstrated to be key for development of anti-dsDNA autoantibodies[94]. A fraction of serosal B-1a cells termed innate response activator (IRA) B cells have additionally been demonstrated to require autocrine GM-CSF for efficient IgM production[95].

Notably, the presence of fat-associated lymphoid clusters (FALCs) as sites of B-1 cell activation and antibody production has been highlighted in recent years[96]. FALCs form independently of canonical mechanisms leading to formation of other secondary lymphoid tissues, like the lymphotoxin-β receptor pathway and lymphoid tissue-inducer cells[97]. Instead, FALC formation increases with age and is inducible by inflammatory

stimuli in a manner dependent on tumor-necrosis factor receptor signaling[97]. FALCs are found primarily in the omentum, pericardium, and mediastinum, and contain abundant numbers of type 2 innate lymphoid cells (ILC2) that produce Th2 cytokines including IL-5[98], and stromal cells that produce IL-33[99]. In a model of pleural infection, IL-5 and IL-33 were both required for the activation of FALC B1 cells and IgM production[99]. Therefore, it is very likely that FALC formation brings into close proximity IL-33, IL-5, and B-1 cells, and may be responsible for the greater IgM production that occurs in adipose tissues relative to that in the serosal cavities. Notably, ILC2 are also found within the PVAT and aortic adventitia, and produce IL-5 after stimulation with IL-33, suggesting that they may contribute to B-1 homeostasis and IgM production within the PVAT[100].

Intrinsic mechanisms contributing to B-1 cell heterogeneity

Intrinsic differences in the B-1 cell ontogeny, BCR repertoire, or intracellular signaling molecules likely also account for differences in IgM production. The source of IgM-secreting B-1 cells in various compartments remains controversial. B-1 cells in adult mice are a largely self-renewing population, derived from precursors from the fetal liver and bone marrow, in contrast to B-2 cells which are continuously generated *de novo* in adult bone marrow. Dorshkind and colleagues have proposed a model in which murine B-1 cell development occurs in waves, with the first wave being the embryonic yolk sac, the second wave arising from the fetal liver and bone marrow, and the third wave arising from neonatal and adult bone marrow during the first few weeks of life[10]. After that, *de novo* B-1 cell development wanes, and the adult B-1 cell pool is primarily maintained through self-renewal. However, distinct B-1a and B-1b progenitors have also been found in adult bone marrow and adult spleen[101-105]. Yet, the capacity of these progenitors to regenerate the B-1 compartment has been demonstrated only after an injury to the B-1

compartment such as lethal irradiation, making it unclear how significantly these progenitors contribute to endogenous B-1a and B-1b subsets in health. Earlier studies suggested that peritoneal B-1 cells arose from precursors within the spleen, because splenectomy reduced peritoneal B-1 number [106,107]. However, in apparent contrast to this, adoptive transfer of adult peritoneal B-1 cells is able to reconstitute all B-1 compartments in adult mice, including in the spleen and bone marrow [91,108,109]. Though the origins and migratory capacities of B-1 cells from different body cavities remains incompletely understood, it is clear that functional heterogeneity exists within the B-1 compartments; some B-1 cells contribute to constitutive natural IgM secretion (predominantly B-1 cells within spleen and bone marrow), while serosal B-1 cells seem to be primed for rapid response to stimuli via migration and differentiation into antibody-secreting cells[41].

Heterogeneity in the B-1 population also occurs at the level of the B cell receptor (BCR), which determines antibody specificity. The variable region of the BCR develops through a process called VDJ recombination, in which V_H, D, and J_H gene family segments rearrange to make the immunoglobulin heavy chain, and V_L and J_L segments make up the immunoglobulin light chain. Pairing and dimerization of two heavy and two light chains and addition of constant region exons forms the mature BCR. Positive and negative selection events strongly influence the development of the BCR and the overall B cell repertoire present in an animal. Additional heterogeneity is introduced through non-template-encoded N nucleotide (N-additions) and nucleotide excisions at the junctions between V-D and D-J gene segments. Antigen binding occurs and is determined by hypervariable regions of IgH V called the complementarity determining regions (CDRs), the most variable of which is CDR-H3, which extends across both V-D and D-J junctions. Several studies have sequenced the variable region of the heavy

chain (IgH V) and shown that significant heterogeneity exists in the IgH V repertoire of B cell subsets from different locations. For example, IgH deep sequencing indicates that the B-1a repertoire (both peritoneal and splenic) is generally more restricted and favors usage of certain V_H genes that encode for autoreactive specificities, compared to the IgH repertoire of splenic marginal zone, splenic follicular B-2, and peritoneal B-2 cells[49]. Moreover, the peritoneal B-1a repertoire is generally less diverse in comparison to the splenic B-1a repertoire regardless of age, containing more recurrent CDR-H3 nucleotide sequences, a bias towards V_H11 and V_H12 gene usage, and little if any N-additions, indicative of a more germline antibody repertoire[49]. In contrast, the splenic B-1a repertoire contains more unique CDR-H3 sequences, and appears to accumulate N-additions and undergo increased somatic hypermutation with age[49]. Because N-additions require the enzyme Tdt, which is only expressed postnatally, it has been proposed that the peritoneal B-1a IgH repertoire is generated primarily from prenatal fetal-derived B-1a cells. However, other studies have demonstrated that N-additions increase in PerC B-1a cells with age[103,110], which may arise from the contribution of postnatally developed B-1a cells, B-1a cells migrating from other compartments, or from selective antigen-induced pressures that are specific to a particular microenvironmental niche. Importantly, given the potential for postnatal diversification and selection of the IgM repertoire, defining the IgM repertoire in the context of atherosclerosis risk factors such as age and hyperlipidemia is of key importance. While BM B-1a cells significantly contribute to IgM production, IgH V analysis of the mature BM B-1a cell population remains undefined.

Certain intracellular signaling pathways may also contribute to differences in IgM antibody production between B-1 cells from different compartments. For example, Holodick and colleagues reported that low-level constitutive IgM production by peritoneal

B-1 cells was independent of the transcription factor IRF4, unlike splenic B-1 cells, which secrete much more IgM on a per cell basis in an IRF4-dependent manner[78]. Additionally, expression of the src family kinase Lck in peritoneal, but not splenic, B-1a cells was demonstrated to contribute to their hyporesponsiveness, and Lck-null mice have increased amounts of circulating natural antibodies[111]. Surface expression of plasma cell alloantigen 1 (PC-1) was also demonstrated to divide the peritoneal B-1a compartment based on high capacity (PC-1^{lo} B-1a) versus low capacity (PC-1^{hi} B-1a) to produce natural IgM[112]. Interestingly, PC-1^{lo} B-1a cells were demonstrated to arise in an earlier wave of B-1a cell development from the fetal liver, while PC-1^{hi} B-1a cells increased in number only after birth. Additionally, certain molecules including Id3[100], Lin28b[113], PIK3CD[114], IgM Fc receptor[115], RasGRP1[116], and CD6[117] have been shown to play a role in B-1a cell development or self-renewal and serum natural IgM production. In these studies, it is important to note the difference between direct modulation of IgM production versus indirect modulation of IgM titers by changes in B-1 cell number. The factors regulating preferential expression of these molecules in a niche-, subset- or antigen-specific manner is an intriguing area for future study.

Niche-specific B-1 cell contributions to atheroprotection

Although B-1 cells in the aorta are present predominantly in the surrounding perivascular adipose tissue and adventitia and only rarely within intimal lesions themselves[77,85], abundant IgM to OSE is present in human and mouse atherosclerotic lesions[54,57,58]. As IgM has been demonstrated to block OSE-induced pro-inflammatory signals within macrophages and this associates with decreased atherosclerosis[74,75], it is thought that IgM limits plaque formation primarily through its actions within the plaque. However, how IgM gets into the lesion and whether it is supplied by systemic plasma

IgM made in peripheral niches, by IgM-producing cells locally within the PVAT and adventitia, or both, remains unclear.

Of all the candidate sites for atheroprotective IgM production, the contribution of the spleen has been most widely studied. B cells in the spleen respond to atherogenesis through expansion of clones reactive to PC and oxLDL[72]. Splenectomy aggravates atherosclerosis in ApoE$^{-/-}$ mice, and adoptive transfer of splenic B cells into splenectomized mice increases circulating titers of anti-OSE IgM and IgG and reduces lesion size even below that of sham-operated controls[11]. Moreover, splenectomy significantly reduces the amount of IgM within aortic root lesions, suggesting that peripheral IgM production significantly contributes to lesional IgM accumulation[37]. These studies demonstrate that the spleen harbors a protective B cell response during atherosclerosis. However, in the splenectomy + adoptive B cell transfer studies, it was not determined to which niche the transferred B cells homed nor where IgM was being generated in the absence of the spleen.

There is evidence that B cell homing to the aorta is atheroprotective. Our lab has demonstrated that adoptively transferred splenic B cells home to the aortic adventitia in a manner dependent on Id3 and CCR6, and that this associates with decreased lesion area and reduced plaque macrophage content[118]. Furthermore, transfer of splenic CCR6$^{+/+}$ApoE$^{-/-}$ B cells into sIgM$^{-/-}$ ApoE$^{-/-}$ mice attenuates atherosclerosis only if those B cells are capable of secreting IgM[119]. Additionally, L-selectin-deficient mice have reduced numbers of aortic B-1a and regulatory B cells, decreased T15 IgM and IL-10 in aortic supernatants, and increased atherosclerosis[35]. These studies suggest that B cell migration to the aorta and subsequent local IgM production is atheroprotective.

Finally, while the bone marrow is an important site of B-1 IgM production, the local B-1 response within the BM during atherosclerosis development is not known. B-1

circulation between all of these sites is likely dynamic and recent studies have shed light on the chemokine axis governing this traffic.

Regulation of B-1 cell trafficking

While there are clear differences in IgM production between B-1 cells from different niches as summarized in the sections above, the factors regulating B-1 cell number at sites of high antibody production, like the bone marrow, both at steady state and in the context of chronic inflammation, remain largely unexplored. Cell trafficking and localization is controlled by a number of cell surface adhesion molecules including chemokine receptors, integrins, and selectins.

Parabiosis studies have demonstrated dynamic circulation of B-1 cells to the PerC between parabiotic partners[79]. Steady-state B-1 localization to the PerC depends on the chemokine/receptor pairs CXCR5/CXCL13[79] and CXCR4/CXCL12[120], as well as the integrins $\alpha 4\beta 1$ and CD9[80] which are important for B-1 cell retention in the PerC. CXCR5/CXCL13 are required for both B-1 cell trafficking to the PerC via the omentum[79,121], as well as B-1 cell trafficking out of the PerC[80]. Sphingosine 1-phosphate (S1P) and one of its receptors S1P1 are also involved in peritoneal B-1 localization, as treatment with the S1P1 agonist FTY720 results in reduction in PerC, blood, and omental B-1 numbers, and accumulation of B-1 cells in the parathymic lymph nodes and bone marrow[122]. Cell transfer studies indicate that the B-1 cell population in the spleen at steady-state is derived partially from B-1 migrants from the PerC[81,123]. Heterogeneity in PerC B-1a migratory capacity has also been demonstrated, with low expression of the surface marker PC-1 on B-1a cells associating with increased capacity to migrate to the spleen compared to PC-1^{hi} B-1a cells after intraperitoneal transfer[112].

In addition to steady-state circulation, PerC B-1 cells can also mobilize in response to activation by inflammatory stimuli[123]. Several studies have used TLR agonists or bacterial ligands to study B-1 migration. For example, intraperitoneal transfer of IgM^b allotype PerC cells into congenic IgM^a allotype hosts and stimulation with intraperitoneal LPS resulted in emigration of donor B-1 cells from PerC to spleen and differentiation into antibody-secreting cells [81]. This study additionally demonstrated that the spleen contains both tissue-resident B-1 cells that rapidly differentiate into CD138+ B-1 plasma cells without dividing first, and a later population of migrated CD11b+ PerC B-1 cells that require cell division before differentiation into CD138+ B-1 plasma cells[81]. TLR4 stimulation induces rapid down-regulation of the integrins α4 and β1 as well as CD9 on PerC B-1 cells, and coincides with B-1 egress from PerC and concomitant increased B-1 numbers in spleen and omentum[80]. Absence of CXCL13 also hampers B-1 emigration from PerC in response to TLR4 agonist, further demonstrating the importance of this chemokine in B-1 trafficking[80]. Additionally, oral or intranasal LPS administration leads to accumulation of IgM-producing B-1 cells in the lamina propria[124] or mediastinal lymph nodes[95] respectively, demonstrating that B-1 cells can have regional responses. CD11b and type I interferon signaling were demonstrated to be necessary for B-1 cell accumulation in mediastinal lymph nodes in response to influenza infection[125].

Importantly, expression of these adhesion molecules is dynamic. Berberich and colleagues have demonstrated that splenic B cells transferred intraperitoneally take on the chemokine receptor profile of peritoneal B cells, and are able to more efficiently migrate to the PerC compared to freshly isolated splenocytes on competitive adoptive transfer[121]. There is also evidence that coordinated regulation of CXCR4 and CXCR5 surface expression coincides with B-1 cell egress from the PerC: after intraperitoneal

LPS administration, CXCR5 expression increases rapidly by 5 hours but wanes by 10 hours, while CXCR4 expression peaks much later (24 hours post-stimulation)[126]. Furthermore, factors that influence the chemokine gradient can also influence cell localization. The atypical chemokine receptor D6 is present on peritoneal cavity B-1 cells[127], and can influence the overall chemokine gradient by functioning as a chemokine scavenger, internalizing chemokines but not inducing Ca^{2+} fluxes or chemotaxis. D6 deficiency results in reduced B-1 cell number in PerC, spleen, and omentum, and reduced serum anti-PC IgA and IgG3[127].

Importantly, a number of these studies demonstrating niche-specific deficits in B-1 cell number in the absence of chemokines/receptors also demonstrate an associated deficit in natural antibody production, highlighting the idea that B-1 cell localization is an important factor influencing IgM production. For example, $CXCL13^{-/-}$ mice that contain diminished PerC B-1 cell numbers have reduced titers of anti-PC and T15 IgM both at steady-state and in response to intraperitoneal immunization with R36A streptococcal vaccine, which expresses phosphocholine that is an antigenic target primarily for B-1a cells[79]. Yet, intravenous administration of R36A did not lead to the same deficit in anti-PC IgM in $CXCL13^{-/-}$ mice[79], and $CXCL13^{-/-}$ mice immunized with B-1b cell-inducing bacterial antigens including *B. hermsii* or PPS did not exhibit a defect in antigen-specific antibody responses[128]. Therefore, the requirement of any specific adhesion molecule in generating an antibody response may differ based on route of antigen administration and the specific cell subset being activated by a particular antigen, and are important factors to consider when interpreting these studies or designing future studies. Furthermore, in the D6 study described above, D6 deficiency did not lead to deficiency in serum anti-PC IgM, despite reduced B-1 cell number in PerC, spleen, and omentum, further highlighting the potential contributions of B-1 cells from other niches, including

the bone marrow, to anti-PC IgM titers. As of the start of this project, factors mediating B-1 cell localization or migration to the bone marrow had yet to be examined.

CXCR4 expression, signaling, and functions

CXCR4 is a broadly expressed G protein-coupled chemokine receptor present on both immune and non-immune cell types. CXCR4 is critical for development, as its global knockout results in fetal lethality due to multiple developmental defects[129]. CXCR4 has a well-established role in retaining hematopoietic stem and progenitor cells (HSPC) in the fetal liver and fetal and adult bone marrow [129,130]. In addition to its role in cell retention, CXCR4 also facilitates cell mobilization into the periphery towards its ligands, CXCL12 and MIF, in health or in response to injury or stress. CXCL12 is similarly broadly expressed, including in bone marrow stroma, high endothelial venules, germinal centers, and peritoneal mesothelial cells. Binding of CXCL12 to CXCR4 triggers dissociation of the coupled heterotrimeric G-protein, into its $G\alpha_i$ subunit and $G\beta\gamma$ dimer. These subunits mediate downstream signaling events that lead to calcium mobilization and activation of the MAPK and PI3K pathways, ultimately resulting in chemotaxis. Ligand binding to CXCR4 can also lead to the recruitment of β-arrestin, which mediates CXCR4 endocytosis and receptor recycling. Therefore, CXCR4 expression is controlled in part by expression and availability of its ligands. Furthermore, an alternative receptor for CXCL12, CXCR7, has gained interest due to its higher affinity for CXCL12 and ability to function as a decoy receptor, competing for available CXCL12 and negatively regulating CXCR4 signaling[131].

Importantly, CXCR4 and its ligand CXCL12 have been implicated in PerC B-1 mobility. At homeostasis, PerC mesothelial cells constitutively produce CXCL12[120], which is important for CXCR4-mediated retention of B-1 cells within the PerC[93]. In

support of this C57BL/6 mice with B cell-specific loss of CXCR4 have reduced numbers of PerC B-1 cells and reduced TI-antibody responses to acute immunization with NP-Ficoll[132]. Soon after a TLR4 stimulus is delivered intraperitoneally, CXCL12 expression in mesothelial cells decreases[80], and CXCR4 expression on B-1 cells increases[126], presumably due to diminished CXCL12-mediated internalization of CXCR4. The LPS-induced increase in surface CXCR4 expression on B-1 cells facilitates B-1 migration towards higher concentrations of CXCL12 in vitro [126], and may also modulate B-1 egress from the PerC down a CXCL12 gradient *in vivo*. In support of this, mice with mutated CXCR4 that is unable to be desensitized display enhanced responses to CXCL12 and leukopenia[133].

In addition to its role in chemotaxis, CXCR4 also has a demonstrated role in mediating cell cycle progression and cell survival. For example, exogenous CXCL12 was demonstrated to have pro-survival and anti-apoptotic effects on murine embryonic stem cells[134], while CXCR4 neutralizing antibody resulted in diminished proliferation and increased apoptosis of pancreatic ductal cells isolated from non-obese diabetic mice[135]. The pro-survival effects of CXCR4 signaling are also often co-opted by transformed and malignant cancer cells, which exhibit heightened expression of this receptor associated with increased proliferation, migration, and invasion[136]. Mechanistically, CXCR4 expressed by malignant peripheral nerve sheath tumors but not by non-transformed cells, was demonstrated to promote cyclin D1 expression and cell-cycle progression through PI3K and β-catenin signaling[137]. Exogenous CXCL12 was also demonstrated to induce expression of the anti-apoptosis protein, survivin, in a glioblastoma cell line[138].

CXCR4 in atherosclerosis

Studies implicating CXCR4 in regulating atherosclerosis development have yielded contrasting results on whether CXCR4 serves an atheroprotective or atherogenic role, likely due to the early use of strategies that targeted CXCR4/CXCL12 globally, through use of small molecule inhibitors or bone marrow transplantation, rather than in a cell type-specific manner (summarized thoroughly by Doring and colleagues[139]). CXCR4 has been suggested to promote atherosclerosis by mediating monocyte adhesion and migration into the artery wall[140,141]. In contrast, CXCR4 involvement in maintenance of endothelial barrier integrity, smooth muscle cell contractile phenotype, and neutrophil homeostasis was linked to reduced atherosclerosis[142,143]. Several human genome wide association studies have identified single nucleotide polymorphisms (SNPs) in CXCR4 and CXCL12 associated with CVD[142,144-149]. However, reports conflict on direction of association with CVD, and whether the risk alleles alter CXCR4/CXCL12 expression or function[139]. These differences may arise from examining CXCR4 expression on total peripheral blood cells, which is a heterogeneous mix of cells with pro- or anti-inflammatory functions depending on context, or plasma CXCL12 levels, which may or may not reflect what is happening at the tissue site during disease. Thus far, it remains unknown what role CXCR4 plays on B cells, specifically B-1 cells, in atherosclerosis, or how hyperlipidemic conditions may affect CXCR4 expression on B cell subsets.

Human B cell subsets and human B-1 cells

In contrast to murine B-1 cells, human B-1 cells have been harder to define. Studies on human B cell subsets were slower compared to their T cell counterparts, in part due to a lack of reagents that clearly distinguished B cell subsets[150]. CD5 was an early marker helpful in a clinical setting for distinguishing lymphomas and leukemias, but

it was less helpful in differentiating healthy B cells. Early studies by Liu and Banchereau in the late 1990's used IgD and CD38 expression to classify naïve, germinal center, and memory B cells from tonsils, and named this the B mature classification system[151,152]. Since then, more surface markers, as well as characterization of BCR affinity, BCR mutation frequency, and functional assays including immunoglobulin secretion have added to our understanding of human B cell populations[150]. In light of these findings, it is clear that a much deeper heterogeneity exists in human B cell subsets that can't be seen when using one or two surface markers. For example, CD27, which is a surface marker used to classify memory B cells, correlates with functional parameters of memory, including greater somatic hypermutation in the IgH V region, proliferation, and ability to differentiate into antibody secreting cells[153-155]. However, the total CD27+ B cell pool is diverse, being expressed on cells with nonmemory phenotypes[156], and there are certain B cells with memory-like phenotype that lack CD27 expression[157]. It is also important to consider that surface marker expression may be dynamic, and a transitioning or polarized population may have altered expression of certain subset-specific markers, yet may be derived or related to a conventional subset.

Rothstein and colleagues identified the putative human B-1 subset using a reverse engineering approach, in which characteristics typical of murine B-1 cells, including spontaneous *in vitro* IgM antibody production, efficient T cell stimulation, and tonic intracellular signaling were used to identify a human B-1 equivalent[158] (**Figure 3**). This subset was identified at low frequency in peripheral and umbilical cord blood and defined as $CD20^{+}CD3^{-}CD27^{+}CD43^{+}$[159,160]. Since its initial discovery, controversy has existed on the frequency of this population in peripheral blood, and the difference between human B-1 cells and plasmablasts or pre-plasmablasts[161-163]. In response, Rothstein and colleagues have extensively and carefully delineated the isolation process

and gating strategy to identify human B-1 cells from peripheral blood[164] and demonstrated that this subset differs from plasmablasts and pre-plasmablasts based on CD38 expression, transcriptional profiling, antibody repertoire, and other characteristics[165]. Yet, studies from Rothstein's lab have also identified further heterogeneity in the $CD20^{+}CD3^{-}CD27^{+}CD43^{+}$ population, including differential CD11b expression, which distinguishes predominantly IgM-secreting B-1 cells ($CD11b^{-}$), from predominantly IL-10-secreting B-1 cells with increased capacity to modulate T cells ($CD11b^{+}$)[166,167]. Thus far, an equivalent to murine B-1a and B-1b subsets has not been identified within the human B-1 population. CD5, which distinguishes these subsets in mice, does not differentiate human B-1 cells; most CD5+ B cells are not $CD20^{+}CD3^{-}CD27^{+}CD43^{+}$ B-1 cells, and CD5 is not expressed on all B-1 cells[158]. Studies from our lab also suggest that deeper heterogeneity exists in this B-1 subset, and more research is necessary to identify potential functionally distinct subpopulations.

Anti-OSE antibodies in human CVD

The role of B cells and their secreted antibodies in human CVD remains an evolving field. A 2013 study utilizing an integrated systems biology approach to analyze data from the Framingham Heart Study revealed that B cell activation genes were enriched in control individuals compared to those with coronary artery disease[168]. Moreover, natural anti-OSE antibodies and human B-1 cells decline in amount, frequency, and avidity with age[169], while prevalence of atherosclerosis increases with age, leading to the interesting hypothesis that natural IgM may serve as a useful metric to predict susceptibility to age-related diseases involving OSE[170]. Indeed, studies in human CVD patient cohorts have demonstrated that increased amounts of circulating IgM antibodies for the OSE malondialdehyde(MDA)-modified LDL are associated with

less coronary artery disease and fewer cardiovascular events [21,22,171,172]. Recent interest has been piqued in examining cardiovascular parameters in human patients receiving B cell-targeted immunotherapies that have been used for decades in treatment of autoimmune diseases, such as systemic lupus erythematosus (SLE) and rheumatoid arthritis (RA)[173]. This is especially so in light of the CANTOS trial, which highlighted the important role of inflammation in CVD progression[6], and in line with this, autoimmune patient populations show increased susceptibility to adverse cardiovascular events[174]. A recent review by Porsch and Binder examining current B cell-targeted therapies and their impact on human CVD indicates that more work in larger human cohorts is necessary to draw conclusions[173]. For example, the anti-CD20 B cell-depleting monoclonal antibody rituximab showed promise in a small-scale study in reducing carotid intima-media thickness (n=55 RA subjects)[175]. However, other studies showed no significant effect of rituximab treatment, while other B-cell immunotherapies either have no effect on CVD parameters, or have simply not yet been assessed[176].

Importantly, human B-1 cells have been shown to produce IgM antibodies that are associated with CVD. Advanced glycation endproduct (AGE) modifications are glycated proteins or lipids that arise after exposure to sugar. AGE modifications have been implicated in progression of CVD associated with oxidative stress, inflammation, and endothelial cell dysfunction[177]. Methylglyoxal (MGO) is a reactive aldehyde that results in AGE modifications, and human B-1 cells have been shown to produce IgM antibodies against methylglyoxal (MGO)-modified apoB100 *in vitro*[178]. Moreover, low levels of MGO-specific IgM antibodies are associated with increased risk of cardiovascular events[178]. These data provide compelling support for the human relevance of murine findings that B-1 derived IgM against modified LDL that arise during chronic inflammatory disease are atheroprotective.

Figure 3. Human B-1 cells. Human B-1 cells were identified in peripheral and cord blood by Rothstein and colleagues as a CD20+CD3-CD27+CD43+ population. Functionally, this subset spontaneously secretes IgM, exhibits tonic intracellular phospholipase C gamma 2 (PLC-γ2) and Syk phosphorylation, and efficiently stimulates T cell proliferation. Heterogeneity has been demonstrated within the human CD20+CD3-CD27+CD43+ B-1 population differentiated by CD11b expression. Human B-1 cells with low or no CD11b expression are better able to spontaneously secrete IgM, thus are termed "B-1 secretors." CD11b+ human B-1 cells have been demonstrated to express higher levels of CD86 and to more efficiently stimulate allogeneic CD4+ T cell proliferation compared to B-1 secretors. CD11b+ B-1 cells also spontaneously secrete IL-10, which is able to suppress intracellular TNF-α expression by anti-CD3 stimulated T cells *in vitro*. CD11b+ B-1 cells are termed "B-1 orchestrators" due to their increased capacity to modulate T cell activation and proliferation.

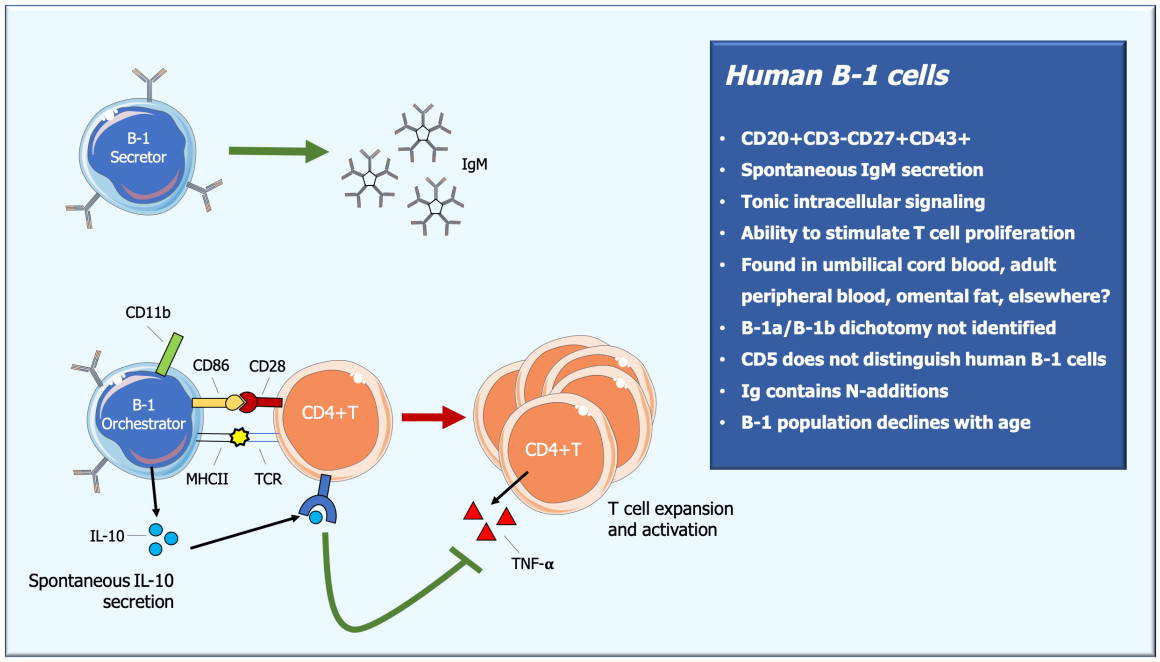

Project rationale

At the outset of this project, it was known that B-1 cells in the bone marrow (BM) contributed significantly to plasma IgM titers[82], and that IgM was critical for mediating protection against atherosclerosis[8,43]. Yet, the factors mediating B-1 cell localization to the BM at steady-state and in the chronic inflammatory state of atherosclerosis were not known. Furthermore, the IgH V repertoire expressed by bone marrow B-1 cells was not yet determined. Additionally, while the putative human B-1 cell subset had been described[158], follow-on studies were revealing that heterogeneity existed within this subset, and knowledge of the factors influencing human B-1 IgM antibody production was limited. We became interested in CXCR4 as a potential regulator of B-1 cell antibody production and atheroprotection due to initial associative findings in a human cohort of CVD, which we then examined in-depth using CXCR4 loss-of-function and gain-of-function mouse models. We hypothesized that CXCR4 was an important regulator of BM B-1 cell localization, anti-OSE IgM production, and atheroprotection.

In chapter 3, we present evidence that CXCR4 maintains the BM B-1a cell population and IgM production within the BM. In $ApoE^{-/-}$ mice either lacking CXCR4 ($CXCR4^{BKO}ApoE^{-/-}$) or overexpressing CXCR4 in B cells, specifically, we found that CXCR4 was necessary for maintaining the number of B-1a cells in the BM, the number of IgM-secreting cells in the BM, and plasma IgM titers. Moreover, we demonstrate using single-cell sequencing of sorted BM or PerC B-1a cells from 100-weeks-aged $ApoE^{-/-}$ mice that the IgH V repertoire of BM B-1a cells is unique and diverse compared to PerC B-1a cells, containing increased N-additions and a greater frequency of unique CDR-H3 sequences. Furthermore, we found that certain CDR-H3 sequences were common to both PerC and BM B-1a cells, indicating potential B-1a migration between compartments. We demonstrate using adoptive cell transfer that migration of PerC B-1a

cells to the BM depended upon CXCR4. Finally, in a 50-subject human cohort of CVD, we find that CXCR4 expression on the putative B-1 subset associates with increased amount of plasma anti-MDA-LDL IgM antibodies, and decreased plaque burden and stenosis. These studies are the first to demonstrate that BM B-1a cells uniquely contribute to the IgM antibody repertoire, and that their maintenance is governed by CXCR4, a novel marker associating with protection in human CVD.

In chapter 4, we discuss the B-1 cell-specific role of CXCR4 in mediating atheroprotection in mice. We examine the local BM and spleen B-1 cell response to atherosclerosis in chow-fed versus Western diet-fed $CXCR4^{BKO}ApoE^{-/-}$ mice. We also go over atherosclerosis studies performed in $CXCR4^{BKO}ApoE^{-/-}$ mice, and after adoptive transfer of CXCR4-sufficient or CXCR4-deficient B-1a cells into lymphocyte-deficient $Rag1^{-/-}ApoE^{-/-}$ mice. We discuss caveats of these mouse models that influence our interpretation of the results.

Chapter 2

Materials and Methods

Human subjects

Patients were recruited for study through the Cardiac Catheterization laboratory at the University of Virginia as previously described[179]. All participants provided written informed consent prior to enrollment, and the study was approved by the Human IRB Committee at UVA. A total of 50 patients presenting for a medically indicated diagnostic cardiac catheterization were enrolled if they met inclusion criteria and had a vessel suitable for intravascular ultrasound (IVUS). All were outpatients with stable coronary syndrome. Patients were excluded if they had: any acute illness, type 1 diabetes, current acute coronary syndrome, autoimmune disease or on immunosuppressive therapy, prior organ transplantation, anemia, pregnancy, HIV infection, or no vessel suitable for IVUS. No patient was on anticoagulation or had deep vein thrombosis or pulmonary embolism.

IVUS

One-vessel IVUS was performed on 50 participants in accordance with the American College of Cardiology standards for image acquisition on a non-infarct related artery as previously described[179]. Summarily, a 2.6 F, 30 MHz IVUS catheter (Volcano Corporation) was advanced over a guidewire into either the left anterior descending coronary artery or the least-angulated vessel providing the longest length for evaluation. Images were obtained at 30 frames/s for a minimum of 40 mm of vessel. IVUS images were analyzed using virtual histology by two blinded investigators according to the guidelines by the American College of Cardiology. Every 60th image was analyzed at 1 mm intervals for a total of 40 mm along the length of the artery beginning at the proximal end. Volcano Image Analysis Software was used to define plaque tissue composition into fibrous, necrotic, or calcified areas, which were expressed as a percentage of total

intima area. Atheroma burden and maximum stenosis were quantified as previously described[179].

Systemic cholesterol measurements

Mouse whole blood was collected with 0.5 M EDTA, centrifuged at 10,000 rpm for 10 minutes, and then plasma was aliquoted in a new tube. Human arterial blood samples were obtained just before IVUS and blood was collected in BD vacutainer serum tubes, centrifuged at 400 rcf for 10 minutes, and then serum was aliquoted into a new tube. Human serum cholesterol quantification was performed by the University of Virginia Medical Laboratories as previously described[118].

Mice

All animal protocols were approved by the Animal Care and Use Committee at the University of Virginia. $CXCR4^{fl/fl}$ and $ApoE^{-/-}$ mice were purchased from Jackson Laboratory. $CD19^{cre/+}$ and $Rag1^{-/-}$ mice were provided by Dr. Timothy Bender (University of Virginia). $CXCR4^{fl/fl}$ mice were bred to the $ApoE^{-/-}$ line and then to $CD19^{cre/+}$ mice to develop $CXCR4^{fl/fl}$ $ApoE^{-/-}$ $CD19^{cre/+}$ mice. These mice were then bred to $CXCR4^{fl/fl}$ $ApoE^{-/-}$ $CD19^{+/+}$ mice to generate $CXCR4^{fl/fl}$ $ApoE^{-/-}$ $CD19^{cre/+}$ ($CXCR4^{BKO}$ $ApoE^{-/-}$) and $CXCR4^{fl/fl}$ $ApoE^{-/-}$ $CD19^{+/+}$ ($CXCR4^{WT}ApoE^{-/-}$) littermate controls. $Rag1^{-/-}$ or $sIgM^{-/-}$ mice were crossed with $ApoE^{-/-}$ mice to generate $Rag1^{-/-}ApoE^{-/-}$ or $sIgM^{-/-}ApoE^{-/-}$ mice. $ApoE^{-/-}$ mice with the CD45.1 allotype were provided by Dr. Gary Owens (University of Virginia). All mice were either purchased on a pure C57BL/6J background from Jackson Laboratory or backcrossed 10 generations with pure C57BL/6J. Mice were fed a standard chow diet (Tekland 7012) or a Western diet (TD.88137, 42% kcal from fat). Mice were euthanized by CO_2 inhalation. Only male mice were used for experiments.

Splenectomy was performed in accordance with ACUC-approved animal protocol by anesthetizing mice with ketamine/xylazine (60-80 mg/5-10kg), excising the spleen, and closing the peritoneal and abdominal wall with absorbable sutures. Sham surgery involved anesthetization, incision, moving spleen with forceps, and suturing the incisions.

Cell preparations for murine and human flow cytometry

During organ harvest, peritoneal cells were harvested by flushing the peritoneal cavity with 10 mL FACS buffer (PBS containing 1% BSA, 0.05% NaN_3). Peripheral blood was collected by cardiac puncture and 20 μL of 0.5 M EDTA was added as an anticoagulant before 50 μL was aliquoted for flow cytometry analysis. Mice were perfused with heparinated PBS then spleen and one femur and tibia were removed. Spleens and flushed bone marrow were filtered through a 70 μm cell strainer. Red blood cells were lysed from single-cell suspensions of bone marrow, spleen and peripheral blood using a lysis buffer containing 155 mM NH_4Cl, 10 mM $KHCO_3$, and 0.1 mM EDTA. Cell surface Fc receptors were blocked using anti-CD16/32 (clone:93, eBioscience), then cells were stained with fluorescently conjugated antibodies against cell surface markers. Cells were stained with fixable Live/Dead Yellow or Live/Dead Aqua (Life Technologies) for dead cell discrimination, then fixed in 2% PFA in PBS. For B-1a cell sorting, dead cell discrimination was determined using DAPI staining. $DAPI^{-}CD19^{+}CD23^{-}B220^{mid\text{-}lo}IgM^{+}CD5^{+}$ B-1a cells were sorted to better than 99% purity from their parent gate. Clone and fluorophore information for the flow cytometry antibodies used in murine experiments to FAC-sort or immunophenotype B cell subsets are given in **Table 1**.

Isolation of PBMC's from human peripheral blood was performed as previously described[38] using Ficoll-Paque Plus (GE Healthcare) and SepMate tubes (Stemcell Technologies), and the buffy coat layer was isolated for staining. Clone and fluorophore information for the flow cytometry antibodies used in human flow cytometry experiments to immunophenotype B cell subsets are given in **Table 2**.

Table 1. Mouse flow cytometry antibodies

Marker	Fluorophore	Clone	Vendor	Catalog Number
CD19	APC-eFluor780, PE-Cy7	eBio1D3	eBioscience	47-0193-82; 25-0193-82
B220	APC, eFluor450, PE-Cy7	RA3-6B2	eBioscience	17-0452-83; 48-0452-82; 25-0452-82
CD5	PE	53-7.3	eBioscience	12-0051-83
CD23	PE-Cy7	B3B4	eBioscience	25-0232-82
IgM	FITC, eFluor450	eB121-15F9	eBioscience	11-5890-82; 48-5890-82
CXCR4	APC	2B11	eBioscience	17-9991-82
CD3	eFluor450	eBio500A2	eBioscience	48-0033-82
CD115	PE	AF598	eBioscience	12-1152-81
Streptavidin	APC-eFluor780	-	eBioscience	47-4317-82
CD43	FITC, Biotin	S7	BD Biosciences	553270; 553269
CD19	PE-CF594	1D3	BD Biosciences	562291
IgM	PE-CF594	R6-60.2	BD Biosciences	562565
CD45.1	PerCP-Cy5.5	A20	BD Biosciences	560580
CD45.2	BV421	104	BD Biosciences	562895
Ly6G	BV711	1A8	Biolegend	127643

Table 2. Human flow cytometry antibodies

Marker	Fluorophore	Clone	Company	Catalog Number
CD3	PE-CF594	UCHT1	BD Biosciences	562280
CD20	APC-H7	2H7	BD Biosciences	560734
CD27	BV421, FITC	M-T271	BD Biosciences	562513; 555440
CD43	FITC, BV421	1G10	BD Biosciences	555475; 562916
CD184	APC	2B11	eBioscience	17-9991-82

All flow cytometry analysis was conducted at the University of Virginia Flow Cytometry Core Facility. Immunophenotyping was performed on a CyAn ADP (Beckman Coulter) or an Attune NxT (ThermoFisher) cytometer. Data analysis and flow plots were generated using FlowJo software (Tree Star Inc). Representative flow plots were chosen

based on the samples whose population frequencies were closest to the mean for that group. B-1a cell sorting was performed on an Influx or FACS Vantage cell sorter (BD Bioscience). Gates on flow plots were set using fluorescence minus one (FMO) controls.

Single-cell sorting and sequencing of the immunoglobulin heavy chain

$CD45^{+}CD19^{+}B220^{mid\text{-}lo}\,CD43^{+}CD5^{+}$ B-1a cells from bone marrow and peritoneal cavity of five 100-week-old chow-fed $ApoE^{-/-}$ mice were single-cell sorted into 96 well plates containing lysis buffer (RNaseOut, 5x Buffer, DTT, IgePAL, carrier RNA, Invitrogen). A 20μl reverse transcription reaction was run per well using the SuperScript III enzyme and random hexamers (Invitrogen). Qiagen's HotStart Taq Plus master mix kit was used to perform the first round of PCR (25μl reaction) using 2.5μl of cDNA diluted 1:2 and the MsVHE and MsCμE primers (**Table 3;**[180]) each at 0.6 μM. Each 25 μl reaction was run as follows: 95°C for 5 minutes; 35 cycles at 94°C for 30 seconds, 50°C for 30 seconds, 72°C for 30 seconds; and then a final extension at 72°C for 10 minutes. The product from this first reaction was then diluted at 1:100 in dH2O and 2 μl was used in the second semi-nested 25 μl reaction using the following MsVHE and MsCμN primers (Supplementary Table 8) each at 0.6 μM. The second reaction was run as follows: 95°C for 5 minutes; 40 cycles at 94°C for 30 seconds, 53°C for 30 seconds, 72°C for 30 seconds; and then a final extension at 72°C for 10 minutes. DNA concentration was determined using the Qiagen Qiaxcel. PCR products were sequenced (Genewiz) using the MsV_HE primer. Sequences were analyzed using an online sequence analysis tool, IMGT/HighV-Quest[181], and only sequences with ≥90% homology to VDJ regions were included.

Table 3. PCR primer sequences

Primer	Sequence
Mouse CXCR4 Forward	5'- TAT TGT CCA CGC CAC CAA -3'
Mouse CXCR4 Reverse	5'- CTT TTC AGC CAG CAG TTT CC-3'
Mouse CXCL12 Forward	5'- GGA CGC CAA GGT CGT CGC CGT G -3'
Mouse CXCL12 Reverse	5'- TTG CAT CTC CCA CGG ATG TCA G -3'
Mouse MIF Forward	5'- TGC CCA GAA CCG CAA CTA CAG TAA -3'
Mouse MIF Reverse	5'- TCG CTA CCG GTG GAT AAA CAC AGA -3'
Mouse CXCL13 Forward	5'- TCC TGG GAA GCT GGT GCA ATG -3'
Mouse CXCL13 Reverse	5'- TCA TCA GGG TCA CAG TGC AAA GG -3'
MsV_HE	5' - GGG AAT TCG AGG TGC AGC TGC AGG AGT CTG G - 3'
MsCμE	5' - ATG GCC ACC GAA TTC TTA TCA GA – 3'
MsCμN	5' - TGT AAA ACG ACG GCC AGT CAT TTG GGA AGG ACT GA - 3'

MDA-LDL generation

MDA-LDL was either provided by Dr. Sotirios Tsimikas (UCSD), or prepared as follows. MDA was freshly generated by incubating malonaldehyde bis dimethylacetal with 1N HCl at 37°C, then the solution was adjusted to pH 7.4 with NaOH. MDA-LDL was prepared by incubating the prepared MDA solution with human LDL (Kalen Biomedical, LLC) at a constant ratio of 100 uL MDA per 1 mg of LDL, for 3 hours at 37°C. After conjugation, MDA-LDL was extensively dialyzed against PBS at 4°C in 10K (10,000 MWCO) Slide-A-Lyzer dialysis cassettes (Thermo Fisher Scientific) to remove excess MDA. Protein concentration was determined by Bradford assay. MDA-LDL was used to coat ELISPOT plates for quantification of anti-MDA-LDL IgM ASC in tissue, as described below.

ELISPOT

Single-cell suspensions of bone marrow and spleen were prepared as described above. ELISPOT to measure total IgM ASC was performed as described previously[38].

Briefly, 10 μg/mL unlabeled anti-mouse IgM antibody (Southern Biotech, 1020-01) or MDA-LDL (prepared as described above) was used to coat Sterile Multiscreen IP-Plates (MSIPS4510). ELISPOT wells were blocked with RPMI1640 containing 10% FCS, then 1-2.5x10^5 spleen or bone marrow cells were added to leading wells and serial 5-fold dilutions of samples were performed. Non-binding cells were washed off with PBS containing 0.01% Tween-20, then ELISPOT wells were incubated in 2 μg/mL biotin-labeled anti-mouse IgM secondary antibody (Southern Biotech, 1020-08) in PBS/0.01% Tween-20. For detection, sequential incubations with streptavidin alkaline phosphatase (Abcam), then BCIP/NBT were performed. Wells were imaged using a Bioreader 4000 (Biosys) and spots were counted manually. Overall IgM ASC number was back-calculated based on sample dilution or total cell count.

ELISA for quantification of total and anti-OSE IgM in mice and humans

Total IgM, IgG1, IgG2b, IgG2c, and IgG3 in mouse serum or plasma was measured using colorimetric ELISA as follows. EIA/RIA high-binding microplates were coated with goat anti-mouse IgM, IgG1, IgG2b, IgG2c, or IgG3 capture antibody (Southern Biotech, 1020-01; 1070-1; 1090-01; 1079-01; 1100-01). Mouse IgM, IgG1, IgG2b, IgG2c, and IgG3 standards (Southern Biotech, 0101-01; 0102-01; 0104-01; 0122-01; 0105-01), or plasma or serum samples were detected with alkaline phosphatase-conjugated goat anti-mouse IgM, IgG1, IgG2b, IgG2c or IgG3 secondary antibody (Southern Biotech, 1020-04; 1070-04; 1090-04; 1079-04; 1100-04) and pNPP substrate (Southern Biotech 0201-01). Absorbance measurements were analyzed with a SpectraMAX 190 microplate reader (Molecular Devices) at 405 nm. The standard curve was determined using a 4-parameter function and concentration measurements were

extrapolated using Softmax Pro 3.1.2 software. Only samples with CV<15% and within the standard curve were included in analysis.

Levels of IgM antibodies specific for MDA-LDL, AB1-2 (anti-idiotypic antibody recognizing E06/T15 specificity), and α-1,3-dextran in mouse serum or plasma were determined by chemiluminescent ELISA as previously described [38,71,182]. In brief, microtiter plates were coated with various antigens at 5 μg/mL in PBS. Antigens used were prepared as previously described [71,182]. Serially diluted plasma was added, and bound plasma IgM was detected with rat anti-mouse IgM μ-chain conjugated to alkaline phosphatase (Abcam) and LumiPhos 530 solution, using a Dynex Luminometer (Dynex Technologies, Chantilly, VA, USA). Data were expressed as relative light units counted per 100 milliseconds (RLU/100 ms). For each set of mice, plasma pools were made initially and used for formal dilution curves to determine optimal dilution for each antigen to use in binding assays. A specific non-saturating dilution was chosen for each antigen, and then plasma samples from each mouse were assayed to determine mean and SD for that determination.

Levels of IgM or IgG against MDA-LDL in human plasma were measured by chemiluminescent ELISA as previously described[171]. Briefly, 5 ug/mL MDA-LDL was coated on microtiter well plates, plasma was added, and IgG or IgM antibodies binding to MDA-LDL were detected with alkaline phosphatase-conjugated goat anti-human IgM or IgG (Sigma).

In vitro LPS stimulation

Peritoneal B-1a cells from $CXCR4^{WT}ApoE^{-/-}$ and $CXCR4^{BKO}ApoE^{-/-}$ mice were sorted as described above, and cultured *in vitro* in B cell media (RPMI-1640, 10% heat-inactivated fetal bovine serum, 10 mM HEPES, non-essential amino acids, 1 mM sodium

pyruvate, 50 ug/mL gentamicin, 55 nM β-mercaptoethanol) containing either 50 μg/mL LPS (Sigma, L4391) or an equivalent volume of PBS. After 72 hours, culture supernatants were harvested, total IgM was measured by ELISA as described above, and normalized to cell counts plated. The fold change in amount of IgM secreted into supernatants from cells cultured with LPS over cells cultured in PBS from each mouse was compared.

Transmigration assay

Peritoneal lavage cells from $CXCR4^{WT}ApoE^{-/-}$ and $CXCR4^{BKO}ApoE^{-/-}$ mice were isolated and $2.5x10^6$ cells were plated into transwell chambers containing 0.4 micron pores (Costar, Corning Incorporated, 3450). Lower wells contained media either with or without 100 ng/mL CXCL12 to distinguish spontaneous migration from migration towards CXCL12. An input aliquot from each sample was additionally analyzed by flow cytometry. Cells were cultured at 37°C for 6 hours then migrated cells in the lower well were harvested for flow cytometry. Percent specific migration towards CXCL12 was defined as the (# of B cells migrating towards CXCL12 - # of B cells migrating spontaneously)/(# of input B cells loaded in the transwell).

Real-time polymerase chain reaction for analysis of chemokine expression

RNA was extracted from CD19+ splenocytes or total bone marrow cells using the RNeasy Plus mini kit (Qiagen, 74134). 1μg of RNA was then treated with DNase (Invitrogen) and used to reverse transcribe cDNA using an iScript cDNA synthesis kit (BioRad). To quantify gene expression, cDNA was diluted 1:10 in water and combined with 0.5mM forward and reverse primers and SYBR Green (SensiFast, BioLine). Semi-quantitative real-time PCR was performed on a CFX96 Real-Time System with an

annealing temperature of 60°C for all reactions (BioRad). Data were calculated by the ΔΔCt method and expressed in arbitrary units that were normalized to 18s ribosomal RNA levels. Primer sequences are listed in **Table 3**.

Cell cycle analysis

8-10 week-old CXCR4^{WT}ApoE$^{-/-}$ and CXCR4^{BKO}ApoE$^{-/-}$ mice were fed 1 week of Western diet, and 1.5 mg BrdU (BD Biosciences 550891) was intraperitoneally injected on days 5, 6, and 7. On day 7, spleen and bone marrow was harvested and prepared for flow cytometry as above. After primary antibody and Live/Dead Yellow staining, cells were fixed, permeabilized, and stained with anti-BrdU FITC (BD 347583) using the BD Cytofix/Cytoperm protocol (554714) according to the manufacturer's instructions. 7-aminoactinomycin (CalBioChem 129935) was used to stain DNA.

Retrovirus production

CXCR4-GFP and Ctl-GFP retroviruses were generated using the pMigR1 retroviral vector (provided by Dr. Timothy Bender, UVA), which expresses GFP. The mouse CXCR4 gene was subcloned from a pCMV-SPORT6 vector (cDNA clone IMAGE:2864967, provided by Dr. Timothy Bender) into the MigR1 retroviral vector using XhoI and EcoRI restriction sites to generate a CXCR4-GFP retroviral vector. The MigR1 (Ctl-GFP) or CXCR4-GFP retroviral vector was co-transfected with the pCL-Eco retroviral packaging vector into 293T cells using calcium phosphate transfection. Transfected 293T cells were incubated at 37°C in an incubator containing 5% CO_2 and viral supernatant was collected 48 hours later. Viral titer was determined by quantifying the frequency of GFP+ cells 24 hours after transduction of 3T3 cells.

Retroviral overexpression of CXCR4 on mouse B cells

Mouse peritoneal B cells were enriched using MACS depletion. Briefly, peritoneal lavage cells from CD45.1^{+} ApoE$^{-/-}$ mice were stained with biotinylated anti-mouse Ter119, CD3e, Gr-1, CD23, NK1.1, and F4/80 antibodies (**Table 4**), secondarily stained with anti-biotin magnetic beads (Miltenyi Biotec), then depleted over Miltenyi MACS LS columns. Enriched B cells were cultured overnight in the presence of 100 nM TLR9 agonist CpG ODN 1668 (Invivogen) to stimulate cell proliferation required for retroviral transduction. Twenty-four hours after stimulation, cells were transduced at a 20:1 multiplicity of infection with Ctl-GFP or CXCR4-GFP retroviral particles using spinfection at 2000 rpm for 90 minutes and cultured for 3 hours at 37°C in the presence of polybrene. Then excess virus was washed off and cells were cultured in fresh B cell media (described above) overnight at 37°C. Cells were FACS-sorted for GFP+ B-1a cells to be used for adoptive transfer. Approximately 30-40% of B-1a cells were successfully transduced by this method.

Table 4. Biotinylated antibodies for MACS depletion.

Marker	Conjugated with:	Clone	Company	Catalog Number
Ter119	Biotin	Ter119	eBioscience	13-5921-82
CD3e	Biotin	eBio500A2	eBioscience	13-0033-85
Gr-1	Biotin	RB6-8C5	eBioscience	13-5931-82
CD23	Biotin	B3B4	eBioscience	13-0232-81
NK1.1	Biotin	PK136	BD Biosciences	553163
F4/80	Biotin	BM8	Life Technologies	MF48015

Adoptive Transfer

Following fluorescence activated cell sorting as described above, B-1a cells were adoptively transferred accordingly:

For short-term transfer of CD45.2^{+} ApoE$^{-/-}$ B-1 cells: 1x10^{6} ApoE$^{-/-}$ peritoneal B-1 cells from CD45.2 allotype mice or an equivalent volume control PBS were intravenously injected into CD45.1 allotype ApoE$^{-/-}$ mice. 4 days later, tissues were harvested for flow cytometry.

For short-term transfer of CXCR4-WT or –BKO B-1 cells: 750,000 CXCR4^{WT} ApoE$^{-/-}$ or CXCR4^{BKO} ApoE$^{-/-}$ B-1 cells or an equivalent volume PBS were intravenously injected into Rag1$^{-/-}$ ApoE$^{-/-}$ mice via retro-orbital injection. Three hours later, tissues were harvested for flow cytometry.

For transfer of virally transduced B-1a cells: 100,000 Ctl-GFP+ or CXCR4-GFP+ B-1a cells from CD45.1 allotype ApoE$^{-/-}$ mice were intravenously injected into CD45.2 allotype Rag1$^{-/-}$ ApoE$^{-/-}$ host mice via retro-orbital injection. Host mice were maintained on chow diet for one week after transfer, then switched to Western diet (TD.88137) for 16 weeks. At the end of diet feeding, tissues were collected for analysis of donor CD45.1+GFP+ B-1a cell localization.

For long-term transfer of B-1a cells: 80,000 CXCR4^{WT} ApoE$^{-/-}$ or CXCR4^{BKO} ApoE$^{-/-}$ B-1a cells or an equivalent volume control PBS were intraperitoneally injected into Rag1$^{-/-}$ ApoE$^{-/-}$ mice. Host mice were maintained on chow diet for one week after transfer, then switched to Western diet (TD.88137) for 16 weeks.

Atherosclerosis analysis

Aortas were perfused with heparinated PBS then opened longitudinally from the aortic arch to the iliac bifurcation, fixed in 4% paraformaldehyde, pinned, and stained

using Sudan IV (Sigma) as previously described [6]. Aortas were imaged using a Nikon D70 DSLR camera and the percentage of the total aorta area that was Sudan IV+ plaque area was quantified using Image-Pro Plus software (Media Cybernetics).

Hearts were separated, cut, embedded in OCT compound (Tissue-Tek), and snap frozen in liquid nitrogen. Serial 7 micron sections from the first appearance of the three aortic leaflets to the aortic arch were collected using a Cryostat (Leica biosystems). 4 slides from each mouse containing sections spanning 21 to 550 microns away from the initiation of the root were stained with Oil Red O. Briefly, slides were fixed in 4% paraformaldehyde, rinsed with 60% isopropanol, stained with a 3mg/mL Oil Red O solution (Sigma, 00625), and counterstained with hematoxylin (Sigma, MHS-16). Tissue sections were imaged on an Olympus BX51 high-magnification microscope. Total lesion area or fraction of lesion area within the external elastic lamina was quantified using Image-Pro Plus software.

Immunofluorescence analysis of IgM and CD68 area within aortic root lesions

Four aortic root sections from each mouse were stained for analysis. Briefly, tissues sections underwent acetone fixation, rehydration with PBS, and incubation with a blocking buffer (10% donkey serum in PBS) to prevent non-specific antibody binding. Slides were stained in blocking buffer containing 1:100 goat anti-mouse IgM (Southern Biotech, 1021-01) or 1:200 rat anti-mouse CD68 (Biolegend, 137001) and the following secondary antibodies: donkey anti-goat Alexa Fluor 555 (Life Technologies, A21432) and donkey anti-rat Alexa Fluor 488 (Life Technologies, A21208). Slides were mounted using Vectashield hardset mounting medium containing DAPI. Tissue sections were imaged on an Olympus BX51 high-magnification microscope. The percentage of total lesion area that was IgM+ or CD68+was quantified using Image-Pro Plus software.

Collagen and necrotic area analysis within aortic root lesions

Four aortic root sections from each mouse were stained for analysis. Briefly, tissue sections were stained with Weigert's iron hematoxylin and Van Gieson solution containing 1% acid fuchsin in aqueous picric acid. Tissue sections were imaged on an Olympus BX51 high-magnification microscope. Dark pink collagen staining and acellular necrotic core area within lesions was quantified using Image-Pro Plus software.

Randomization, blinding, power calculation

To avoid differences arising from cage to cage variation in mouse experiments, each cage had at least one mouse from each experimental group, but otherwise, experimental groups were allocated randomly, and investigators were blinded to group allocation when performing all data collection. No power calculation was performed in mouse experiments, but the sample size of 5-10 is similar to what has been reported in previous publications.

Statistics

Statistics were performed as indicated using GraphPad Prism Version 7.0a (GraphPad Software, Inc). For comparison of data containing two groups, Mann-Whitney test was performed. Potential single outliers were tested in data sets using two-sided Dixon's outlier test and excluded if $p<0.05$. For comparing more than two groups of data, one-way ANOVA with Tukey's multiple comparisons test was used where data was normally distributed. For comparing more than two groups of non-parametric data, Kruskal-Wallis test was used. χ^2 analysis was performed using 2x4 and 2x2 comparisons as indicated. Results from all replicated experiments are displayed and bar

graphs display mean ± standard error of the mean. Correlations were determined using Pearson correlation coefficient (r-value) when both variables passed the D'Agostino and Pearson test for normality. Where one or both variables being correlated failed the D'Agostino and Pearson test for normality, Spearman correlation coefficients are reported. For correlation and in multivariate analysis, log transformation was applied to the MFI of CXCR4 on B1 cells to transform the highly skewed variable into an approximately normal variable. To exclude co-linearity between variables, a Spearman correlation matrix was generated using the PROC CORR procedure in SAS 9.4. Additional co-linearity diagnostics was performed by including tolerance and variance inflation terms in multivariate linear regression modeling using the PROC REG procedure in SAS 9.4. P-values were adjusted for multiple testing by using False Discovery Rate, determined in SAS 9.4.

Data availability

The datasets generated and analyzed in this study are available from the corresponding author upon reasonable request (C.A.M). The human data are not publicly available as they contain information that could compromise research participant privacy and consent.

Chapter 3

Diversification and CXCR4-dependent establishment of the bone marrow B-1a cell pool governs atheroprotective IgM production linked to human coronary atherosclerosis

As published in Upadhye A. et al. *Circulation Research*, 2019.
DOI 10.1161/CIRCRESAHA.119.315786

ABSTRACT

Rationale: B-1 cell-derived natural IgM antibodies against oxidation-specific epitopes (OSE) on low-density lipoprotein are anti-inflammatory and atheroprotective. Bone marrow (BM) B-1a cells contribute abundantly to IgM production, yet the unique repertoire of IgM antibodies generated by BM B-1a, and the factors maintaining the BM B-1a population remain unexplored. The chemokine receptor CXCR4 has been implicated in human CVD and B cell homeostasis, yet the role of B-1 cell CXCR4 in regulating atheroprotective IgM levels and human CVD is unknown.

Objective: To characterize the BM B-1a IgM repertoire and to determine whether CXCR4 regulates B-1 production of atheroprotective IgM in mice and humans.

Methods and Results: Single-cell sequencing demonstrated that BM B-1a cells from aged ApoE$^{-/-}$ mice with established atherosclerosis express a unique repertoire of IgM antibodies containing increased N-additions and a greater frequency of unique CDR-H3 sequences compared to peritoneal (PerC) B-1a cells. Some CDR-H3 sequences were common to both compartments suggesting B-1a migration between compartments. Indeed, mature PerC B-1a cells migrated to BM in a CXCR4-dependent manner. Furthermore, BM production of anti-OSE IgM and plasma IgM levels were reduced in ApoE$^{-/-}$ mice with B cell-specific knockout of CXCR4, and overexpression of CXCR4 on B-1a cells increased bone marrow localization and plasma anti-OSE IgM, including IgM against malondialdehyde (MDA)-modified LDL. Finally, in a 50-subject human cohort, we find that CXCR4 expression on circulating human B-1 cells positively associates with plasma levels of anti-MDA-LDL IgM antibodies and inversely associates with human coronary artery plaque burden and necrosis.

Conclusions: These data provide the first report of a unique BM B-1a cell IgM repertoire and identifies CXCR4 expression as a critical factor selectively governing BM B-1a localization and anti-OSE IgM production. That CXCR4 expression on human B-1 cells

was greater in humans with low coronary artery plaque burden suggests a potential targeted approach for immune modulation to limit atherosclerosis.

INTRODUCTION

A wealth of evidence in murine models demonstrates an atheroprotective role for B-1 cells, primarily through their ability to produce anti-inflammatory IgM antibodies against oxidation-specific epitopes (OSE), such as malondialdehyde (MDA)[7,14,37,38,54,55]. Studies in human cardiovascular disease (CVD) patients have demonstrated that increased amounts of circulating IgM antibodies specific for MDA-modified-LDL are associated with less coronary artery disease and fewer cardiovascular events[21,22], yet the factors regulating production of IgM to MDA-LDL in humans are unknown. A putative human equivalent of the murine B-1 cell was identified by Rothstein and colleagues as a CD20+CD27+CD43+ subset present in peripheral blood that demonstrated key functional hallmarks of murine B-1 cells, including spontaneous T cell-independent IgM production[158]. However, functional and phenotypic heterogeneity in the CD20+CD27+CD43+ B-1 subset suggests additional markers may further refine the phenotype of anti-OSE IgM producing human B-1 cells[162,165,167].

In mice, B-1 cells can be further divided into phenotypically distinct B-1a and B-1b subsets based on expression of the surface marker CD5, and both subsets secrete anti-OSE IgM and protect against atherosclerosis [37,38]. While peritoneal cavity (PerC) B-1 cells constitutively secrete a small amount of IgM, B-1 cells in the bone marrow (BM) and spleen secrete larger amounts of antibody per cell and significantly contribute to plasma IgM titers[78,82,83]. However, the factors that regulate B-1 cell number at sites of

high antibody production like the BM, both at steady-state and in the context of chronic inflammation, remain largely unexplored.

Further heterogeneity in the B-1 population occurs at the level of the B cell receptor, which consists of heavy and light chains containing variable regions that determine the specificity of IgM antibodies. The variable region of the immunoglobulin heavy chain (IgH V) is formed by combinatorial joining of germline V_H, D, and J_H family gene segments through a process called VDJ recombination, and additional heterogeneity is introduced through non-template-encoded N nucleotides (N-region additions) at the junctions between V-D and D-J gene segments. Antigen binding occurs at and is determined by hypervariable regions of IgH V called the complementarity determining regions (CDRs), the most variable of which is CDR-H3, which extends across both V-D and D-J junctions. Analyses of IgH V sequences to date demonstrate that PerC B-1a cells express a restricted VDJ repertoire containing a paucity of N-additions, consistent with their origins from primarily fetal liver precursors that lack expression of Tdt, the enzyme mediating N-additions[48,49,183]. However, the prevalence of N-additions increases in PerC and splenic B-1a cells with age, which may arise from the contribution of postnatally developed B-1a cells, from the contribution of B-1 cells from other compartments such as the BM, or from selective antigen-induced pressures that are specific to a particular microenvironmental niche[41,49,103,110]. While BM B-1a cells significantly contribute to IgM production, IgH V analysis of the mature BM B-1a cell population remains undefined. Moreover, given the potential for postnatal diversification and selection, defining the BM B-1a IgM repertoire in the context of atherosclerosis risk factors such as age and hyperlipidemia is of key importance.

Abundant IgM and specifically IgM to OSE are present in human and mouse atherosclerotic lesions [54,57], and administration or overexpression of anti-OSE IgM antibodies *in vivo* can inhibit oxidized LDL-induced activation of inflammatory pathways

and reduce lesion area [74,75]. However, targeted B-1 cell-specific strategies to increase IgM antibody production *in vivo* have been limited, likely due to an incomplete understanding of factors that regulate B-1 production of atheroprotective IgM in the setting of hyperlipidemia.

The chemokine receptor CXCR4 regulates cell trafficking and localization[120,130,184]. Genome-wide association studies have implicated CXCR4 and its ligand CXCL12 in human CVD [139,144,146,147], although results demonstrate conflicting effects, likely due to the broad expression of CXCR4 on a myriad of cell types with both pro- and anti-inflammatory functions. Prior studies have demonstrated that CXCR4 mediates IgM responses to acute immunization with the T-independent antigen NP-Ficoll[132], suggesting a role for CXCR4 on B-1 cells. Whether CXCR4 regulates B-1 cell production of anti-OSE IgM in the setting of hyperlipidemia, and the mechanisms underlying this regulation are unknown. Moreover, whether B-1 cell CXCR4 expression is linked to circulating anti-OSE IgM levels or CVD in humans has not been explored.

The present study provides novel characterization of the the BM B-1a IgH V repertoire in aged mice with hyperlipidemia and examines the factors maintaining B-1a number and IgM production within the BM. We demonstrate that the BM B-1a IgH V repertoire in aged ApoE$^{-/-}$ mice is distinct from the PerC B-1a repertoire, containing increased N-additions and greater frequency of unique CDR-H3 sequences. Using adoptive transfer studies, we find that the BM B-1a population is replenished by trafficking of mature B-1a cells from the periphery to the BM in a CXCR4-dependent manner. Furthermore, B cell-specific loss of CXCR4 decreases B-1a number and IgM production specifically within the BM, resulting in decreased plasma IgM. Conversely, B-1a cell-specific overexpression of CXCR4 *in vivo* associates with increased B-1a localization to the bone marrow and increased plasma anti-OSE IgM. Finally, in a 50-subject human cohort, CXCR4 expression on the circulating human

CD20+CD27+CD43+ B-1 subset significantly positively associates with the amount of plasma anti-MDA-LDL IgM, and inversely associates with plaque burden and necrotic area in human coronary arteries. Overall these data indicate that BM B-1a cells uniquely contribute to the IgM antibody repertoire, and that their maintenance is governed by CXCR4, a novel marker associating with protection in human CVD.

RESULTS

IgM of mature bone marrow B-1a cells is distinct from IgM of peritoneal B-1a cells in atherosclerotic mice

To characterize the immunoglobulin repertoire of the mature bone marrow B-1a cell population in the context of atherosclerosis, we utilized 100-week-old chow-fed ApoE$^{-/-}$ mice. B-1a cells from BM and PerC were single-cell sorted and the variable region of the immunoglobulin heavy chain was sequenced. BM B-1a cells displayed increased diversity at the V-D and D-J junctions, as evidenced by an increase in N-additions, with 32% of sequences containing ≥1 N-additions at both junctions, compared to 2% of PerC B-1a sequences ($P<0.0001$ by 2X4 χ^2 analysis, df=3; **Figure 4a**). Moreover, the average number of N-additions at the V-D and D-J junctions, as well as the average sum of N-additions at both junctions was significantly greater in BM B-1a cells (**Figure 4b**). Together, these data indicate increased diversity and a shift away from germline in the BM B-1a immunoglobulin heavy chain repertoire of aged ApoE$^{-/-}$ mice as compared to PerC B-1a cells.

Comparison of V_H, D, and J_H gene segment usage revealed marked differences between the BM and PerC B-1a repertoire, with increased V_H1, V_H2, V_H3, V_H5, V_H6, V_H10, V_H11, V_H14, D_H1-1, J_H2, J_H3, and J_H4 gene family usage in BM B-1a cells

compared to PerC B-1a (**Figure 4c**). In contrast, PerC B-1a cells showed increased usage of V_H12, D_H2, and J_H1 family genes.

Importantly, sequence comparison between PerC and BM B-1a cells revealed that a high frequency of PerC B-1a cells (92%) and to a lesser extent BM B-1a cells (65%) were replicate sequences present in more than one B-1a cell in these compartments. Notably, the sequence of the most common CDR-H3 in the BM, AGDYDGYWYFDV, was also the most common CDR-H3 sequence in the PerC (**Fig. 4d**) and other sequences were also common to both BM and PerC (**Table 5**), suggesting that B-1a migration between compartments could be occuring.

Intriguingly, AGDYDGYWYFDV accounted for 70% of total PerC B-1a sequences, while it only accounted for 11.6% of total BM B-1a sequences **(Fig. 4d)**, suggesting that selection pressure driving the presence or survival of B-1a cells expressing AGDYDGYWYFDV is stronger in the PerC than the BM in aged $ApoE^{-/-}$ mice. Additionally, the presence of more unique CDR-H3 sequences in the BM also suggests that the BM B-1a microenvironment is more permissive for IgH V diversification.

Figure 4. The bone marrow B-1a cell IgH V repertoire is distinct from the peritoneal B-1a cell IgH V repertoire. (a) Percentage of total sequences with 0 N-additions at both V-D and D-J junctions (lower left), 1 or more N-additions at both junctions (upper right), or one or more N-addition at either the V-D or D-J junction (upper left or lower right) in the variable region of the immunoglobulin heavy chain of sorted bone marrow or perC B-1a cells. **(b)** Average number of N-additions at either the V-D junction, the D-J junction, or the average sum of N-additions at both junctions in sorted bone marrow and peritoneal cavity B-1a cells. $P<0.0001$ by Mann-Whitney test. **(c)** Frequency of total sequences utilizing the given V_H, D, and J_H gene segments in the variable region of the immunoglobulin heavy chain from single cell-sorted B-1a cells from peritoneal cavity (black bars) or bone marrow (checkered bars) of 100-week-old chow-fed $ApoE^{-/-}$ mice. ****$P<0.0001$, **$P<0.01$, or *$P<0.05$ by 2x2 χ^2 analysis, df=1. **(d)** VDJ usage, CDR-H3 amino acid sequence, and number and frequency of replicates for the top three most frequent replicate sequences found in sorted PerC or BM B-1a cells.

Figure 4

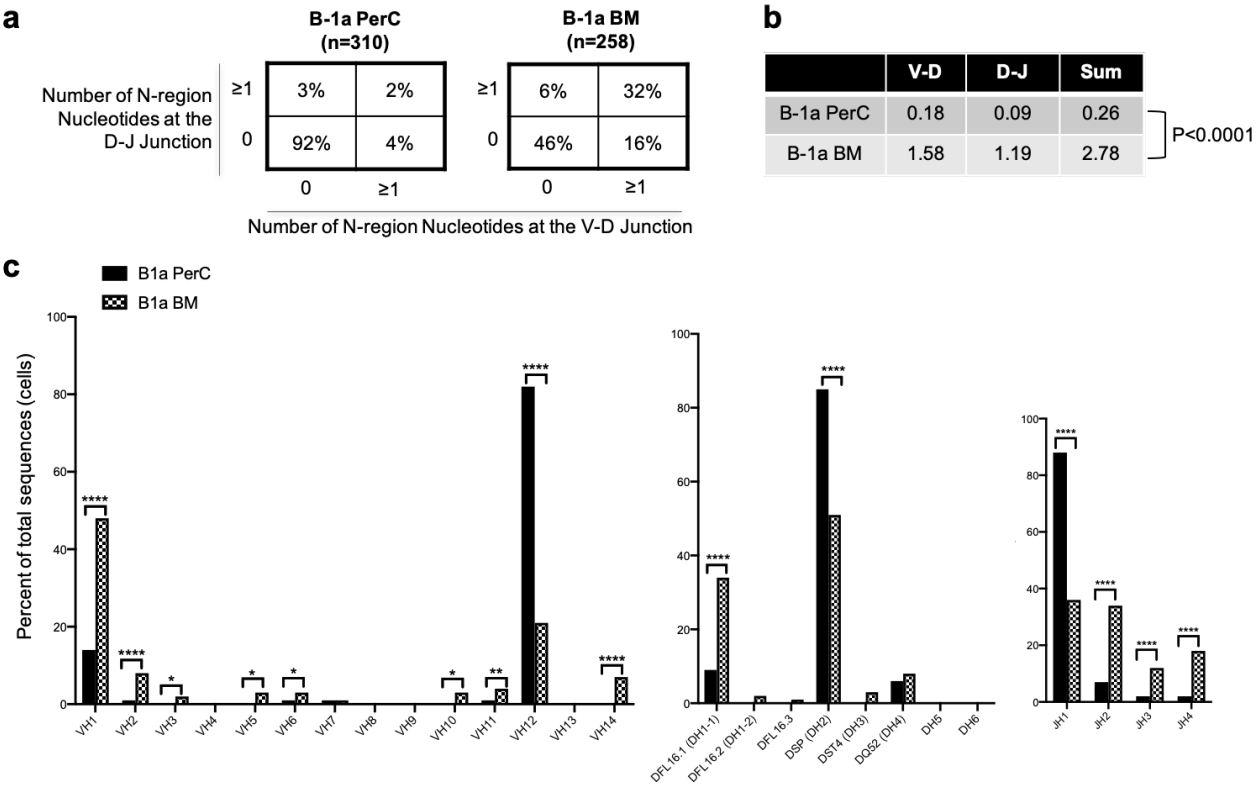

d

Sample	V-D-J	CDR-H3	Number of CDR-H3 specific replicates (%)
PerC B-1a (n=310 total sequences)	VH12 - DH2 - JH1	AGDYDGYWYFDV	218 (70.0%)
	VH12 - DH4 - JH1	AGDRWGYWYFDV	13 (4.2%)
	VH1 - DH1-1 - JH2	ARSYYYGSSYYFDY	13 (4.2%)
BM B-1a (n=258 total sequences)	VH12 - DH2 - JH1	AGDYDGYWYFDV	30 (11.6%)
	VH1 - DH2 - JH2	AREVTTMYYFDY	26 (10.1%)
	VH1 - DH1-1 - JH2	ARSYYYGSSYYFDY	21 (8.1%)

Table 5. Replicate CDR-H3 amino acid sequences (those present more than once) and frequency present in single cell-sorted BM and PerC B-1a cells

BM B-1a (n=258 total sequences)			PerC B-1a (n=310 total sequences)		
CDR-H3 Sequence	**# of CDR-H3 replicates**	**% of total sequences**	**CDR-H3 Sequence**	**# of CDR-H3 replicates**	**% of total sequences**
AGDYDGYWYFDV	30	11.6	AGDYDGYWYFDV	217	70.0
AREVTTMYYFDY	26	10.1	AGDRWGYWYFDV	13	4.2
ARSYYYGSSYYFDY	21	8.1	ARSYYYGSSYYFDY	13	4.2
AREDYYGSSYYFDY	8	3.1	ARYYGNYWYFDV	6	1.9
AGDRTGYWYFDV	6	2.3	AGDLLGYWYFDV	5	1.6
AIYYGNYWYFDV	5	1.9	ARDYYWYFDV	4	1.3
ATYYSNYWYFDV	5	1.9	AGDSDGYWYFDV	4	1.3
TTYYYGSAWFAY	5	1.6	AGDYYGYWYFDV	3	1.0
AKRDYYSNYFGLGYYYAMDY	5	1.6	ASYYGNYWYFDV	2	0.6
ATGSSFDY	4	1.6	ATYYSNYWYFDV	2	0.6
ASYYGNYWYFDV	4	1.6	AREGDYYYGSSYWFAY	2	0.6
MRYSNYWYFDV	4	1.6	MRYSNYWYFDV	2	0.6
AKNDYGIYYYAMDY	4	1.6	AGDTTGYWYFDV	2	0.6
ARSNYYAMDY	3	1.2	AGDRTGYWYFDV	2	0.6
MRYGDYWYFDV	3	1.2	AGDPYDGYYGFAY	2	0.6
AGDADGYWYFDV	3	1.2	AGDRDGYWYFDV	2	0.6
AGDYYGYWYFDV	3	1.2	AKLR*XLL*L	2	0.6
TPHYYGSSWFAY	3	1.2	ARYYYGSSYAMDY	2	0.6
ARNGGLWSYYAMDY	3	1.2			
ARMGNYGSRYFDV	2	0.8			
AREQLRLYYFDY	2	0.8			
ARRYYYGSSYAMDY	2	0.8			
ANWAY	2	0.8			
ARSSNYAMDY	2	0.8			
ARDYYWYFDV	2	0.8			
MRYGYDWYFDV	2	0.8			
AGDRWGYWYFDV	2	0.8			
AGYAWFAY	2	0.8			
TYYGNYENYTVDY	2	0.8			
AKNNYYGGYFDV	2	0.8			
TRPSTVHFDY	2	0.8			

Mature PerC-derived B-1a cells migrate to the bone marrow and the bone marrow B-1 population does not rely on the spleen

To examine the factors that maintain BM B-1 cells, we first determined whether the BM B-1 population can be replenished by B-1 cells from the circulation. Short-term intravenous transfer of CD45.2 ApoE$^{-/-}$ PerC B-1 cells into CD45.1 ApoE$^{-/-}$ hosts revealed that a small fraction of the total B-1 population in PerC and spleen were emigrated CD45.2^{+} donor cells, as expected in immunocompetent hosts with an endogenous B cell compartment (**Fig. 5**). Importantly, CD45.2+ B-1 cells were also present in the bone marrow, indicating that mature PerC B-1 cells can migrate from the periphery to the BM (**Fig. 5**).

The adult PerC B-1 cell population has previously been shown to depend upon the spleen[37,107]. To determine whether the adult BM B-1 cell population relies upon splenic migrants, we performed sham or splenectomy surgery on ApoE$^{-/-}$ mice and quantified BM B-1 cell populations after 4 weeks of Western diet feeding (**Fig. 6a**). Bone marrow B-1a and B-1b cell numbers were not altered by absence of the spleen, suggesting that B-1a migrants to the BM may come from locations other than the spleen (**Fig. 6b**).

Figure 5. Mature peritoneal B-1 cells migrate to the bone marrow.

(a) Experimental schematic for short-term 4-day adoptive transfer. (**b**) Calculated frequency of CD45.2^{+} donor B-1 cells recovered from peritoneal cavity (PerC), bone marrow, or spleen of CD45.1 ApoE$^{-/-}$ mice receiving control PBS (n=1) or 1x10^{6} CD45.2^{+} CD19^{+} CD23^{-} peritoneal cavity B-1 cells (n=4).

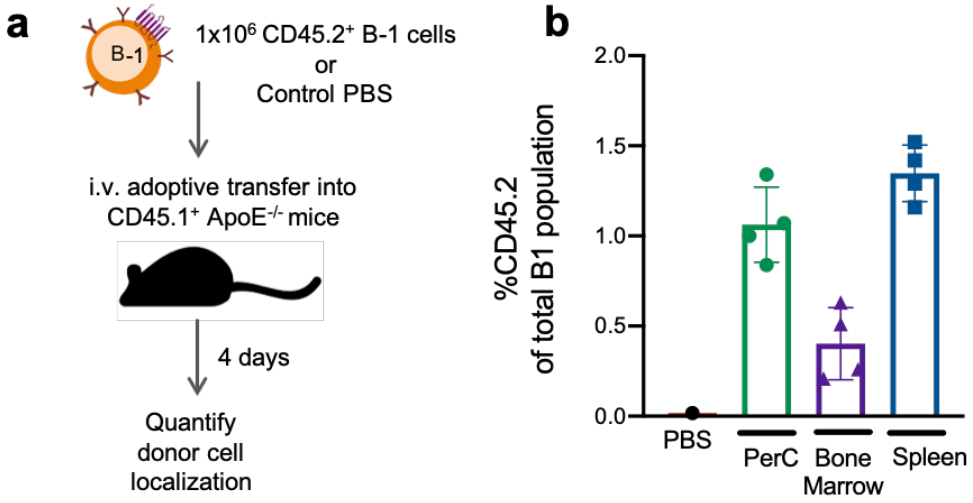

Figure 6. The adult bone marrow B-1 population does not rely on the spleen. (a) Experimental schematic for splenectomy. (**b**) Calculated number of $CD19^{+}$ $B220^{mid\text{-}lo}$ IgM^{+} $CD23^{-}$ $CD43^{+}$ $CD5^{+ \text{ or } -}$ B-1a or B-1b cells recovered from bone marrow of $ApoE^{-/-}$ mice receiving splenectomy (n=6) or sham surgery (n=5). N.s. indicates non-significant p-value by Mann-Whitney test.

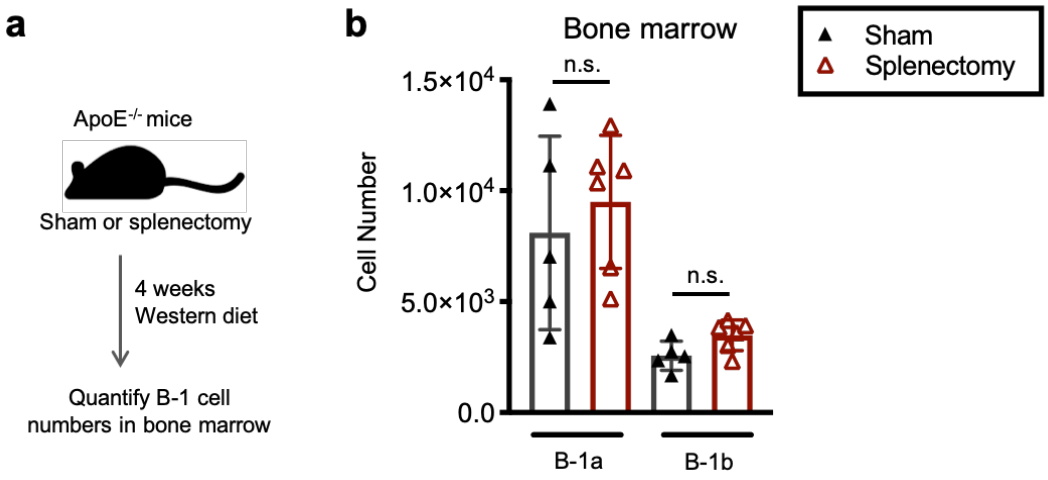

CXCR4 facilitates mature B-1a migration to the bone marrow

CXCR4 has a well-established role in mediating progenitor cell retention in the BM[130], yet whether CXCR4 is needed for mature B-1a cell homing to BM is unknown. To examine the role of B cell CXCR4 on B-1a cell BM migration, we developed a B cell-specific CXCR4 knockout mouse model on the atherosclerosis-prone $ApoE^{-/-}$ background. This is a Cre-Lox model in which Cre recombinase is under control of the CD19 promoter, thereby deleting floxed CXCR4 alleles in all B cells (B-1 and B-2). $ApoE^{-/-}$ mice lacking CXCR4 in B cells ($CXCR4^{BKO}ApoE^{-/-}$) display efficient knockdown of CXCR4 mRNA and protein expression in B cells, and a defect in migratory capacity towards its ligand CXCL12 relative to littermate control mice that retain expression of CXCR4 ($CXCR4^{WT}$ $ApoE^{-/-}$) (**Figure 7**).

Adoptive transfer of PerC B-1 cells from $CXCR4^{WT}$ $ApoE^{-/-}$ or $CXCR4^{BKO}ApoE^{-/-}$ mice into T- and B cell-deficient $Rag1^{-/-}$ $ApoE^{-/-}$ hosts (**Fig. 8a**) revealed that B-1a cells migrated to both the BM and spleen, however only BM homing was CXCR4-dependent (**Fig. 8b-d**). To examine why CXCR4 might preferentially facilitate B-1a migration to the BM, and how that is altered in an inflammatory state, we compared mRNA expression of the CXCR4 ligands, CXCL12 and MIF, as well as another important B cell chemokine, CXCL13, in spleen and BM of C57BL/6J and $ApoE^{-/-}$ mice. Results demonstrate greater expression of CXCL12 in BM of C57BL/6J and $ApoE^{-/-}$ mice compared to spleen, and increased CXCL12 expression in $ApoE^{-/-}$ BM compared to C57BL/6J BM (**Fig. 8e**). MIF expression was not significantly different between BM and spleen, but was increased in $ApoE^{-/-}$ mice compared to C57BL/6J (**Fig. 8f**). CXCL13 expression was significantly higher in spleen than BM, and was not significantly different between $ApoE^{-/-}$ and C57BL/6J mice (**Fig. 8g**). These results provide evidence for differential chemokine expression in spleen and BM at baseline and in hyperlipidemic states, providing a likely

mechanism for CXCR4-dependent B-1a migration preferentially to the BM over the spleen.

Figure 7. Generation of a B cell specific knockout of CXCR4 on an atherogenic ApoE$^{-/-}$ background. (**a**) Quantification of CXCR4 mRNA expression in CD19+ splenocytes isolated from CXCR4^{WT} ApoE$^{-/-}$ (n=3) or CXCR4^{BKO} ApoE$^{-/-}$ (n=4) mice. *P<0.05 by two-tailed t-test. (**b**) Surface CXCR4 expression on CD19+ B cells or CD3+ T cells in peripheral blood from CXCR4^{WT} ApoE$^{-/-}$ (solid black histogram) or CXCR4^{BKO} ApoE$^{-/-}$ mice (dashed line histogram). Shaded histograms indicate FMO-CXCR4 control. (**c**) Representative flow plots of the frequency of CXCR4^{WT} ApoE$^{-/-}$ (top) or CXCR4^{BKO} ApoE$^{-/-}$ (bottom) CD19+ cells migrating spontaneously (left) or towards CXCL12 . (**d**) Frequency of B cells isolated from CXCR4^{WT} ApoE$^{-/-}$ (n=3) or CXCR4^{BKO} ApoE$^{-/-}$ (n=2) mice that migrated towards CXCL12 as a percentage of the total number of B cells loaded in transwell. Error bars represent mean ± s.e.m.

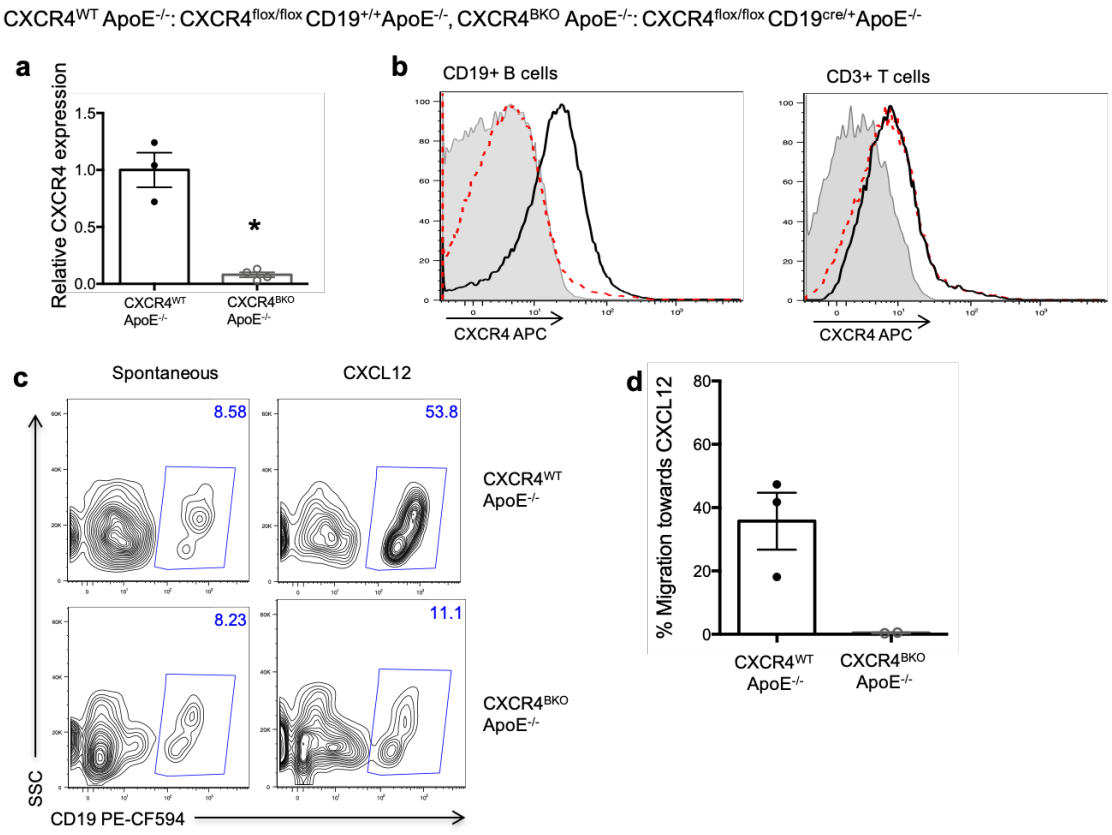

Figure 8. B-1a cells traffic to the bone marrow in a CXCR4-dependent manner. (**a**) Experimental schematic for short-term adoptive transfer. (**b**) Representative gating strategy from one bone marrow sample per transfer condition for quantification of adoptively transferred B-1 cells in $Rag1^{-/-}ApoE^{-/-}$ mice receiving control PBS (n=1) or $7.5x10^5$ $CD19^+$ $B220^{lo}$ IgM^+ $CD23^-$ peritoneal cavity B-1 cells from $CXCR4^{WT}$ $ApoE^{-/-}$ (n=3) or $CXCR4^{BKO}$ $ApoE^{-/-}$ (n=3) donor mice. Quantification of the number of donor B-1a cells ($CD19^+IgM^+CD23^-CD5^+$) recovered in bone marrow (**c**) and spleen (**d**) of $Rag1^{-/-}$ $ApoE^{-/-}$ recipient mice 3 hours post-intravenous transfer. *P<0.05 or n.s. indicates non-significant p-value by Kruskal-Wallis test. Quantification of CXCL12 (**e**), MIF (**f**), and CXCL13 (**g**) mRNA expression normalized to 18s ribosomal RNA expression in total bone marrow and spleen single cell suspensions isolated from C57BL/6 mice (n=5) or $ApoE^{-/-}$ mice (n=5) ***P<0.001, **P<0.01, *P<0.05 or n.s. indicates non-significant p-value by one-way ANOVA with Tukey's multiple comparisons test. Error bars represent mean ± s.e.m.

Figure 8.

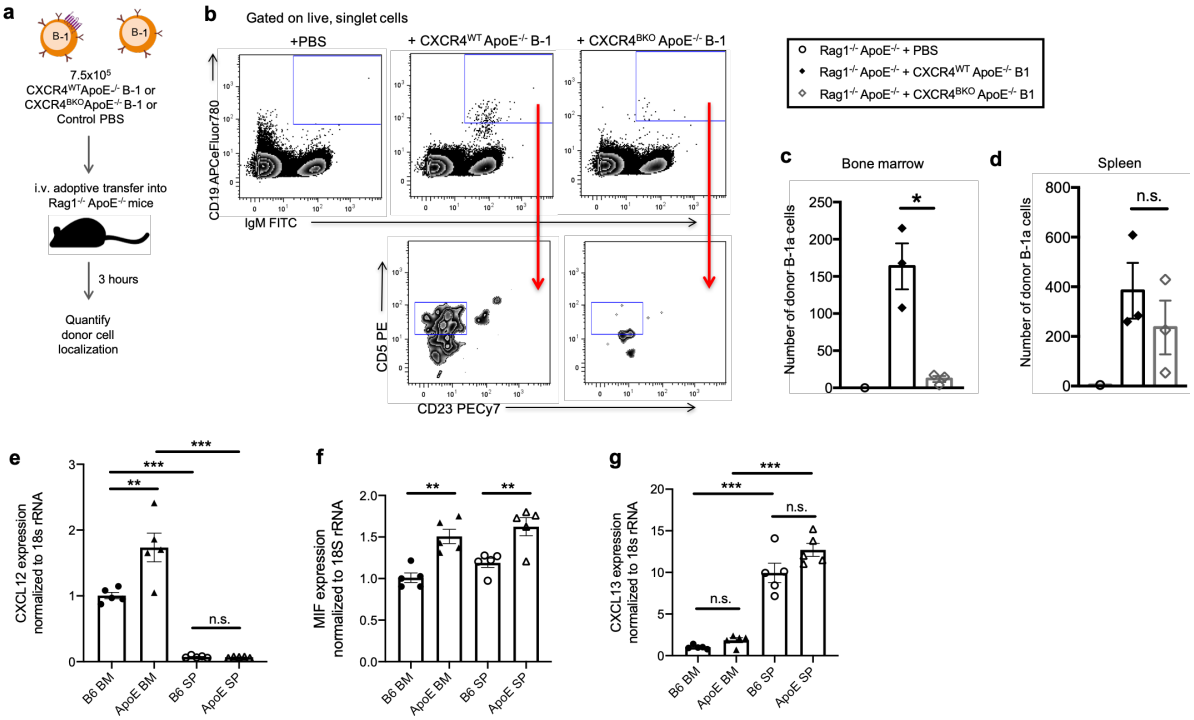
a
B-1
B-1
7.5x10^5
CXCR4^WT ApoE^-/- B-1 or
CXCR4^BKO ApoE^-/- B-1 or
Control PBS
i.v. adoptive transfer into
Rag1^-/- ApoE^-/- mice
3 hours
Quantify
donor cell
localization
b
Gated on live, singlet cells
+PBS
+ CXCR4^WT ApoE^-/- B-1
+ CXCR4^BKO ApoE^-/- B-1
CD19 APCeFluor780
IgM FITC
CD5 PE
CD23 PECy7
Rag1^-/- ApoE^-/- + PBS
Rag1^-/- ApoE^-/- + CXCR4^WT ApoE^-/- B1
Rag1^-/- ApoE^-/- + CXCR4^BKO ApoE^-/- B1
c
Bone marrow
Number of donor B-1a cells
*
d
Spleen
Number of donor B-1a cells
n.s.
e
CXCL12 expression
normalized to 18s rRNA
***
**
n.s.
B6 BM
ApoE BM
B6 SP
ApoE SP
f
MIF expression
normalized to 18S rRNA
**
**
B6 BM
ApoE BM
B6 SP
ApoE SP
g
CXCL13 expression
normalized to 18s rRNA
***
***
n.s.
n.s.
B6 BM
ApoE BM
B6 SP
ApoE SP

CXCR4 is critical for maintaining bone marrow B-1a cell number, bone marrow IgM ASC, and circulating IgM levels

To determine if B cell-specific loss of CXCR4 impacts the endogenous BM B-1a population, we quantified BM B-1 cells in $CXCR4^{BKO}ApoE^{-/-}$ mice by flow cytometry. We identified B-1 cells as live $CD19^{+}$ IgM^{+} $B220^{mid\text{-}lo}$ $CD23^{-}$ $CD43^{+}$ cells in the bone marrow and further classified into B-1a and B-1b subsets based on expression of CD5 (**Fig. 9a**). $CXCR4^{BKO}ApoE^{-/-}$mice harbor a significant reduction in total B-1 cells in the bone marrow and blood, but not spleen or peritoneal cavity (**Fig. 9b)**. Importantly, the reduction in B-1 number in the bone marrow was attributable to a loss specifically in the B-1a subset, while B-1b numbers were equal between genotypes (**Fig. 9c,d**). Loss of CXCR4 additionally reduced the number of $CD19^{+}B220^{hi}CD23^{+}CD43^{-}$ B-2 cells in the bone marrow, but did not impact B-2 cell numbers in blood, spleen, or perC (**Fig. 10a**). There were no significant differences in other immune cell types, including $CD3^{+}$ T cells, $CD115^{+}$ monocytes, and $Ly6G^{+}$ neutrophils in the spleen, bone marrow, and blood between $CXCR4^{WT}$ $ApoE^{-/-}$ and $CXCR4^{BKO}ApoE^{-/-}$ mice (**Fig. 11**).

Consistent with fewer BM B-1a cells, total circulating IgM in $CXCR4^{BKO}ApoE^{-/-}$ mice was significantly reduced compared to $CXCR4^{WT}$ $ApoE^{-/-}$ littermate controls (**Fig. 9e**). Sort-purified B-1a and B-1b cells from $CXCR4^{WT}$ $ApoE^{-/-}$ and $CXCR4^{BKO}ApoE^{-/-}$ mice secreted equivalent amounts of IgM after stimulation with LPS, a TLR4 agonist which induces B-1 cell IgM production (**Fig. 9f**), indicating that loss of CXCR4 does not reduce the ability of B-1 cells to produce and secrete IgM. Instead, B cell-specific loss of CXCR4 resulted in reduced numbers of IgM antibody-secreting cells (ASC) and MDA-LDL-specific IgM ASC in the bone marrow but not in the spleen (**Fig. 9g-k**). Titers of IgG1, IgG2b, IgG2c, and IgG3 were not significantly different between $CXCR4^{WT}$ $ApoE^{-/-}$ and $CXCR4^{BKO}ApoE^{-/-}$ mice (**Fig. 10b-e**). Taken together, these data provide evidence that

CXCR4 regulates plasma IgM titers by maintaining the number of IgM antibody-secreting B-1a cells specifically within the bone marrow.

Figure 9. CXCR4 is critical for maintaining bone marrow B-1a cell number, bone marrow IgM ASC, and circulating IgM levels in ApoE$^{-/-}$ mice. (**a**) Representative gating strategy for quantification of bone marrow B-1 cells by flow cytometry. (**b**) Quantification of B-1 cells from the bone marrow, blood, spleen, and peritoneal cavity of 8-week-old CXCR4^{WT} ApoE$^{-/-}$ (n=6) or CXCR4^{BKO} ApoE$^{-/-}$ (n=8) mice using flow cytometry. (**c**) Quantification of B-1a and B-1b cell number in bone marrow of CXCR4^{WT} ApoE$^{-/-}$ (n=6) and CXCR4^{BKO} ApoE$^{-/-}$ (n=8) mice. (**d**) Representative flow plots of B-1a and B-1b gating from bone marrow of CXCR4^{WT} ApoE$^{-/-}$ or CXCR4^{BKO} ApoE$^{-/-}$ mice. (**e**) Calculated concentration of total IgM in sera of 8-week-old CXCR4^{WT} ApoE$^{-/-}$ (n=10) or CXCR4^{BKO} ApoE$^{-/-}$ (n=10) mice. (**f**) Fold change in concentration of IgM in supernatants of cultured peritoneal B-1a or B-1b cells from CXCR4^{WT} ApoE$^{-/-}$ (n=5) or CXCR4^{BKO} ApoE$^{-/-}$ (n=6) mice in response to 50 μg/mL LPS over the amount secreted in response to control PBS. (**g**) Representative ELISPOT wells depicting IgM antibody-secreting cells (ASC) from bone marrow and spleen of 8-week-old CXCR4^{WT} ApoE$^{-/-}$ or CXCR4^{BKO} ApoE$^{-/-}$ mice. Calculated numbers of IgM ASC in bone marrow (**h**) and spleen (**i**) of 8-week-old CXCR4^{WT} ApoE$^{-/-}$ (n=6) or CXCR4^{BKO} ApoE$^{-/-}$ (n=6) mice. Calculated numbers of anti-MDA-LDL IgM ASC in bone marrow (**j**) and spleen (**k**) of 8-week-old CXCR4^{WT} ApoE$^{-/-}$ (n=6) or CXCR4^{BKO} ApoE$^{-/-}$ (n=6) mice. Error bars represent mean ± s.e.m. *P<0.05, **P<0.01, ***P<0.001, or n.s. indicating non-significant p-value by Mann-Whitney test.

Figure 9.

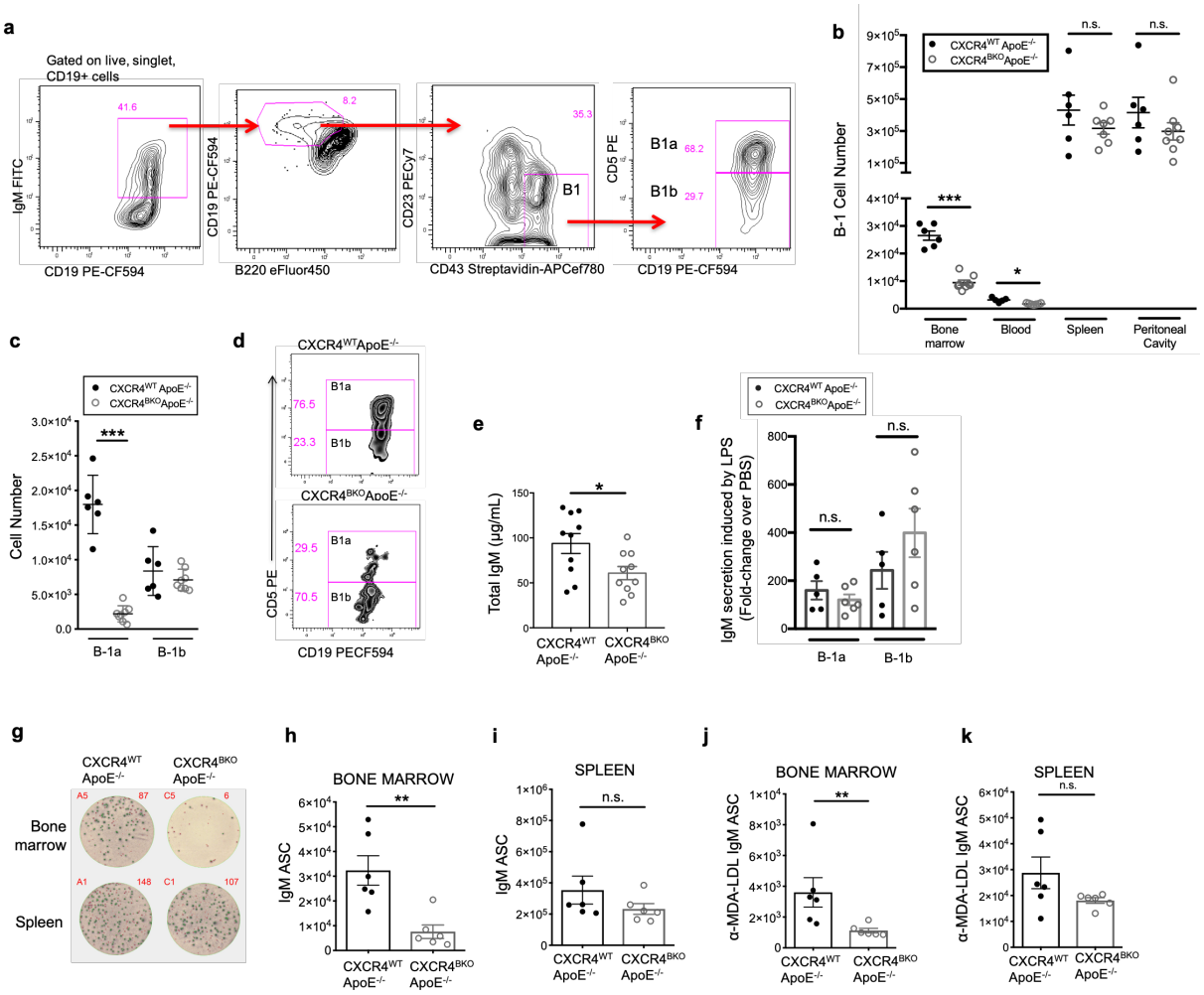
a
Gated on live, singlet, CD19+ cells
IgM FITC
CD19 PE-CF594
B220 eFluor450
CD23 PECy7
CD43 Streptavidin-APCef780
CD5 PE
B1a
B1b
B1
b
B-1 Cell Number
CXCR4WT ApoE-/-
CXCR4BKO ApoE-/-
Bone marrow
Blood
Spleen
Peritoneal Cavity
n.s.
c
Cell Number
B-1a
B-1b
d
CD19 PECF594
e
Total IgM (μg/mL)
f
IgM secretion induced by LPS (Fold-change over PBS)
g
Bone marrow
Spleen
h
BONE MARROW
IgM ASC
i
SPLEEN
j
α-MDA-LDL IgM ASC
k

Figure 10. B cell-specific loss of CXCR4 reduces mature B-2 number in the BM but does not significantly impair production of IgG antibodies in young ApoE$^{-/-}$ mice. **(a)** Quantification of CD19^{+}B220^{hi}CD23^{+} B-2 cells from bone marrow, blood, spleen, and peritoneal cavity of 8-week-old CXCR4^{WT} ApoE$^{-/-}$ (n=6) or CXCR4^{BKO} ApoE$^{-/-}$ (n=8) mice. Relative titers of **(b)** IgG1, **(c)** IgG2b, **(d)** IgG2c, and **(e)** IgG3 in sera of 8-week-old CXCR4^{WT} ApoE$^{-/-}$ (n=10) or CXCR4^{BKO} ApoE$^{-/-}$ (n=10) mice. 4 samples excluded in IgG1 dataset due to duplicate measurements having CV>30%. ***P<0.001 or n.s. indicates non-significant p-value using Mann-Whitney test.

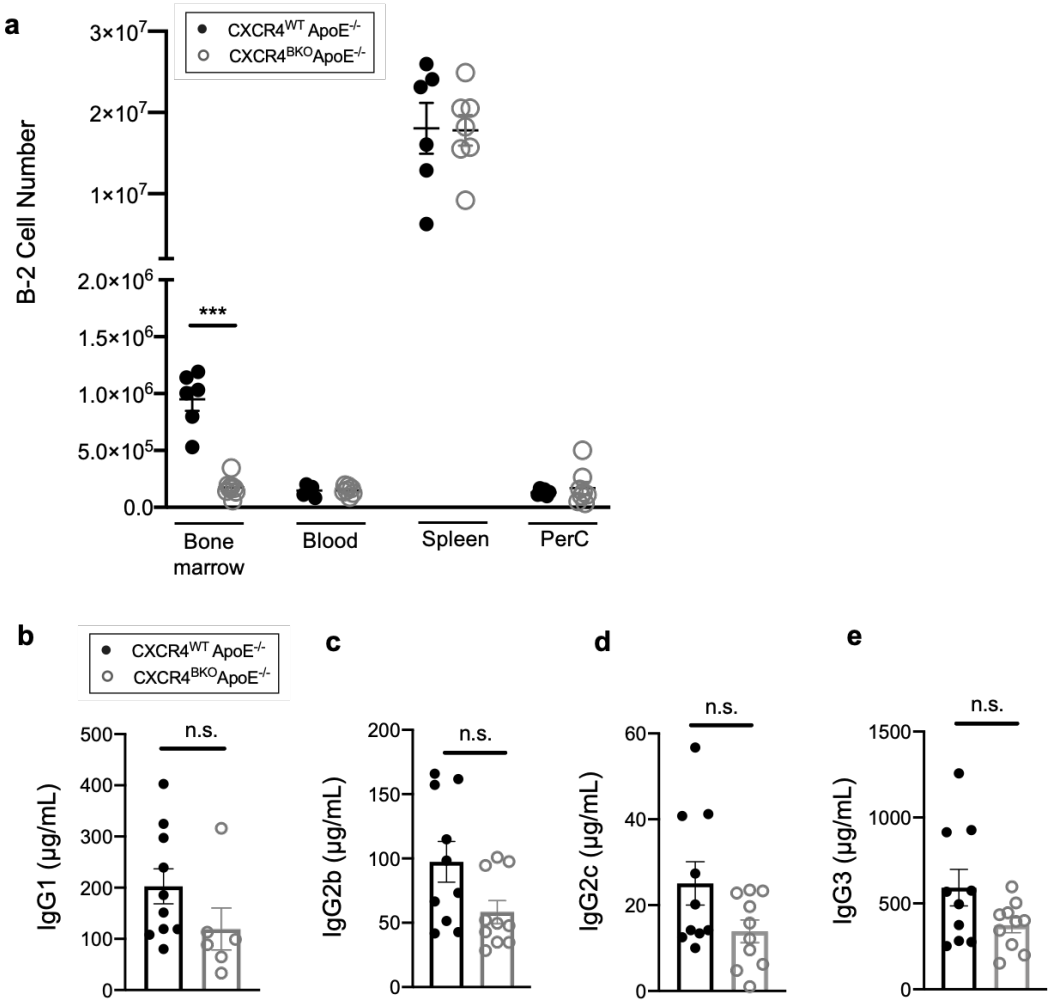

Figure 11. B cell-specific loss of CXCR4 does not significantly impact numbers of other immune cell types in the spleen, bone marrow, or blood. Calculated numbers of CD3+ T cells, CD115+ monocytes, and Ly6G+ neutrophils in spleen (**a**), bone marrow (**b**), or circulating blood (**c**) of 8-week-old CXCR4^{WT} ApoE$^{-/-}$ (n=5) or CXCR4^{BKO} ApoE$^{-/-}$ (n=5) mice. Error bars represent mean ± s.e.m.

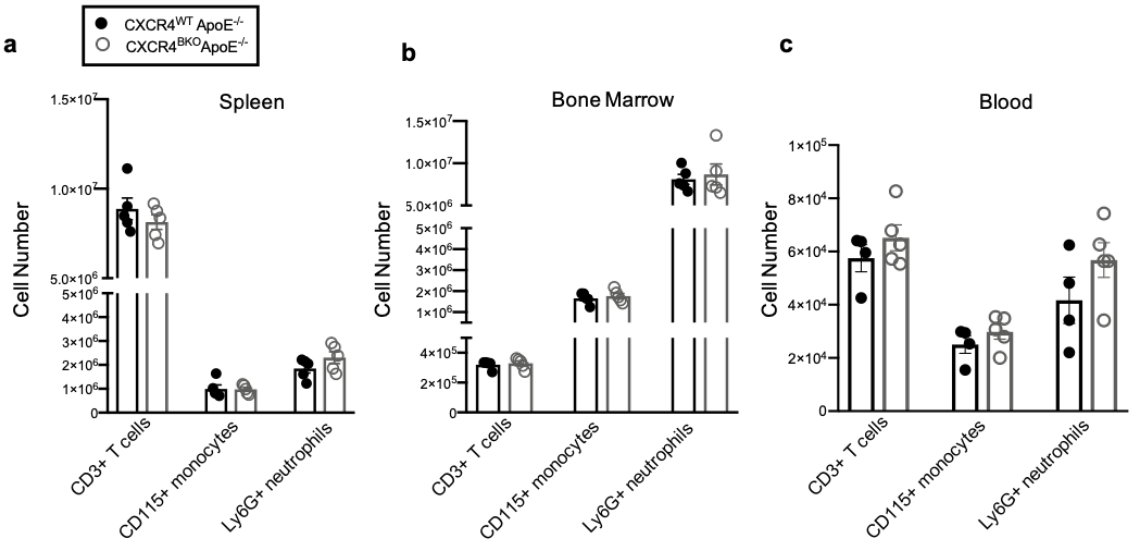

CXCR4 overexpression associates with increased B-1a localization to the bone marrow and increased plasma anti-OSE IgM levels

To determine if increasing CXCR4 expression in wild-type B-1a cells could increase localization to the bone marrow and boost IgM production, CXCR4 was overexpressed in B-1a cells using a retroviral approach. The generated CXCR4-GFP retrovirus was able to effectively increase B-1 cell surface CXCR4 expression and functional migration towards CXCL12 compared to a control (Ctl-GFP) retrovirus (**Fig. 12a-c**), without affecting B cell viability (**Fig. 12d-e**). $Rag1^{-/-}ApoE^{-/-}$ recipient mice were adoptively transferred with Ctl-GFP+ B-1a cells, CXCR4-GFP+ B-1a cells, or control PBS and fed Western diet for 16 weeks (**Fig. 13a**). Donor B-1a cells recovered in the bone marrow and spleen of recipients given CXCR4-GFP+ B-1a cells maintained increased CXCR4 expression after 16 weeks (**Fig. 13b,c**). However, the degree of CXCR4 overexpression varied between mice. Therefore, correlative analysis of the full experimental cohort was performed to determine the effect of CXCR4 overexpression on donor B-1a cell localization. A positive association was identified with the MFI of CXCR4 on donor B-1a cells and the number of donor B-1a cells in the bone marrow but not spleen (**Fig. 13d**). These data provide further evidence that CXCR4 expression preferentially mediates B-1a migration to the bone marrow. Furthermore, the number of donor B-1a cells in the bone marrow positively associated with circulating levels of IgM against MDA-LDL and a trend towards increased IgM against phosphocholine (plasma E06/T15 IgM), but not with IgM against α-1,3-Dextran, a classic T-independent bacterial surface antigen used as a non-OSE type antigen control (**Fig. 13e**).

Figure 12. Retroviral-mediated overexpression of CXCR4 on CXCR4^{BKO} ApoE$^{-/-}$ B cells. Peritoneal B cells from CXCR4^{BKO}ApoE$^{-/-}$ mice were isolated and transduced with Ctl-GFP or CXCR4-GFP retrovirus, or cultured without transduction. (**a**) Representative flow plots of CXCR4 and GFP expression on B-1 cells from non-transduced (upper left), Ctl-GFP transduced (lower left), or CXCR4-GFP transduced (lower right) conditions. FMO-CXCR4 (upper right) used to set CXCR4 positive gate. (**b**) Quantification of the MFI of CXCR4 on GFP+ B-1 cells from non-transduced (n=1), Ctl-GFP transduced (n=2), or CXCR4-GFP transduced (n=2) conditions. *P<0.05 by one-way ANOVA with Tukey's multiple comparisons test. (**c**) Frequency of non-transduced (n=1), Ctl-GFP transduced (n=2), or CXCR4-GFP transduced (n=2) B-1 cells that migrated towards CXCL12 as a percentage of the total number of B-1 cells loaded in transwell. (**d**) Representative gating strategy for quantification of viable cells within the successfully transduced B cell population (CD19+GFP+). (**e**) Frequency of live B cells after transduction with Ctl-GFP (n=2) or CXCR4-GFP retrovirus (n=2). Error bars represent mean ± s.e.m.

Figure 12.

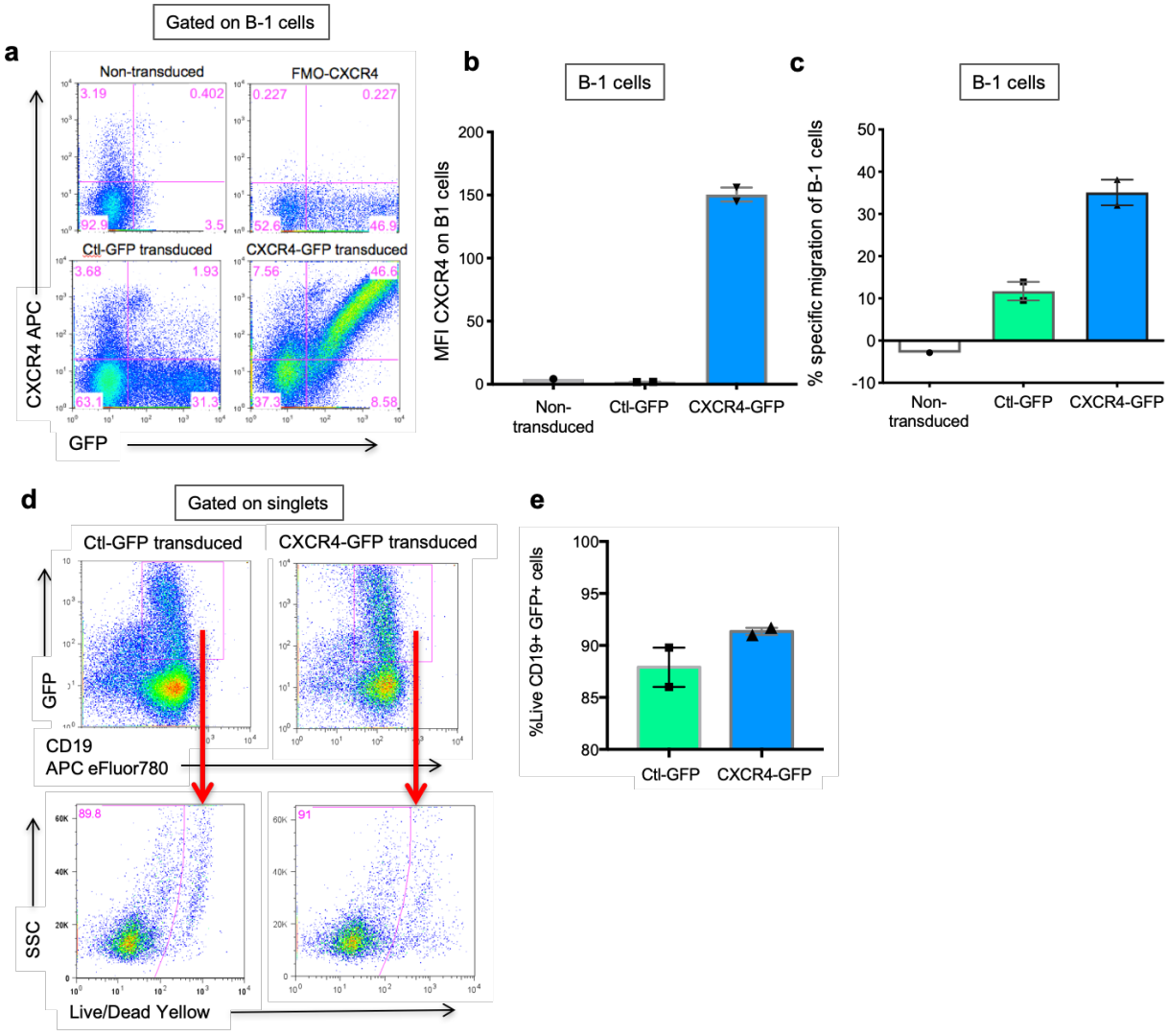
a
Gated on B-1 cells
Non-transduced
FMO-CXCR4
Ctl-GFP transduced
CXCR4-GFP transduced
3.19
0.402
92.9
3.5
0.227
0.227
52.6
46.9
3.68
1.93
63.1
31.3
7.56
46.6
37.3
8.58
CXCR4 APC
GFP
b
B-1 cells
MFI CXCR4 on B1 cells
200
150
100
50
0
Non-transduced
Ctl-GFP
CXCR4-GFP
c
B-1 cells
% specific migration of B-1 cells
50
40
30
20
10
0
-10
Non-transduced
Ctl-GFP
CXCR4-GFP
d
Gated on singlets
Ctl-GFP transduced
CXCR4-GFP transduced
GFP
CD19
APC eFluor780
89.8
91
60K
40K
20K
SSC
Live/Dead Yellow
e
%Live CD19+ GFP+ cells
100
95
90
85
80
Ctl-GFP
CXCR4-GFP

Figure 13. Overexpression of CXCR4 in murine B-1a cells associates with increased B-1a cell localization to the bone marrow and increased plasma anti-OSE IgM levels. (**a**) Experimental setup: Peritoneal B cells from CXCR4 wild-type CD45.1 allotype ApoE$^{-/-}$ mice were transduced with CXCR4-GFP or Ctl-GFP retrovirus and 1x10^{5} successfully transduced B-1a cells were intravenously transferred into Rag1$^{-/-}$ ApoE$^{-/-}$ hosts, which were fed 16 weeks of Western diet. Quantification of the mean fluorescence intensity (MFI) of CXCR4 on recovered CD45.1^{+}GFP^{+} donor B-1a cells in bone marrow **(b)** or spleen **(c)** of Rag1$^{-/-}$ApoE$^{-/-}$ mice receiving CXCR4-GFP+ B-1a cells (n=5) or Ctl-GFP+ B-1a cells (n=6) after 16 weeks Western diet feeding. *P<0.05 or **P<0.01 by Mann-Whitney test. (**d**) The MFI of CXCR4 on donor B-1a cells correlated with the number of donor B-1a cells in bone marrow or spleen of Rag1$^{-/-}$ApoE$^{-/-}$recipient mice after 16 weeks Western diet feeding. N=11 mice. (**e**) The number of donor B-1a cells in bone marrow correlated with circulating levels of anti-MDA-LDL IgM, E06/T15 IgM specific for phosphocholine, or anti-1,3-Dextran IgM after 16 weeks Western diet feeding. Data presented as correlation coefficient (r) and statistical significance (p).

Figure 13.

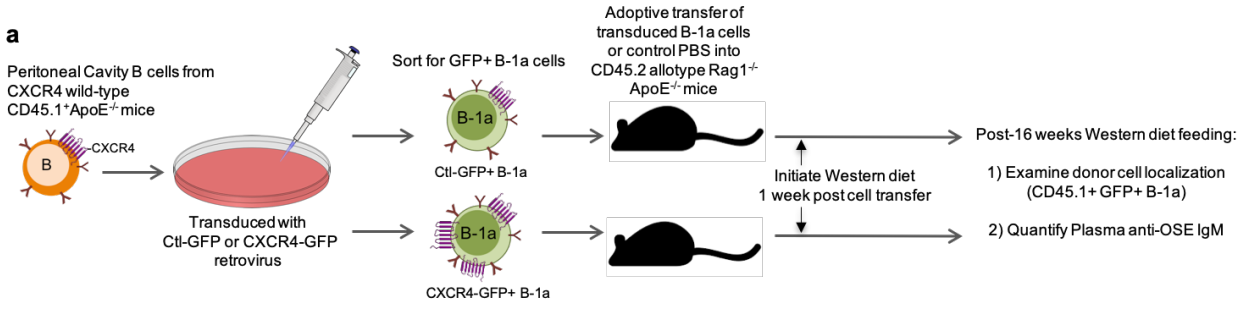

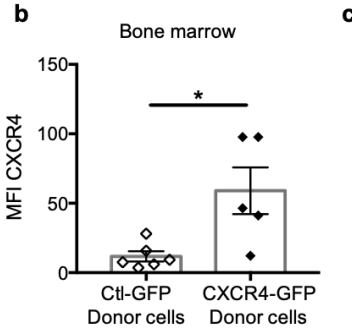

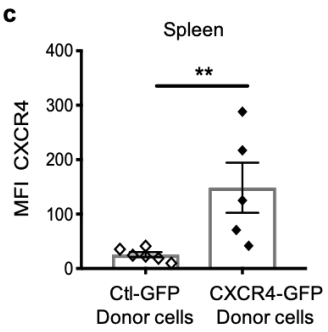

d

Variable	MFI of CXCR4 on donor B-1a cells	
	r-value	p-value
# of donor B-1a cells in bone marrow	0.71	*0.014
# of donor B-1a cells in spleen	0.43	0.18

e

Variable	# of donor cells in bone marrow	
	r-value	p-value
Plasma α-MDA-LDL IgM	0.67	*0.028
Plasma E06/T15 IgM	0.56	0.076
Plasma 1,3-Dextran IgM	0.29	0.39

Loss of secreted IgM enhances atherosclerosis in aged ApoE$^{-/-}$ mice with modest cholesterol levels

To determine if secreted IgM impacts atherogenesis in a setting relevant to human disease, we examined atherosclerosis by *en face* analysis in 80-week-old chow-fed ApoE$^{-/-}$ mice lacking secreted IgM (sIgM$^{-/-}$). As age has been shown to accelerate atherogenesis[185], one might consider this model more comparable to a 70-year-old human with hypercholesterolemia. Aged chow-fed ApoE$^{-/-}$ sIgM$^{-/-}$ mice had significantly increased atherosclerosis compared to chow-fed ApoE$^{-/-}$ controls (**Figure 14a,b**) and had cholesterol levels of 421-468 mg/dL (**Figure 14e**). In contrast, in a typical model of murine atherosclerosis (young mice fed Western diet for 8 weeks), atherosclerosis did not differ between genotypes (**Fig. 14c,d**). Notably, this model is comparable to a much younger human and has total cholesterol levels approaching 2000 mg/dL (**Fig. 14e**), representing an extreme atherogenic pressure not encountered in human CVD. These findings suggest that typical murine models of atherosclerosis may not be appropriate for determining if CXCR4 mediates B-1 cell production of anti-OSE IgM and atheroprotection.

Figure 14. Loss of secreted IgM enhances atherosclerosis in aged ApoE$^{-/-}$ mice with modest cholesterol levels. Representative images **(a)** and quantification **(b)** of Sudan-IV+ lesion area in aortas from 80-week-old ApoE$^{-/-}$ (n=4) and sIgM$^{-/-}$ApoE$^{-/-}$ (n=6) mice fed normal chow diet. Representative images **(c)** and quantification **(d)** of Sudan-IV+ lesion area in aortas from 16-week-old ApoE$^{-/-}$ (n=9) and sIgM$^{-/-}$ApoE$^{-/-}$ (n=9) mice fed 8 weeks of Western diet. *P<0.05 or non-significant (n.s.) by Mann-Whitney test. **(e)** Total cholesterol levels in ApoE$^{-/-}$ and sIgM$^{-/-}$ApoE$^{-/-}$ mice fed 8 weeks of Western diet or 80 weeks normal chow diet.

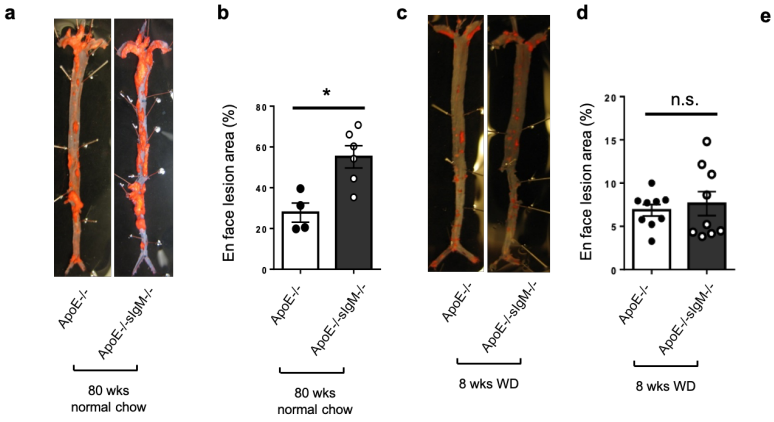

e

Group	Total Cholesterol (mg/dL)
ApoE$^{-/-}$ 80 weeks normal Chow	421 ± 68.3
ApoE$^{-/-}$ sIgM$^{-/-}$ 80 weeks normal Chow	468 ± 87.9
ApoE$^{-/-}$ 8 weeks Western diet	1918 ± 286
ApoE$^{-/-}$ sIgM$^{-/-}$ 8 weeks Western diet	1962 ± 174

CXCR4 expression on human peripheral B-1 cells associates with increased amount of plasma anti-MDA-LDL IgM antibodies

Accordingly, we turned to a human atherosclerosis cohort to test for association between B-1 cell CXCR4 expression and anti-OSE IgM and coronary artery disease. We analyzed a cohort of 50 human subjects presenting to the cardiac catheterization laboratory at the University of Virginia. We quantified circulating levels of IgM and IgG antibodies specific for MDA-LDL and CXCR4 expression on circulating B-1 cells (**Fig. 15a,b**). We used the flow cytometry strategy originally defined by Rothstein and colleagues [158] when quantifying the B-1 population. In this strategy, and for all findings in this report, human B-1 cells are defined as live, singlet, CD20+CD3-CD27+CD43+ cells. Representative flow cytometry plots of circulating immune cells from one subject (**Fig. 15b,c**) reveal a diffuse population of human B-1 cells, when gated based on an FMO-CD43 control (**Fig. 15d**). Cell surface expression of CXCR4 was measured as mean fluorescence intensity (MFI) of CXCR4 on B-1 cells (**Fig. 15e**). As the MFI of CXCR4 on B-1 cells was a skewed variable, we performed log transformation to approximate normality for use in correlative analysis. The frequency of CD20+CD3-CD27+CD43+ B-1 cells within the total CD20+ B cell population displayed no significant association with plasma levels of anti-MDA-LDL IgM (**Fig. 15f**). Notably, the addition of cell surface expression of CXCR4 to the analysis of B-1 cells significantly improved the positive association with amount of plasma anti-MDA-LDL IgM (**Fig. 15f**). No associations were identified between anti-MDA-LDL IgG levels and CXCR4 expression on B-1 cells (**Fig. 15f**) or anti-MDA-LDL IgG or IgM levels and CXCR4 expression on other peripheral B cell subsets including naïve CD20+CD3-CD27-CD43- B cells and memory CD20+CD3-CD27+CD43- B cells (**Table 6**).

Figure 15. CXCR4 expression on peripheral human B-1 cells associates with increased circulating amounts of anti-MDA-LDL IgM antibodies. (**a**), A 50-subject human cohort was analyzed for circulating anti-MDA-LDL IgM or IgG antibody levels and CXCR4 expression on peripheral blood B cell subsets. (**b**) Representative flow cytometry of peripheral blood mononuclear cells subset into CD20+ B cells and CD3+ T cells. (**c**) CD20+ B cells further subset into CD27+CD43+ B-1 cells. (**d**) FMO minus CD43 control used to set CD43 positivity. (**e**) Representative histograms depicting CXCR4 expression on the CD27+CD43+ B-1 subset from an FMO minus CXCR4 control (blue histogram) or a representative patient sample (red histogram). Dashed lines indicate mean fluorescence intensity (MFI) of CXCR4. (**f**) The percentage of CD20+CD3-CD27+CD43+ B-1 cells of total CD20+ B cells, or CXCR4 expression on B-1 cells (log(MFI CXCR4)) correlated with circulating amounts of anti-MDA-LDL IgM or IgG antibodies in 50 subjects. Correlation data presented as correlation coefficient (r) and statistical significance (p).

Figure 15.

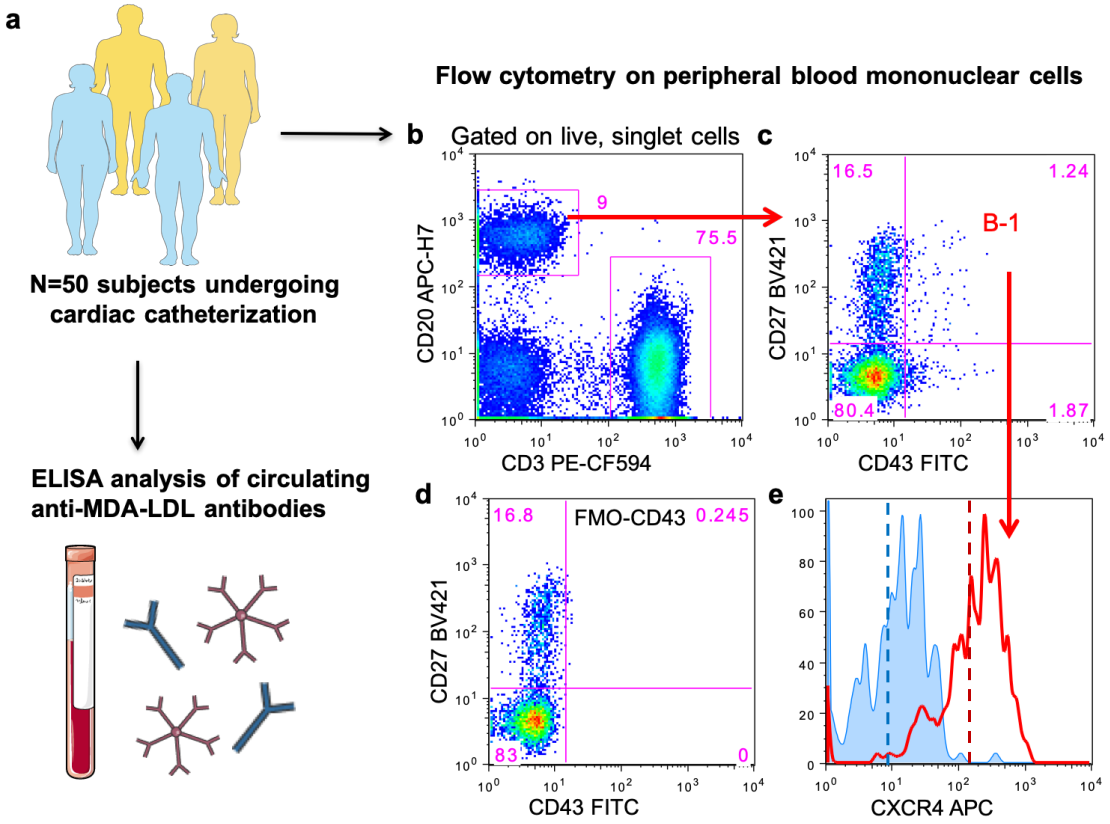

f

Variable	anti-MDA-LDL IgM r-value	anti-MDA-LDL IgM p-value	anti-MDA-LDL IgG r-value	anti-MDA-LDL IgG p-value
%CD27+CD43+ B-1 of total CD20+ B cells	0.11	0.45	-0.086	0.55
Log(MFI CXCR4 on CD27+CD43+ B-1 cells)	0.35	0.012*	-0.057	0.69

Table 6. Associations between circulating levels of anti-MDA-LDL antibodies and CXCR4 expression on other B cell subsets or the frequency of other B cell subsets. Data presented as correlation coefficient (r) and statistical significance (p). N=50 subjects. *P<0.05.

Variable	MDA-LDL IgM		MDA-LDL IgG	
	R-value	p-value	R-value	p-value
MFI CXCR4 total CD20+ B cells	0.05	0.73	0.20	0.16
%CD27-CD43- naïve B of total CD20+ B cells	-0.31	0.031*	0.048	0.74
MFI CXCR4 CD27-CD43- naïve B	0.18	0.22	0.22	0.12
%CD27+CD43- memory B of total CD20+ B cells	0.30	0.031*	-0.059	0.69
MFI CXCR4 CD27+CD43- memory B	-0.056	0.70	0.11	0.45

CXCR4 expression on human peripheral B-1 cells inversely associates with plaque volume and stenosis and indices of plaque instability.

Next, we analyzed the relationship between human B-1 CXCR4 expression and plaque burden and composition in human coronary arteries, as quantified by intravascular ultrasound and virtual histology (IVUS-VH) (**Fig. 16a**). Clinical and laboratory characteristics of this patient cohort are provided in **Table 7**. Consistent with the positive association of CXCR4 expression on human B-1 cells with circulating levels of IgM to MDA-LDL, human B-1 CXCR4 expression showed an inverse association with plaque burden and stenosis (**Fig. 16b,c**). Furthermore, while the frequency of circulating B-1 cells was not significantly associated with plaque burden, stenosis, or plaque characteristics (**Table 8**), CXCR4 expression on these B-1 cells demonstrated a trending positive association with the percentage of fibrous area in plaque and a trending inverse association with the percentage of necrotic area in plaque (**Fig. 16d)**, indicative of a more stable plaque phenotype. Additionally, there were no significant associations of B-1 CXCR4 expression and circulating levels of HDL, LDL, or triglycerides (**Fig. 16d**). Consistent with these findings, CXCR4 expression was not different on B cell subsets between age-matched C57BL/6 mice and hypercholesterolemic $ApoE^{-/-}$ mice fed chow or Western diet (**Fig. 17**). Multivariate analysis indicated that CXCR4 expression on human B-1 cells predicted plaque burden independently of LDL cholesterol, age, or gender in this 50-subject cohort (β coefficient= -11.33; standard error 3.04; P-value=0.0005). Finally, no significant associations were seen between human B-1 CXCR4 expression and other CAD risk factors such as hsCRP, BMI, HbA1c%, or creatinine **(Table 9).**

Figure 16. CXCR4 expression on peripheral human B-1 cells associates with decreased plaque volume and a protected plaque phenotype. (**a**) Plaque burden, stenosis, and composition were measured in human coronary arteries by intravascular ultrasound (IVUS) and virtual histology (VH). (**b**) Correlation plot of plaque burden with CXCR4 expression on B-1 cells (log(MFI CXCR4)) in 50 subjects. (**c**) Correlation plot of maximum stenosis with CXCR4 expression on B-1 cells (log(MFI CXCR4)) in 50 subjects. (**d**) Associations between CXCR4 expression on peripheral human B-1 cells and plaque burden, stenosis, plaque characteristics, or plasma cholesterol levels in 50 subjects. Data presented as correlation coefficient (r) and False Discovery Rate (FDR)-corrected statistical significance (p). *P<0.05 for FDR-corrected p-values.

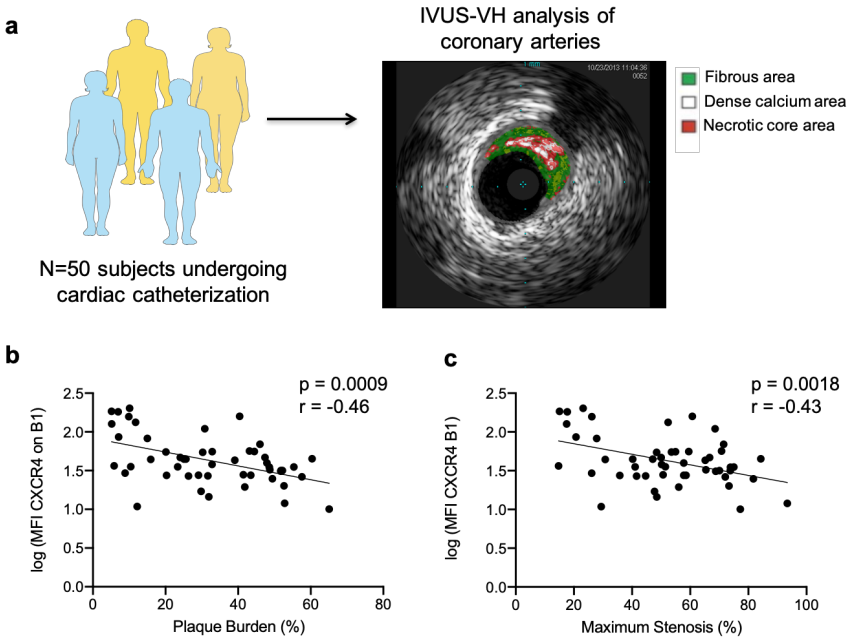

d

Variable	log(MFI CXCR4 on B-1 cells) r-value	p-value
Plaque Burden	-0.46	0.0072*
Stenosis	-0.43	0.0072*
%Fibrous	0.30	0.072
%Necrotic	-0.31	0.072
%Calcium	-0.24	0.14
HDL (mg/dL)	0.066	0.74
LDL (mg/dL)	-0.035	0.81
Triglycerides (mg/dL)	-0.13	0.47

Table 7. Clinical and laboratory characteristics of IVUS subjects. Values are presented as n(%) for binary measures or as mean± SD.

Subject Characteristics	**Values**
Age (y)	58.7 ± 9.6
Gender n (%male) n (%female)	27 (54%), 23 (46%)
Race n (%African Americans) n (%Caucasians)	3 (6%), 47 (94%)
Body Mass Index (kgm^{-2})	31.7 ± 7.0
Hypertension n(%)	41(82%)
Type-2 Diabetes n (%)	20 (40%)
Statin use n (%)	42 (84%)
Hemoglobin (k/µl)	12.7 ± 2.4
Hematocrit (%)	38.2 ± 4.3
Platelets (k/µl)	221 ± 55
White blood cell count (k/µl)	7.2 ± 2.7
Serum Creatinine (mg/dl)	0.9 ± 0.17
eGFR (MDRD) (ml/min per 1.73 m^2)	87.2 ± 14.2
Total cholesterol (mg/dl)	148 ± 35
Triglycerides (mg/dl)	116 ± 71
High density lipoprotein cholesterol (mg/dl)	39.8 ± 11
Low density lipoprotein cholesterol (mg/dl)	89.3 ± 30

Table 8. Associations of the frequency of circulating B-1 cells with IVUS virtual histology measurements. Given values represent correlation coefficient (r), and statistical significance (p). N=50 subjects.

Variable	**%CD27+CD43+ B-1 cells of total CD20+ B cells**	
	R-value	**p-value**
Plaque Burden	-0.0073	0.96
Stenosis	-0.042	0.77
%Fibrous	-0.028	0.84
%Necrotic	0.011	0.94
%Calcium	-0.11	0.46

Table 9. Associations of the MFI of CXCR4 on circulating human B-1 cells with other clinical characteristics. Given values represent correlation coefficient (r), and statistical significance (p). N=50 subjects.

Variable	**MFI CXCR4 on B-1 cells**	
	R-value	**p-value**
hsCRP (mg/L)	0.20	0.16
BMI	0.025	0.86
A1c%	-0.18	0.23
Creatinine (mg/dL)	-0.053	0.71

Figure 17. CXCR4 expression on B cell subsets is not modulated by ApoE knockout or Western diet. Quantification of CXCR4 MFI on splenic, bone marrow, blood, and peritoneal B cell subsets isolated from age-matched male C57BL/6 (n=5), ApoE$^{-/-}$ chow-fed (n=4), and ApoE$^{-/-}$ 8 weeks Western diet-fed (n=4) mice. B-2 cells were identified as CD19^{+}B220^{hi}CD23^{+} cells; B-1 cells were identified as CD19^{+} B220$^{mid\text{-}lo}$ CD23^{-} CD43^{+} IgM^{+} cells, then CD5 was used to discriminate B-1a and B-1b cells. CXCR4 expression was determined using an FMO control. Error bars represent mean ± s.e.m.

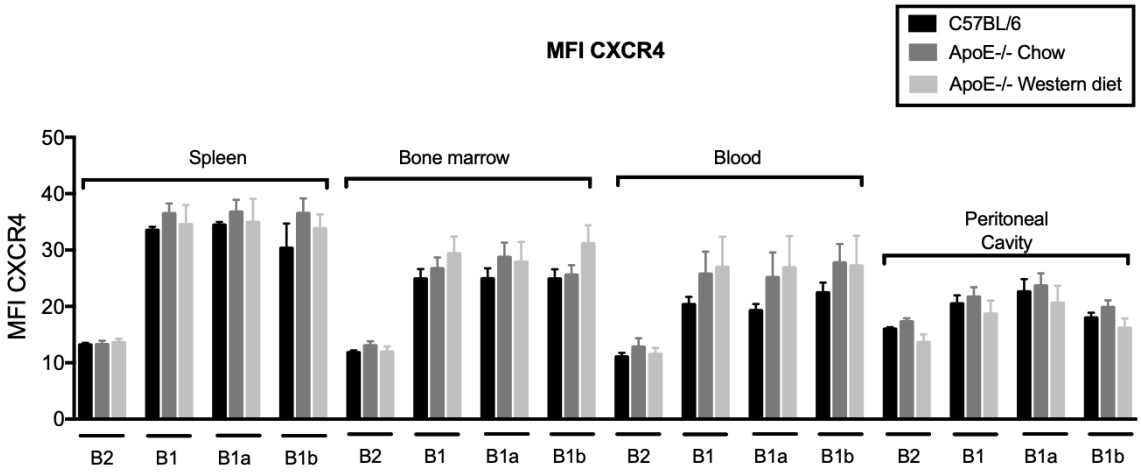

DISCUSSION

As B-1 cell-derived anti-OSE IgM antibodies have been demonstrated to be atheroprotective, identifying the factors that regulate their production has potential therapeutic implications. BM B-1a cells are known to be major contributors to circulating IgM levels[82]. While comparisons in immunoglobulin repertoire and circulatory patterns between splenic and peritoneal B-1a populations in non-atherosclerotic mice have been explored[48,49,80,81,103,110,112,123,183], little is known about what maintains the BM B-1a population or their IgM repertoire, particularly in the setting of atherosclerosis. Here we characterize, for the first time, the immunoglobulin heavy chain repertoire of BM B-1a cells in the context of atherosclerosis, and find that it is distinct from that of PerC B-1a cells. Moreover, we identify CXCR4 as a critical factor regulating BM B-1a number, BM IgM ASC number, and plasma levels of anti-OSE IgM in mice, and further as a novel marker associating with atheroprotection in humans (**Fig. 18**).

Figure 18. CXCR4 mediates atheroprotective IgM production in the bone marrow, a niche permissive for a unique repertoire of IgM antibodies. In mice (left), the BM IgH V repertoire is distinct and diversified compared to B-1a cells in the peritoneal cavity. The IgH V repertoire displayed by BM B-1a cells contains increased V_H1 gene segment usage, more N-additions, and a greater frequency of unique CDR-H3 sequences, resulting in greater IgH V repertoire diversity. The BM B-1a compartment is maintained by CXCR4, as loss of CXCR4 results in reduced B-1a migration to the BM and decreased anti-OSE IgM production in the BM. Conversely, overexpression of CXCR4 results in increased B-1a migration to the BM and increased anti-OSE IgM levels. In humans (right) CXCR4 expression on the human B-1 cell subset associates with increased circulating IgM, decreased atherosclerotic plaque burden, and a protected plaque phenotype in coronary arteries.

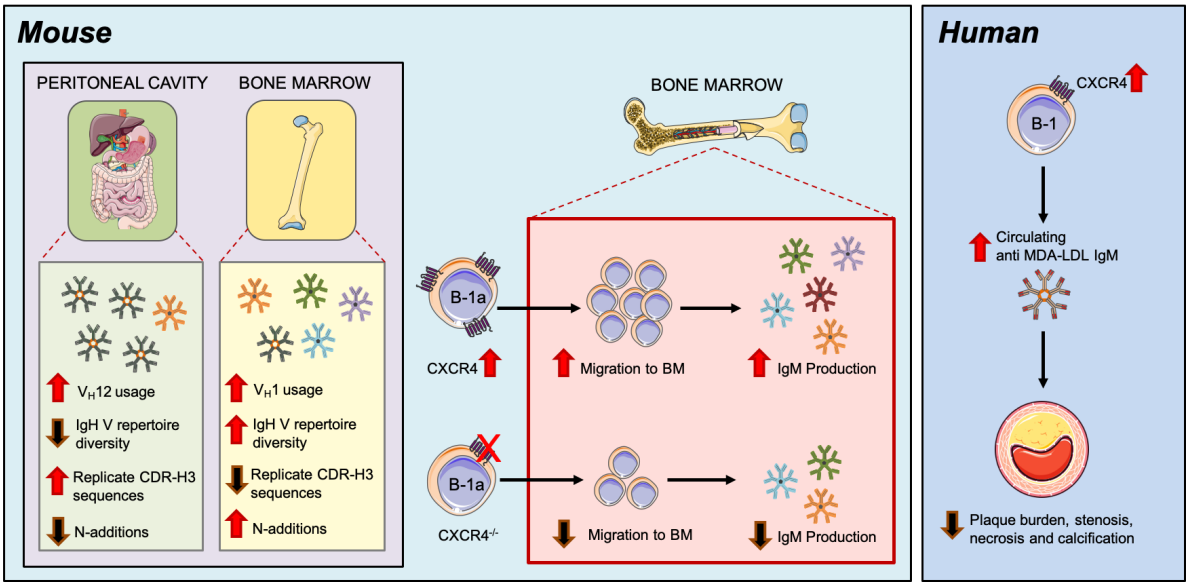

Previous studies comparing the IgH V region of single cell-sorted or bulk-sorted PerC B cell subsets from non-immune C57BL/6 or BALB/c-ByJ mice have demonstrated that PerC B-1a cells have a restricted heavy chain VDJ repertoire, and lose diversity in VDJ rearrangements and gain N-additions with age[48,49,110]. In line with these studies, we found that the PerC B-1a repertoire from 100-week aged ApoE$^{-/-}$ mice was very limited. Some CDR-H3 sequences in our dataset were previously observed on deep sequencing of bulk peritoneal B-1a cells from young C57BL/6 mice[48], supporting the conservation of B-1a sequences. Notably in aged ApoE$^{-/-}$ mice, we found that 70% of PerC B-1a sequences utilized one identical VH12-DH2-JH1 nucleotide sequence that encoded one identical CDR-H3 amino acid sequence, a significantly higher frequency than previously reported in C57BL/6 mice, in which two CDR-H3 sequences comprised 43% of total PerC B-1a sequences[48]. Strikingly, we also found that N-additions in aged ApoE$^{-/-}$ PerC B-1a cells were very limited, with 92% of sequences containing 0 N-additions at both V-D and D-J junctions. These data contrast with previous studies, which showed that PerC B-1a from 7-24 month old BALB/c-ByJ mice contained 28% of sequences with 0 N-additions[110], and from 12-week-old C57BL/6 mice that contained ~60% of sequences with no N-additions[48]. These differences may be due to differences in mouse background, vivarium conditions, or perhaps the heightened inflammatory microenvironment of the 100-weeks-aged ApoE$^{-/-}$ mouse, which may drive preferential selection for germline sequences in the PerC.

In contrast, our novel BM B-1a repertoire data in aged ApoE$^{-/-}$ mice reveals significantly more N-additions and fewer replicate sequences, indicating a shift away from germline and increased antibody diversity compared to PerC B-1a. Despite this diversity, some CDR-H3 sequences were common to both BM and PerC B-1a cells. It remains undetermined whether the adult BM B-1a population is maintained by circulating B-1a cells from PerC or elsewhere, or from resident adult BM B-1 cell progenitors, or

both. On one hand, the commonalities seen between PerC and BM B-1a sequences raise the intriguing hypothesis that certain B-1 cell clones preferentially migrate to the BM for antibody production. Consistent with this hypothesis, our data utilizing adoptive transfer of B-1a cells either overexpressing or deficient in CXCR4 demonstrate that PerC-derived mature B-1a cells traffic to the BM in a CXCR4-dependent manner. Alternatively, the differences observed between PerC and BM B-1a IgH V sequences suggest that niche-specific signals within the BM may also permit antibody repertoire diversification.

The most frequently utilized CDR-H3 in both BM and Perc B-1a was AGDYDGYWYFDV, a sequence previously observed to be associated with binding to phosphatidylcholine (PtC)[49]. Prior studies by Witztum and colleages have demonstrated that another PtC-binding antibody binds oxidized LDL and specifically, the phosphocholine (PC) head group present on PtC and oxidized phospholipids[48]. Our finding of high prevalence of AGDYDGYWYFDV in PerC and BM B-1a cells of aged ApoE$^{-/-}$ mice, coupled with the known abundance of PC-containing oxidized phospholipids in atherosclerosis[74] leads us to speculate that the hyperlipidemic conditions in ApoE$^{-/-}$ mice may drive preferential selection and expansion of IgM antibodies against PC and perhaps other OSE.

We additionally provide evidence that B-1a cell trafficking to the BM likely does not depend on B-1a cell migration from the spleen, as splenectomy does not alter B-1 cell numbers within the BM. Instead, the preferential expression of CXCL12 in the BM and CXCL13 expression in the spleen may guide B-1 cells with varying expression of CXCR4 or CXCR5 (receptor for CXCL13), to the BM or spleen, respectively. We found that CXCR4 expression on B cell subsets remains constant between C57BL/6, ApoE$^{-/-}$ chow-fed and ApoE$^{-/-}$ Western diet-fed mice. Future analysis of CXCR5 expression, or

the ratio of CXCR4:CXCR5 on B-1 cells, may further help delineate additional trafficking patterns of B-1 cells.

To examine the relationship between B-1 CXCR4 expression and atherosclerosis, we utilized a human CVD cohort. We chose this approach due to significant caveats of available murine models, including the lack of B-1a-specificity in the $CXCR4^{BKO}ApoE^{-/-}$ model, and the marked hyperlipidemia and immunodeficient setting of the Western diet-fed $Rag1^{-/-}$ $ApoE^{-/-}$ model. While a protective role for B-1 cells in murine atherosclerosis is well established, translating these findings to humans has been challenging. The human equivalent of the murine B-1 cell has remained elusive due to its distinct cell surface phenotype and low frequency in peripheral blood [164]. Since its initial discovery, controversy has existed on the difference between human B-1 cells and plasmablasts (PB) or pre-plasmablasts (pre-PB) [161], though Rothstein and colleagues have since demonstrated that the CD20+CD27+CD43+ B-1 subset differs from pre-PB and PB based on CD38 expression, transcriptional profiling, antibody repertoire, and other characteristics [165]. Additionally, differential expression of CD11b on the CD27+CD43+ B-1 population has been shown to associate either with increased IgM production (CD11b- human B-1) or increased IL-10 production and capacity to modulate T cells (CD11b+ human B-1)[167]. This suggests that a deeper heterogeneity within the CD27+CD43+ B-1 subset exists, and additional surface markers may correlate with functional differences. We found in a 50-subject human cohort that B-1 CXCR4 expression significantly positively associated with plasma levels of IgM to MDA-LDL, echoing our murine findings that CXCR4 is critical for maintaining circulating anti-OSE IgM levels.

Advances in coronary artery imaging, such as the use of IVUS-VH, have also improved our abilities to translate murine discoveries to humans. By utilizing IVUS-VH to quantify coronary artery plaque volume and characteristics, we provide the first evidence

that B-1 CXCR4 expression inversely associates with plaque burden and stenosis, and positively associates with a more stable plaque phenotype. These correlations support a hypothesis in which CXCR4 directs B-1 migration to sites of IgM antibody production like the bone marrow, thereby increasing circulating anti-OSE IgM levels that can modify plaque phenotype and reduce plaque burden.

In sum, this report provides novel findings demonstrating a distinct IgM repertoire between PerC and BM B-1a cells in the setting of atherosclerosis, and niche-specific differences in CXCR4-dependent B-1a cell maintenance and IgM production. Furthermore, our initial proof-of-concept study overexpressing CXCR4 on B-1a cells *in vivo* provides a rationale for future studies investigating whether modulating chemokine receptor expression in a targeted manner can have therapeutic potential. Our initial findings in a 50-subject cohort, coupled with our novel murine findings that production of circulating IgM to OSE and B-1a homeostasis depends on CXCR4, underscore the need for larger studies examining the association between human B-1 CXCR4 expression and plaque characteristics.

ACKNOWLEDGEMENTS

We thank Joanne Lannigan, Mike Solga, and Claude Chew from the UVa flow cytometry core, and Naomi Tsuji and Alexander Ludlow from Western Michigan University Homer Stryker M.D. School of Medicine for their excellent technical assistance. We thank Fabrizio Drago from University of Virginia for his assistance with statistical analysis. We thank Thomas Prohaska at University of California San Diego for assistance in comparative analysis to previously identified sequences.

SOURCES OF FUNDING

This work was supported by 1R01 HL107490, 1R01 HL136098, Project 3 of P01 HL055798 and P01 HL136275-01 (CAM), Core B of P01 HL055798 and P01 HL136275-01 (CAM and AMT), and R01AI142004. AU was supported by AHA Predoctoral fellowship 16PRE30300002 and 5T32AI007496-20.

DISCLOSURES

Drs. Tsimikas and Witztum are co-inventors and receive royalties from patents owned by UCSD on oxidation-specific antibodies and of biomarkers related to oxidized lipoproteins, and are co-founders of Oxitope, Inc. Dr. Tsimikas currently has a dual appointment with UCSD and is an employee of Ionis Pharmaceuticals. Dr. Witztum is a consultant to Ionis Pharmaceuticals.

Novelty and Significance

What is known?

- IgM antibodies against oxidation-specific epitopes (OSE), like malondialdehyde (MDA)-modified LDL are associated with atheroprotection in mouse models and in human patients with cardiovascular disease (CVD).
- Bone marrow (BM) B-1a cells contribute significantly to amount of plasma IgM.
- The putative human B-1 cell subset was previously identified as a CD20+CD3-CD27+CD43+ population in the circulation.

What new information does this article contribute?

- The repertoire of IgM expressed by BM B-1a cells is unique and displays greater heterogeneity compared to B-1a cells in the peritoneal cavity, where B-1 cells are found in abundance but where IgM secretion is low.
- The chemokine receptor CXCR4 regulates BM B-1a cell number in mice through mediating B-1a trafficking to the BM, and consequently sustains IgM production in the bone marrow.
- CXCR4 expression on human B-1 cells associates with increased amount of plasma anti-MDA-LDL IgM antibodies and decreased atherosclerosis in human coronary arteries.

B-1 cells in mice and humans produce atheroprotective anti-OSE IgM antibodies. While BM B-1a cells contribute significantly to overall plasma IgM titers, little is known about what mechanisms maintain the BM B-1a population. Here we show that CXCR4 is necessary for maintaining B-1a and IgM secreting-cell number in the BM, and consequently plasma IgM levels. Moreover, we find that the repertoire of IgM expressed

by BM B-1a cells during atherosclerosis is unique and displays greater heterogeneity than that of peritoneal cavity B-1a cells. Certain IgM sequences were commonly expressed by both peritoneal cavity and BM B-1a cells, suggesting that B-1a migration between compartments may be occurring. We show that, indeed, CXCR4 mediates the migration of peritoneal B-1a cells to the BM. Finally, in 50 human CVD subjects, CXCR4 expression on the putative human B-1 subset associated with increased levels of plasma anti-MDA-LDL IgM antibodies and less coronary artery plaque burden. These findings highlight a previously underappreciated diversity in human and murine B-1 cell populations and identify CXCR4 as a novel biomarker associating with protection in human CVD. Moreover, these results suggest that a targeted approach for limiting atherosclerosis via increasing B-1 CXCR4 expression may be relevant to humans.

Chapter 4

The Role of CXCR4 in B-1a cell homeostasis and murine atherosclerosis

ABSTRACT

Rationale: CXCR4 expression on human B-1 cells associates with less coronary artery atherosclerosis, and CXCR4 expression in mice is important for maintaining bone marrow B-1a number. However, whether CXCR4 expression is necessary for B-1a-mediated atheroprotection is not known, and the local bone marrow B-1a cell response during atherosclerosis has not been examined. Mice with B cell-specific knockout of CXCR4 have reduced B-1a cell number in the bone marrow partly due to a defect in migration, but alternative mechanisms may be responsible for this phenotype, due to CXCR4's roles in cell survival and turnover.

Objective: To examine the bone marrow B-1 cell response during atherosclerosis, to determine if CXCR4 is necessary for B-1a-mediated atheroprotection, and to examine alternative mechanisms responsible for the loss of B-1a number in the bone marrow in $CXCR4^{BKO}ApoE^{-/-}$ mice.

Methods and Results: We demonstrate that 9 weeks of Western diet (WD) feeding does not significantly induce B-1a cell or IgM antibody secreting cell (ASC) expansion in the bone marrow compared to age-matched chow-fed mice. CXCR4 was necessary for maintaining bone marrow B-1a cell number in both chow-fed and WD-fed conditions. Western diet induced a mild non-significant expansion of IgM ASC in the spleen that was not dependent on CXCR4. Plasma amounts of total IgM and anti-MDA-LDL IgM increased upon 9 weeks WD feeding, while E06/T15 IgM levels remained stable. $CXCR4^{BKO}ApoE^{-/-}$ mice had no significant differences in atherosclerotic lesion area in the aorta both after 9 weeks and 18 weeks of WD feeding. Long-term $CXCR4^{BKO}ApoE^{-/-}$ B-1a cell transfer into lymphocyte-deficient $Rag1^{-/-}$ $ApoE^{-/-}$ mice resulted in reduced donor B-1a and IgM ASC number in multiple niches and reduced plasma total IgM and anti-

OSE IgM compared to $CXCR4^{WT}ApoE^{-/-}$ B-1a cell transfer. Yet, surprisingly, atherosclerosis was reduced to a similar extent in both cell transfer groups compared to control $Rag1^{-/-}$ $ApoE^{-/-}$ mice receiving PBS. Intriguingly, B-1a cell transfer reduced plasma cholesterol in a CXCR4-independent manner. To determine whether bone marrow B-1a cell turnover or survival were impacted upon loss of CXCR4, BrdU uptake analysis was performed in $CXCR4^{WT}ApoE^{-/-}$ and $CXCR4^{BKO}ApoE^{-/-}$ mice. In the absence of CXCR4, bone marrow B-1a cells incorporated BrdU to much greater extent and the frequency of dead B-1a cells in the bone marrow was significantly increased. Bone marrow B-1a cells from $CXCR4^{BKO}ApoE^{-/-}$ mice also expressed less IL-5R, a cytokine receptor important for B-1a survival and homeostasis.

Conclusions: Our findings suggest that the bone marrow is a site of constitutive natural IgM antibody production and is not a site for B-1a/IgM ASC expansion in response to hyperlipidemia. Our findings also suggest that B cell CXCR4 expression is not essential for protection from WD-induced atherosclerosis in mice, but potential caveats of the utilized mouse models are additionally discussed. Finally, CXCR4 also has a role in maintaining bone marrow B-1a cell homeostasis and survival.

INTRODUCTION

While B-1a cells have a known atheroprotective function through production of IgM[37], less is known about the niche-specific nature of the B-1a cell response during atherosclerosis. It has previously been shown that spleens of hyperlipidemic ApoE$^{-/-}$ mice contain increased numbers of PC-specific IgM ASC compared to spleens of C57BL/6 mice[72]. Moreover, transfer of splenic B cells from aged atherosclerotic ApoE$^{-/-}$ mice reduces atherosclerosis in young ApoE$^{-/-}$ mice[11], suggesting that the spleen contains a protective B cell response to hyperlipidemia and atherosclerosis. However, the local bone marrow B-1a cell and IgM ASC response to hyperlipidemia has not yet been examined, but may be important since the BM is another site of constitutive IgM production[82]. In the previous chapter, we demonstrated that CXCR4 regulates bone marrow B-1a cell number and IgM production in young ApoE$^{-/-}$ mice, but whether CXCR4 regulates the BM B-1a response to hyperlipidemia remains to be tested.

In chapter 3 we also provided evidence that human B-1 CXCR4 expression associates with less coronary artery plaque burden and necrosis. Yet, whether CXCR4 is necessary for B-1a cell-mediated atheroprotection, and the mechanisms underlying this have not been examined. A few studies have provided evidence that it is important to examine the role of CXCR4 in atherosclerosis in a cell-type specific manner. Deletion of CXCR4 in arterial endothelial cells reduced endothelial barrier function and resulted in a more permeable vasculature, increased leukocyte adhesion to endothelium, increased macrophage content in aortic root lesions, and increased atherosclerosis[142]. Deletion of CXCR4 in vascular smooth muscle cells (VSMC) also resulted in increased atherosclerosis, though not by promoting immune cell recruitment[142]. Instead, CXCR4 was responsible for maintaining VSMC in a contractile state, and CXCR4 deficiency

resulted in reduced aortic root SMC content and VSMC dedifferentiation. Another study additionally demonstrated that CXCR4 deficiency or antagonism resulted in increased neutrophil recruitment into lesions and aggravated atherosclerosis[143]. These studies indicate that CXCR4 is protective in atherosclerosis through its regulation of multiple cell types. Conversely, other studies have demonstrated that CXCR4 may promote atherosclerotic lesion development through recruitment of smooth muscle progenitor cells and their differentiation into lesional SMC[186,187]. The role for CXCR4 on B cells, and specifically B-1a cells, in atherosclerosis remains to be examined.

We also provided evidence in the previous chapter that CXCR4 regulates bone marrow B-1a cell number through mediating B-1a migration to the bone marrow. However, much fewer B-1a cells migrated to the bone marrow compared to the spleen after adoptive transfer (**Chapter 3, Figure 8**). Because CXCR4 has functions outside of chemotaxis, including regulating cell cycle and cell survival, we hypothesized that alternative mechanisms could also be responsible for the loss of BM B-1a number seen in $CXCR4^{BKO}ApoE^{-/-}$ mice.

Here, we demonstrate that the bone marrow B-1a and IgM ASC population does not increase in response to hyperlipidemia. Moreover, while CXCR4 was necessary for maintaining the bone marrow B-1a/IgM ASC population and circulating amount of T15/E06 IgM, it was not necessary for maintaining the splenic B-1a/IgM ASC population or plasma amount of total or anti-MDA-LDL IgM after WD feeding in the $CXCR4^{BKO}$ $ApoE^{-/-}$ model. $CXCR4^{BKO}$ $ApoE^{-/-}$ and littermate control mice additionally had no significant differences in atherosclerotic lesion area after WD feeding, though knockout of CXCR4 in multiple B cell subsets in this model made it difficult to interpret this result. In order to examine the B-1a cell-specific role of CXCR4 in regulating atherosclerosis, we utilized adoptive B-1a cell transfer into $Rag1^{-/-}ApoE^{-/-}$ mice and Western diet feeding.

In contrast to results in CXCR4^{BKO} ApoE$^{-/-}$ mice, we demonstrate that CXCR4 expression on donor B-1a cells was necessary for maintaining their number in BM, spleen, and PerC after long-term adoptive transfer and for generating plasma total and anti-MDA-LDL IgM. Yet, CXCR4 was not required for B-1a-mediated protection from atherosclerosis. This was perhaps due to a CXCR4-independent lipid-lowering effect of B-1a cell transfer, however, caveats of the adoptive transfer model system are also discussed. Finally, we provide evidence that CXCR4 also regulates BrdU uptake, cell survival, and IL-5R expression specifically in bone marrow B-1a cells.

RESULTS

The bone marrow B-1a and IgM ASC population does not expand upon Western diet feeding

To examine the local BM B-1a response to atherosclerosis and to see if it was regulated by CXCR4, we quantified B-1a number in chow-fed or 9 weeks WD-fed $CXCR4^{WT}ApoE^{-/-}$ or $CXCR4^{BKO}ApoE^{-/-}$ mice. CXCR4 was necessary for maintaining BM B-1a number both in chow and WD-feeding conditions, however, B-1a cells did not significantly expand in the bone marrow upon WD feeding (**Fig. 19a**). B-1a cell number also did not increase in the spleen in response to WD, and loss of CXCR4 did not significantly impact splenic B-1a number (**Fig. 19b**).

To examine whether BM IgM production was altered upon WD feeding, we quantified IgM ASC using ELISPOT. Similar to flow cytometry results, loss of CXCR4 resulted in fewer IgM ASC in the bone marrow regardless of feeding condition, and no significant expansion of BM IgM ASC occurred upon WD-feeding (**Fig. 19c**). In contrast, a trend towards increased splenic IgM ASC was seen in WD-fed mice compared to chow, which was not dependent on CXCR4 (**Fig. 19d**).

Next, to examine whether the changes in the BM B-1a and IgM ASC populations impacted circulating levels of IgM, we measured plasma amount of total IgM, E06/T15 IgM specific for PC, and anti-MDA-LDL IgM. Western diet induced an increase in total plasma IgM, an effect that was not entirely CXCR4-dependent, though WD-fed $CXCR4^{BKO}ApoE^{-/-}$ mice had a trend towards lower amount of total IgM compared to WD-fed wild-type littermate controls (**Fig. 19e**). Intriguingly, anti-OSE IgM specificities were induced differently upon WD. The amount of PC-specific E06/T15 IgM did not increase

after WD-feeding, but depended upon CXCR4 (**Fig. 19f**), while anti-MDA-LDL IgM was induced upon WD-feeding and was less dependent on CXCR4 (**Fig. 19g**).

In sum, these data indicate that the bone marrow does not contain local B-1a or IgM ASC expansion in response to hyperlipidemia, and that the WD-induced increases in plasma total and anti-MDA-LDL IgM may arise from IgM production in other niches, or by other cell types, such as B-1b or plasma cells. Alternatively, though B-1a and IgM ASC cell number was not increased, the amount of IgM secreted by B-1a cells on a per cell basis could be increased in hyperlipidemic conditions.

Figure 19. Western diet does not induce a local bone marrow B-1a cell or IgM ASC response. Calculated number of B-1a cells in the bone marrow (**a**) or spleen (**b**) of age-matched male $CXCR4^{WT}ApoE^{-/-}$ or $CXCR4^{BKO}ApoE^{-/-}$ mice fed chow or 9 weeks of Western diet. ***P<0.001, **P<0.01, or n.s. indicates non-significant differences using Kruskal-Wallis test. Calculated number of IgM antibody secreting cells (ASC) in the bone marrow (**c**) or spleen (**d**) of age-matched $CXCR4^{WT}ApoE^{-/-}$ or $CXCR4^{BKO}ApoE^{-/-}$ mice fed chow or 9 weeks of Western diet. *P<0.05, or #p=0.07 with removal of outlier in spleen $CXCR4^{WT}ApoE^{-/-}$ chow group by Kruskal-Wallis test. Plasma amount of total IgM (**e**), E06/T15 IgM (**f**), or anti-MDA-LDL IgM (**g**) in age-matched $CXCR4^{WT}ApoE^{-/-}$ or $CXCR4^{BKO}ApoE^{-/-}$ mice fed chow or 9 weeks of Western diet. *P<0.05 by Kruskal-Wallis test.

Figure 19.

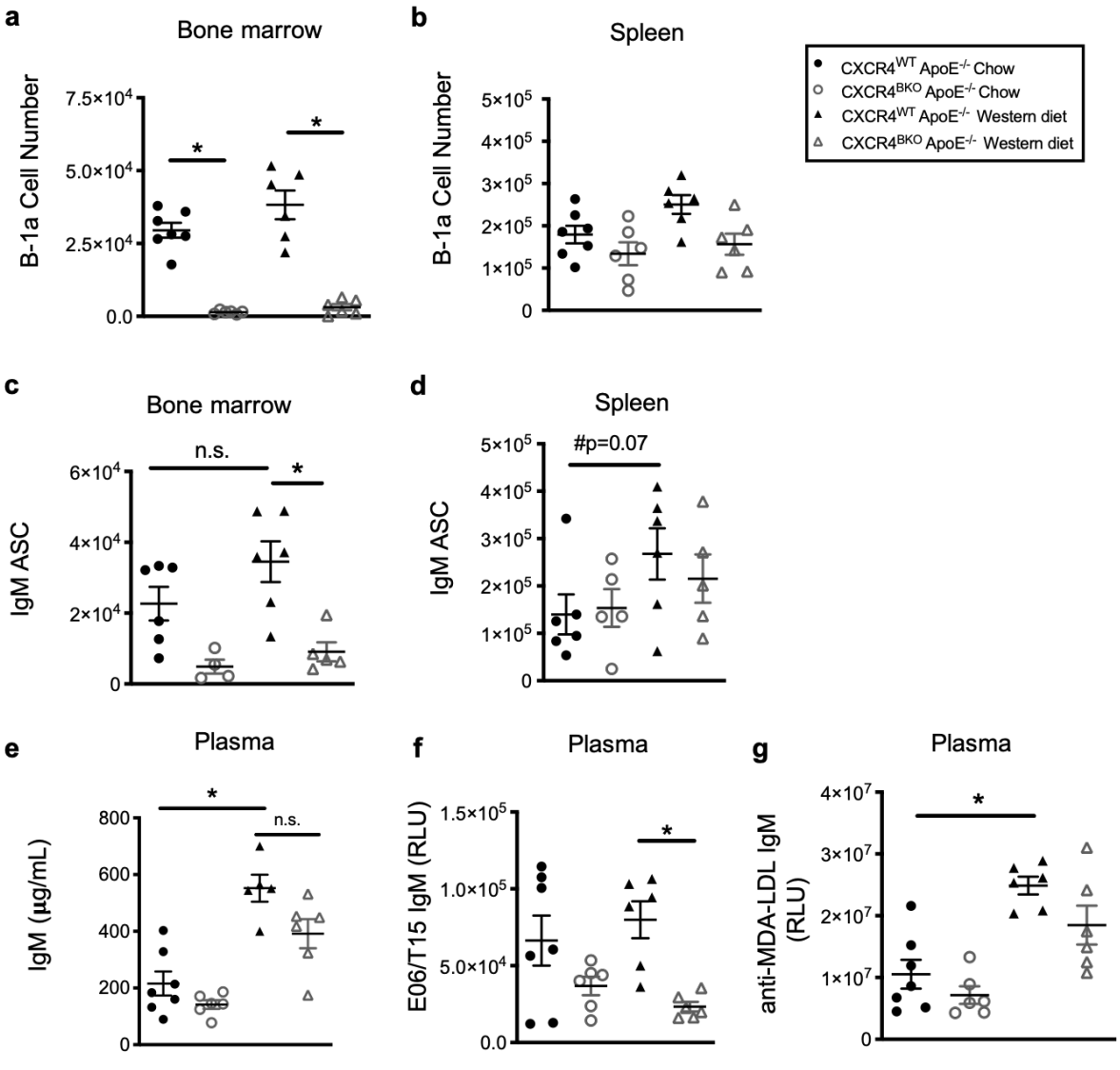
a
Bone marrow
B-1a Cell Number
7.5×10^4
5.0×10^4
2.5×10^4
0.0
*
*
b
Spleen
B-1a Cell Number
5×10^5
4×10^5
3×10^5
2×10^5
1×10^5
0
CXCR4^WT ApoE^-/- Chow
CXCR4^BKO ApoE^-/- Chow
CXCR4^WT ApoE^-/- Western diet
CXCR4^BKO ApoE^-/- Western diet
c
Bone marrow
IgM ASC
6×10^4
4×10^4
2×10^4
0
n.s.
*
d
Spleen
IgM ASC
5×10^5
4×10^5
3×10^5
2×10^5
1×10^5
0
#p=0.07
e
Plasma
IgM (µg/mL)
800
600
400
200
0
*
n.s.
f
Plasma
E06/T15 IgM (RLU)
1.5×10^5
1.0×10^5
5.0×10^4
0.0
*
g
Plasma
anti-MDA-LDL IgM (RLU)
4×10^7
3×10^7
2×10^7
1×10^7
0
*

B cell-specific knockout of CXCR4 does not impact atherosclerosis in WD-fed ApoE$^{-/-}$ mice

Next, to determine whether B cell-specific loss of CXCR4 impacted atherosclerosis development, we examined atherosclerotic lesion area in the aorta of CXCR4^{WT}ApoE$^{-/-}$ or CXCR4^{BKO}ApoE$^{-/-}$ mice fed 9 weeks of Western diet. Loss of CXCR4 did not significantly alter Sudan IV+ lesion area in the aorta (**Fig. 20a,b**). However, an important caveat of this model is that CXCR4 is lost on all subsets of B cells, not only B-1a, and different B cell subsets can have opposing effects on atherosclerosis[7]. Indeed, B cell-specific loss of CXCR4 additionally led to loss of mature B-2 cells in the bone marrow (**Fig. 20c**).

After 9 weeks of WD feeding, lesion development in the aorta was minimal (<5%). Therefore, we also examined atherosclerosis in CXCR4^{WT}ApoE$^{-/-}$ or CXCR4^{BKO}ApoE$^{-/-}$ mice fed 18 weeks of Western diet. Loss of CXCR4 also did not impact atherosclerosis with this longer WD feed (**Fig. 20d,e**). Interestingly, at this later time point, the trend towards decreased amount of total plasma IgM in CXCR4^{BKO}ApoE$^{-/-}$ mice was lost (**Fig. 20f**), though the defect in bone marrow B-1a number persisted to this age (**Fig. 20g**). These data again suggest that BM B-1a cells, though necessary for generating homeostatic levels of circulating IgM (**Chapter 3-Figure 9e** and Choi et al[82]), may not be the primary B cell population responsible for generating IgM during hyperlipidemic WD feeding.

Altogether, these data indicate that total B cell knockout of CXCR4 does not impact atherosclerosis development in the aorta. Whether aortic root lesion development, aortic root plaque composition, lesion IgM accumulation, or levels of plasma or lesional IgG isotypes differ between Western diet-fed CXCR4^{WT}ApoE$^{-/-}$ or

CXCR4^{BKO}ApoE$^{-/-}$ mice remains unanswered. We chose to move away from this model as it did not allow us to parse out the B-1a cell-specific role of CXCR4 in atherosclerosis.

Figure 20. B-cell specific loss of CXCR4 does not impact atherosclerosis after 9 or 18 weeks of Western diet. Representative images of Sudan-IV stained aortas (**a**) and quantification of Sudan IV+ area (**b**) in age-matched $CXCR4^{WT}ApoE^{-/-}$ or $CXCR4^{BKO}ApoE^{-/-}$ mice fed 9 weeks of Western diet. P=0.16 by Mann-Whitney test. (**c**) Calculated number of $CD19^{+}CD23^{+}CD43^{-}B220^{hi}$ B-2 cells in bone marrow of $CXCR4^{WT}ApoE^{-/-}$ or $CXCR4^{BKO}ApoE^{-/-}$ mice fed 9 weeks of chow or Western diet. ***P<0.001 or **P<0.01 using Kruskal-Wallis test. Representative images of Sudan-IV stained aortas (**d**) and quantification of Sudan IV+ area (**e**) in age-matched $CXCR4^{WT}ApoE^{-/-}$ or $CXCR4^{BKO}ApoE^{-/-}$ mice fed 18 weeks of Western diet. (**f**) Plasma amount of total IgM in age-matched $CXCR4^{WT}ApoE^{-/-}$ or $CXCR4^{BKO}ApoE^{-/-}$ mice fed 18 weeks of Western diet. (**g**) Quantified number of $CD19^{+}CD23^{-}CD43^{+}B220^{lo}IgM^{+}CD5^{+}$ B-1a cells in bone marrow of $CXCR4^{WT}ApoE^{-/-}$ or $CXCR4^{BKO}ApoE^{-/-}$ mice fed 18 weeks of Western diet.

Figure 20.

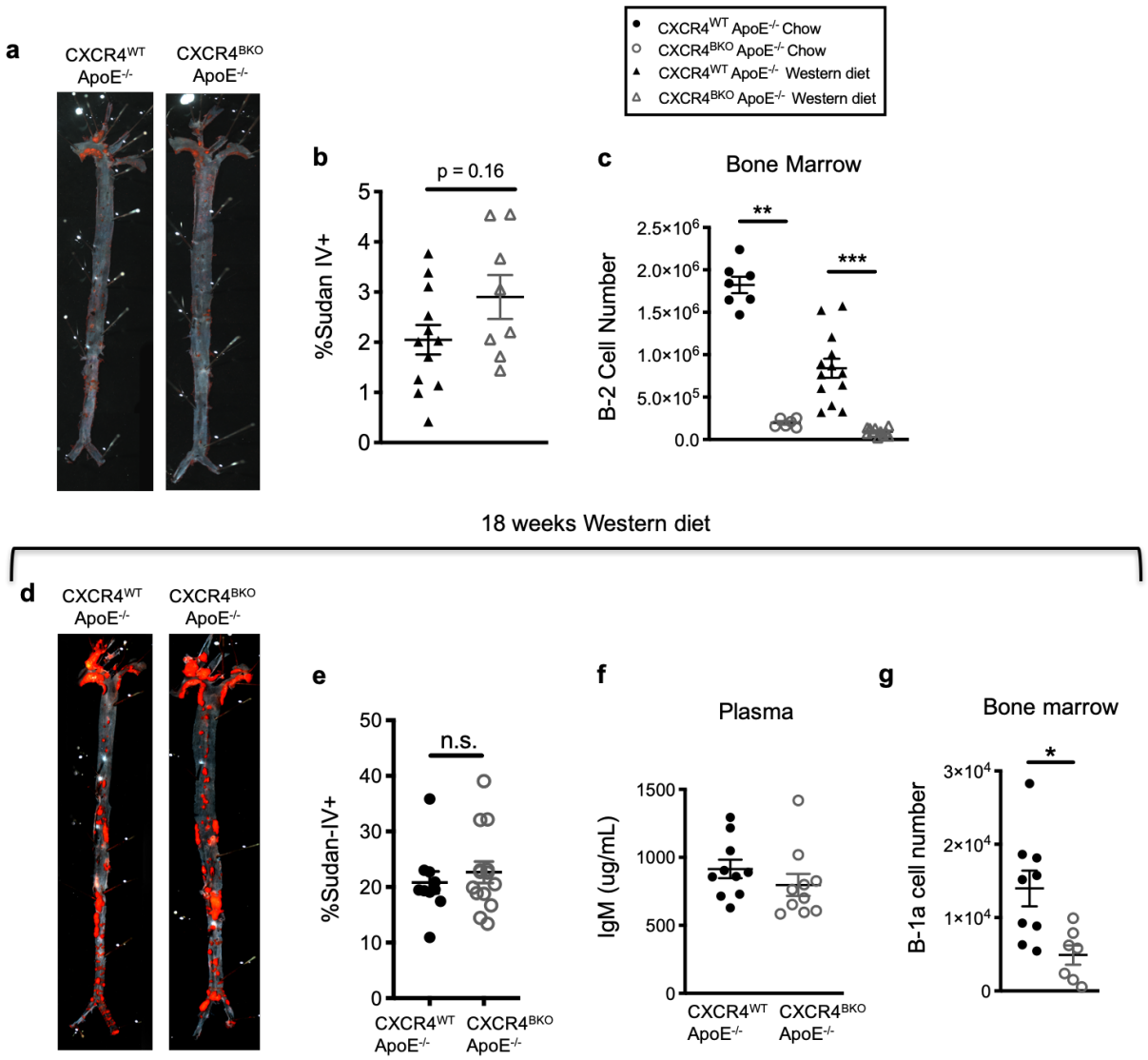
a
CXCR4WT ApoE-/-
CXCR4BKO ApoE-/-
CXCR4WT ApoE-/- Chow
CXCR4BKO ApoE-/- Chow
CXCR4WT ApoE-/- Western diet
CXCR4BKO ApoE-/- Western diet
b
p = 0.16
%Sudan IV+
c
Bone Marrow
B-2 Cell Number
**
***
18 weeks Western diet
d
e
n.s.
%Sudan-IV+
f
Plasma
IgM (ug/mL)
g
Bone marrow
B-1a cell number
*

Absence of CXCR4 on B-1a cells significantly reduces cell number and IgM production in lymphoid tissues after adoptive transfer into Rag1$^{-/-}$ ApoE$^{-/-}$ mice

To examine the role of CXCR4 specifically on the B-1a subset under conditions of hypercholesterolemia, we instead turned to an adoptive transfer model. Lymphocyte-deficient Rag1$^{-/-}$ ApoE$^{-/-}$ recipient mice were adoptively transferred with FAC-sorted CXCR4^{WT} ApoE$^{-/-}$ or CXCR4^{BKO}ApoE$^{-/-}$ B-1a cells or control PBS and fed Western diet for 16 weeks (**Fig. 21a**). In contrast to the results in CXCR4^{BKO}ApoE$^{-/-}$ mice in which B-1a cell loss was limited to the bone marrow (**Fig. 19a,b**, and **Chapter 3 Fig 9b**), flow cytometry on tissues revealed fewer B-1a cells present in the bone marrow, spleen, and peritoneal cavity of Rag1$^{-/-}$ ApoE$^{-/-}$ recipients given CXCR4^{BKO}ApoE$^{-/-}$ B-1a cells compared to those given CXCR4^{WT}ApoE$^{-/-}$ B-1a cells (**Fig. 21b-e**). B-1a cell transfer also resulted in an increase in the number of Ly6G+ neutrophils in the spleen, bone marrow, and blood of Rag1$^{-/-}$ ApoE$^{-/-}$ recipients, but no significant differences in CD3+T cells or CD115+ monocytes (**Fig. 22**).

ELISPOT analysis revealed fewer IgM ASC in the bone marrow and spleen of recipients given CXCR4^{BKO}ApoE$^{-/-}$ B-1a cells compared to those given CXCR4^{WT}ApoE$^{-/-}$ B-1a cells (**Fig. 21f-h**). In contrast to WD-fed CXCR4^{BKO}ApoE$^{-/-}$ mice, in which absence of CXCR4 did not impact circulating total or anti-MDA-LDL IgM (**Fig. 19 e,g**), lower titers of total IgM and anti-MDA-LDL IgM were found in plasma of recipients given CXCR4^{BKO}ApoE$^{-/-}$ B-1a cells (**Fig. 21i,j**). Titers of IgM against CuOx-LDL and PC were lower in recipients given CXCR4^{BKO}ApoE$^{-/-}$ B-1a cells, although these did not reach statistical significance (**Fig. 21k,l**).

In sum, these results after B-1a adoptive transfer differed from what was observed in the WD-fed CXCR4^{BKO}ApoE$^{-/-}$ model, and indicated that CXCR4 specifically on B-1a cells was important for maintaining B-1a number in niches not limited to the

bone marrow, and for generating plasma total and anti-MDA-LDL IgM in WD-fed Rag1$^{-/-}$ ApoE$^{-/-}$ hosts. The fact that we saw a defect in B-1a number in multiple niches in the absence of CXCR4 further indicated that CXCR4 may also regulate B-1a survival. The implications of these findings are discussed below.

Figure 21. CXCR4^{BKO} ApoE$^{-/-}$ B-1a cells are defective in the ability to generate circulating IgM and retain their numbers in lymphoid tissues after adoptive transfer into Rag1$^{-/-}$ ApoE$^{-/-}$ mice. (a) Experimental setup: Control PBS or 8x10^4 peritoneal B-1a cells from CXCR4^{WT} ApoE$^{-/-}$ or CXCR4^{BKO} ApoE$^{-/-}$ mice were adoptively transferred into Rag1$^{-/-}$ApoE$^{-/-}$ hosts, which were fed 16 weeks of Western diet. (**b**) Representative gating strategy for quantification of donor B-1a cells in B cell-deficient Rag1$^{-/-}$ApoE$^{-/-}$ hosts. Calculated number of CD19$^+$IgM$^+$CD23$^-$ donor cells recovered in bone marrow (**c**), spleen (**d**), and peritoneal cavity (**e**) of Rag1$^{-/-}$ ApoE$^{-/-}$ recipient mice adoptively transferred with CXCR4^{WT} ApoE$^{-/-}$ B-1a cells (n=12), CXCR4^{BKO} ApoE$^{-/-}$ B-1a cells (n=12), or control PBS (n=11) after 16 weeks Western diet feeding. (**f**) Representative ELISPOT wells depicting splenic IgM ASC in Rag1$^{-/-}$ApoE$^{-/-}$ recipients after 16 weeks Western diet feeding. Calculated number of IgM ASC in cell suspensions of total bone marrow (**g**) or spleen (**h**) of Rag1$^{-/-}$ApoE$^{-/-}$ hosts receiving control PBS (n=11), CXCR4^{WT} ApoE$^{-/-}$ B-1a cells (n=12), or CXCR4^{BKO} ApoE$^{-/-}$ B-1a cells (n=12) after 16 weeks Western diet feeding. (**i**) Calculated concentration of total IgM in plasma of Rag1$^{-/-}$ApoE$^{-/-}$ recipient mice adoptively transferred with CXCR4^{WT} ApoE$^{-/-}$ B-1a cells (n=7), CXCR4^{BKO} ApoE$^{-/-}$ B-1a cells (n=7), or control PBS (n=7) after 16 weeks Western diet feeding. Relative titer of IgM reactive to MDA-LDL (**j**), CuOx-LDL (**k**), or PC-KLH (**l**) in plasma of Rag1$^{-/-}$ApoE$^{-/-}$ recipient mice after 16 weeks Western diet feeding. ****P<0.0001, ***P<0.001, **P<0.01 using one-way ANOVA with Tukey's multiple comparisons test. Error bars represent mean ± s.e.m.

Figure 21.

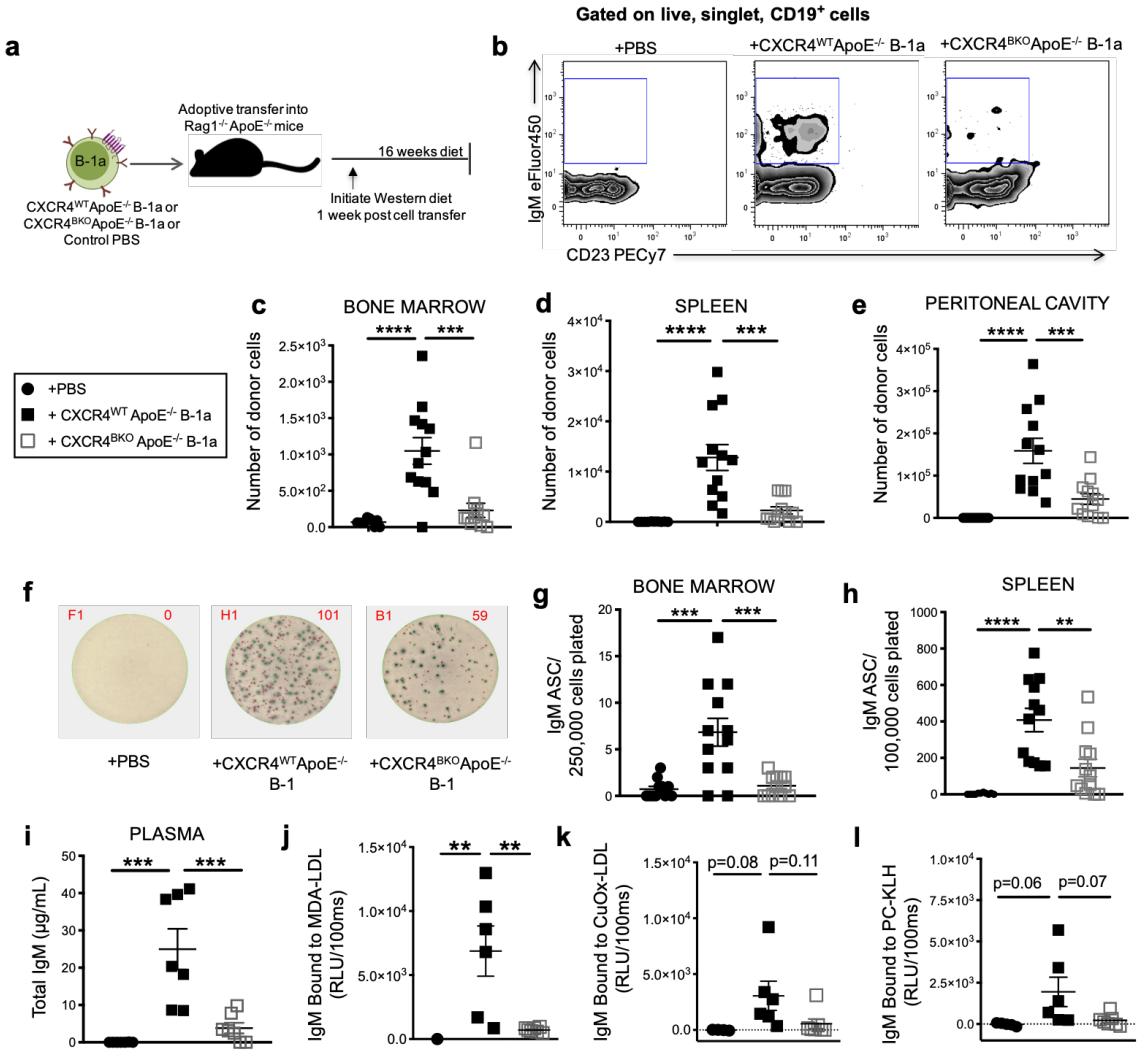
a
Adoptive transfer into Rag1-/- ApoE-/- mice
B-1a
16 weeks diet
Initiate Western diet 1 week post cell transfer
CXCR4WTApoE-/- B-1a or CXCR4BKOApoE-/- B-1a or Control PBS
b
Gated on live, singlet, CD19+ cells
+PBS
+CXCR4WTApoE-/- B-1a
+CXCR4BKOApoE-/- B-1a
IgM eFluor450
CD23 PECy7
+PBS
+ CXCR4WT ApoE-/- B-1a
+ CXCR4BKO ApoE-/- B-1a
c
BONE MARROW
Number of donor cells
d
SPLEEN
e
PERITONEAL CAVITY
f
F1 0
H1 101
B1 59
+PBS
+CXCR4WTApoE-/- B-1
+CXCR4BKOApoE-/- B-1
g
BONE MARROW
IgM ASC/ 250,000 cells plated
h
SPLEEN
IgM ASC/ 100,000 cells plated
i
PLASMA
Total IgM (µg/mL)
j
IgM Bound to MDA-LDL (RLU/100ms)
k
IgM Bound to CuOx-LDL (RLU/100ms)
p=0.08
p=0.11
l
IgM Bound to PC-KLH (RLU/100ms)
p=0.06
p=0.07

Figure 22. Effect of B-1a adoptive transfer on other immune cell populations in spleen, bone marrow, and blood. Calculated numbers of CD3+ T cells, CD115+ monocytes, and Ly6G+ neutrophils in spleen (**a**), bone marrow (**b**), or circulating blood (**c**) of B- and T-cell deficient Rag1$^{-/-}$ApoE$^{-/-}$ recipient mice adoptively transferred with 8x10^{4} CXCR4^{WT} ApoE$^{-/-}$ B-1a cells (n=5), CXCR4^{BKO} ApoE$^{-/-}$ B-1a cells (n=5), or control PBS (n=3), after 16 weeks of Western diet feeding. Error bars represent mean ± s.e.m.

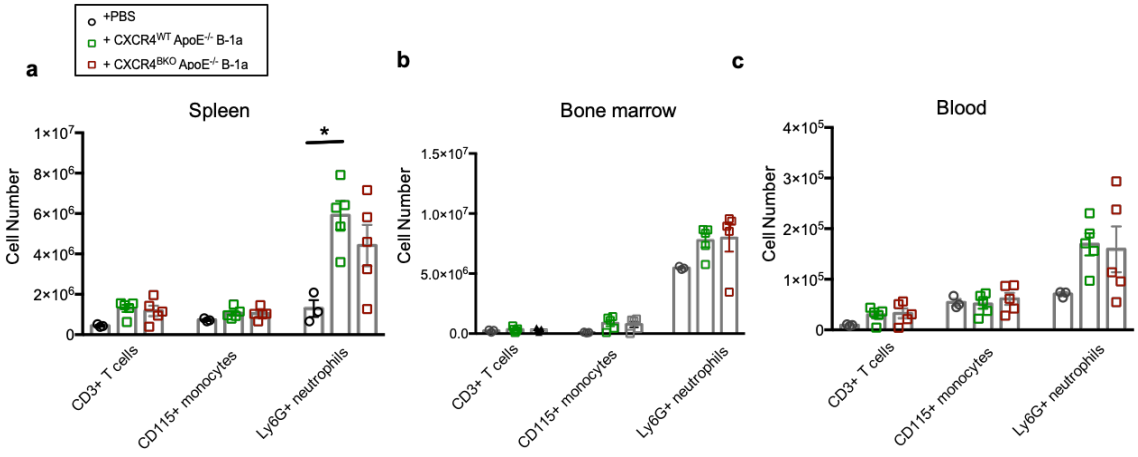

B-1a cell transfer attenuates atherosclerosis in Western diet-fed Rag1$^{-/-}$ ApoE$^{-/-}$ mice in a region-specific but CXCR4-independent manner

Next, we examined atherosclerosis in B-1a adoptive transfer recipients. Consistent with previous studies[37], transfer of CXCR4-sufficient B-1a cells attenuated atherosclerosis in the aorta relative to PBS controls (**Fig. 23a,b**). Notably, the B-1a effect on atherosclerosis was seen only in the aortic arch and thoracic aorta, not in the abdominal aorta (**Fig. 23c-e**). There were no significant differences in Sudan-IV+ lesion area between Rag1$^{-/-}$ ApoE$^{-/-}$ recipients given CXCR4^{WT}ApoE$^{-/-}$ and CXCR4^{BKO}ApoE$^{-/-}$ B-1a cells. Cross-sectional analysis of Oil Red O-stained aortic root sections additionally confirmed that B-1a cell transfer attenuated atherosclerotic lesion development in a CXCR4-independent manner (**Fig. 23f-h**).

Intriguingly, despite significant differences in plasma IgM titers between the two B-1a cell transfer groups (**Fig. 21i**), there was only a non-significant trend towards reduced lesional IgM in Rag1$^{-/-}$ ApoE$^{-/-}$ recipients given CXCR4^{BKO}ApoE$^{-/-}$ B-1a cells compared to CXCR4^{WT}ApoE$^{-/-}$ B-1a cells (**Fig. 24a,b**). B-1a cell transfer did not significantly modulate CD68+ macrophage, necrotic core, or collagen content in aortic root lesions **(Fig. 24c-f**). Unexpectedly, we also found that B-1a cell transfer reduced total cholesterol, specifically non-HDL cholesterol, and overall body weight, in a CXCR4-independent manner (**Fig. 25**).

In sum, these data indicate that CXCR4 on B-1a cells is not necessary for B-1a-mediated atheroprotection in WD-fed Rag1$^{-/-}$ApoE$^{-/-}$ mice. Moreover, protection from atherosclerosis did not correlate with plasma IgM levels in this study. To understand this finding, it is important to consider caveats of the atherosclerosis model we used. One explanation for why plasma IgM levels did not correlate with reduced atherosclerosis in our adoptive transfer experiment is that perhaps sufficient IgM was not generated to

mitigate the significantly heightened lipid burden present in Western diet-fed $Rag1^{-/-}$ $ApoE^{-/-}$ mice. Indeed, $CXCR4^{WT}$ $ApoE^{-/-}$ B-1a cell transfer resulted in only ~25 ug/mL plasma IgM (**Fig. 21i**), in comparison to 100 ug/mL present in young $CXCR4^{WT}ApoE^{-/-}$ mice (**Chapter 3, Fig. 9e**) and ~900 ug/mL present in 18 weeks Western diet-fed $CXCR4^{WT}ApoE^{-/-}$ mice (**Fig. 20f**). Moreover, attenuation of atherosclerosis was IgM-dependent only in the setting of more moderate lipid levels such as in aged chow-fed $ApoE^{-/-}$ mice that had average total cholesterol of approximately 450 mg/dL, but not in young $ApoE^{-/-}$ mice fed 8 weeks of Western diet, which had average total cholesterol of almost 2000 mg/dL (**Chapter 3, Fig. 14**). Thus, the combination of insufficient IgM production and extreme, non-physiologic cholesterol levels may have overwhelmed the ability of IgM to be protective in this 16 week-WD fed model, and may be why we do not observe further reduced atherosclerosis after $CXCR4^{WT}$ $ApoE^{-/-}$ B-1a cell transfer compared to $CXCR4^{BKO}$ $ApoE^{-/-}$ B-1a cell transfer. The fact that we do see a CXCR4-independent reduction in atherosclerosis after B-1a transfer could be due to 1) IgM made in a CXCR4-independent manner in other niches like the PVAT that generates enough lesional IgM to mediate atheroprotection without impacting plasma IgM levels, or 2) the CXCR4-independent lipid-lowering effect of B-1a transfer. Overall, we now know that there are significant pitfalls to using the WD-induced atherosclerosis model to answer our specific question of whether CXCR4 on B-1a cells is atheroprotective, especially because it is not likely to represent the human condition, which involves significantly less cholesterol burden. The implications of these findings and potential alternative approaches are discussed in Chapter 5.

Figure 23. B-1a cell transfer attenuates atherosclerosis in Western diet-fed Rag1$^{-/-}$ ApoE$^{-/-}$ mice in a region-specific but CXCR4-independent manner

(a) Representative images of Sudan IV staining and quantification of the percentage of Sudan IV^{+} atherosclerotic lesion area in the total aorta (**b**), aortic arch (**c**), thoracic aorta (**d**), or abdominal aorta (**e**) from Rag1$^{-/-}$ApoE$^{-/-}$ mice adoptively transferred with 8x10^{4} CXCR4^{WT} ApoE$^{-/-}$ B-1a cells (n=12), CXCR4^{BKO} ApoE$^{-/-}$ B-1a cells (n=12), or control PBS (n=11), after 16 weeks of Western diet feeding. **P<0.01; ***P<0.001, using one-way ANOVA with Tukey's multiple comparisons test. (**f**) Representative images of Oil Red O-stained aortic root sections from Rag1$^{-/-}$ApoE$^{-/-}$ mice adoptively transferred with CXCR4^{WT} ApoE$^{-/-}$ B-1a cells, CXCR4^{BKO} ApoE$^{-/-}$ B-1a cells, or control PBS, after 16 weeks of Western diet feeding. Quantification of total lesion area (**g**) or fraction of lesion+ area within the external elastic lamina (EEL) (**h**) measured over the length of the aortic root in Rag1$^{-/-}$ApoE$^{-/-}$ mice adoptively transferred with CXCR4^{WT} ApoE$^{-/-}$ B-1a cells (n=5), CXCR4^{BKO} ApoE$^{-/-}$ B-1a cells (n=5), or control PBS (n=9). ****P<0.0001 by 2-way ANOVA ($F(2,225)=20.38$ for (**g**); $F(2,225)=18.11$ for (**h**)). n.s. indicates non-significant p-value. Error bars represent mean ± s.e.m.

Figure 23.

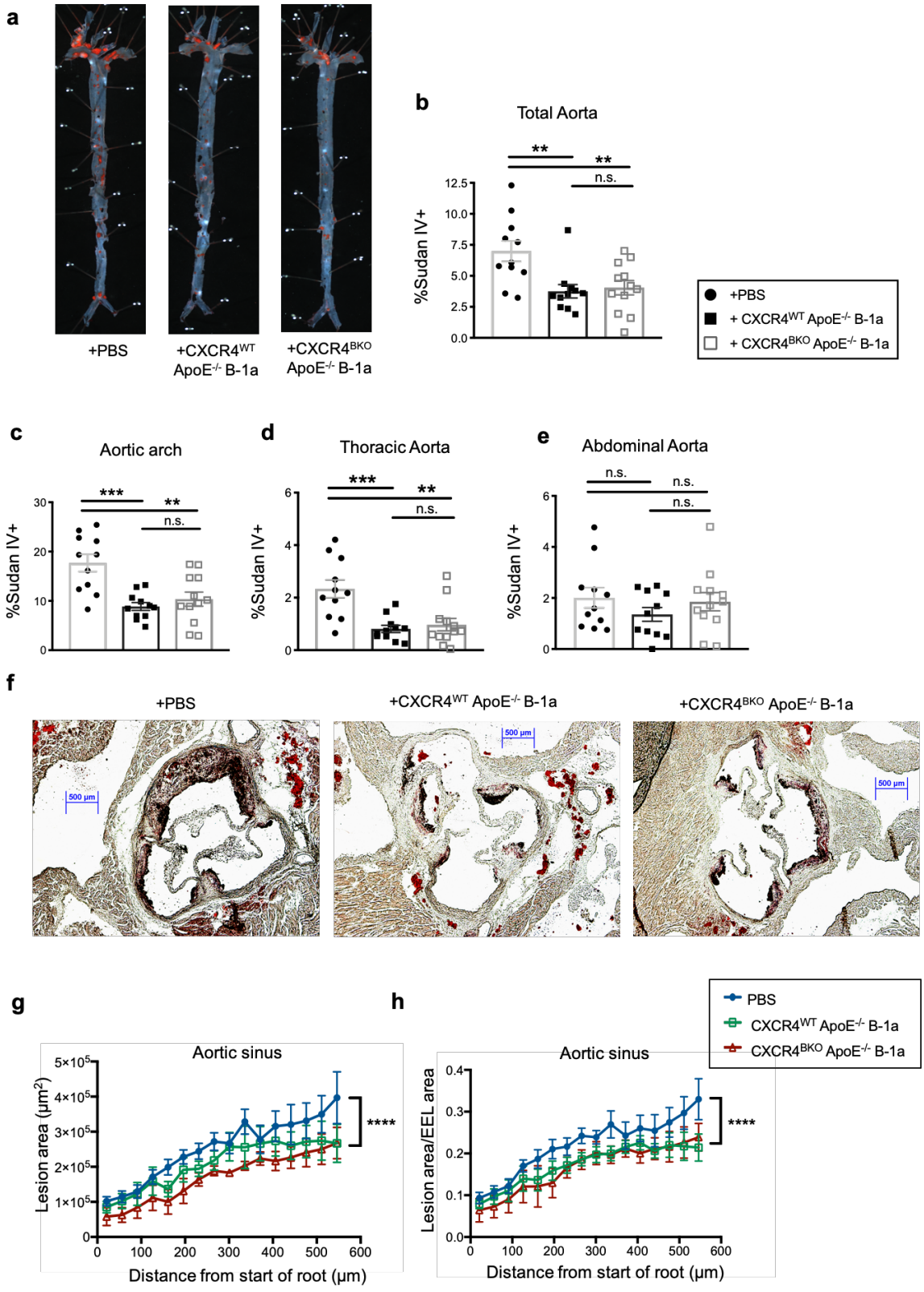
a
+PBS
+CXCR4WT ApoE-/- B-1a
+CXCR4BKO ApoE-/- B-1a
b
Total Aorta
%Sudan IV+
**
**
n.s.
+PBS
+ CXCR4WT ApoE-/- B-1a
+ CXCR4BKO ApoE-/- B-1a
c
Aortic arch
%Sudan IV+
***
**
n.s.
d
Thoracic Aorta
%Sudan IV+
***
**
n.s.
e
Abdominal Aorta
%Sudan IV+
n.s.
n.s.
n.s.
f
+PBS
+CXCR4WT ApoE-/- B-1a
+CXCR4BKO ApoE-/- B-1a
500 µm
g
Aortic sinus
Lesion area (µm2)
Distance from start of root (µm)
****
h
Aortic sinus
Lesion area/EEL area
Distance from start of root (µm)
****
PBS
CXCR4WT ApoE-/- B-1a
CXCR4BKO ApoE-/- B-1a

Figure 24. B-1a cell transfer increases lesional IgM in a CXCR4-independent manner, but does not modulate lesional CD68^{+} content, necrotic area, or collagen content

(**a**) Representative brightfield images (top row), IgM immunofluorescence staining (middle row), or CD68 immunofluorescence staining (bottom row) at 4x magnification in aortic root sections of Rag1$^{-/-}$ApoE$^{-/-}$ recipients. Scale bar=500 μm. Quantification of the percentage of aortic root lesion area that is IgM+ (**b**), or CD68+ (**c**) in Rag1$^{-/-}$ ApoE$^{-/-}$ recipients transferred with CXCR4^{WT} ApoE$^{-/-}$ B-1a cells (n=5), CXCR4^{BKO} ApoE$^{-/-}$ B-1a cells (n=5), or control PBS (n=9), after 16 weeks of Western diet feeding. (**d**) Representative images of van Gieson collagen staining in aortic root sections from Rag1$^{-/-}$ApoE$^{-/-}$ recipient mice. Acellular necrotic regions indicated by yellow arrows. Quantification of the percentage of acellular necrotic area (**e**) or collagen+ area (**f**) within aortic root lesions of Rag1$^{-/-}$ApoE$^{-/-}$ hosts receiving CXCR4^{WT} ApoE$^{-/-}$ B-1a cells (n=5), CXCR4^{BKO} ApoE$^{-/-}$ B-1a cells (n=5), or control PBS (n=9), after 16 weeks of Western diet feeding. ****P<0.0001, ***P<0.001, *P<0.05, or n.s. indicates non-significant difference by one-way ANOVA with Tukey's multiple comparisons test. Error bars represent mean ± s.e.m.

Figure 24.

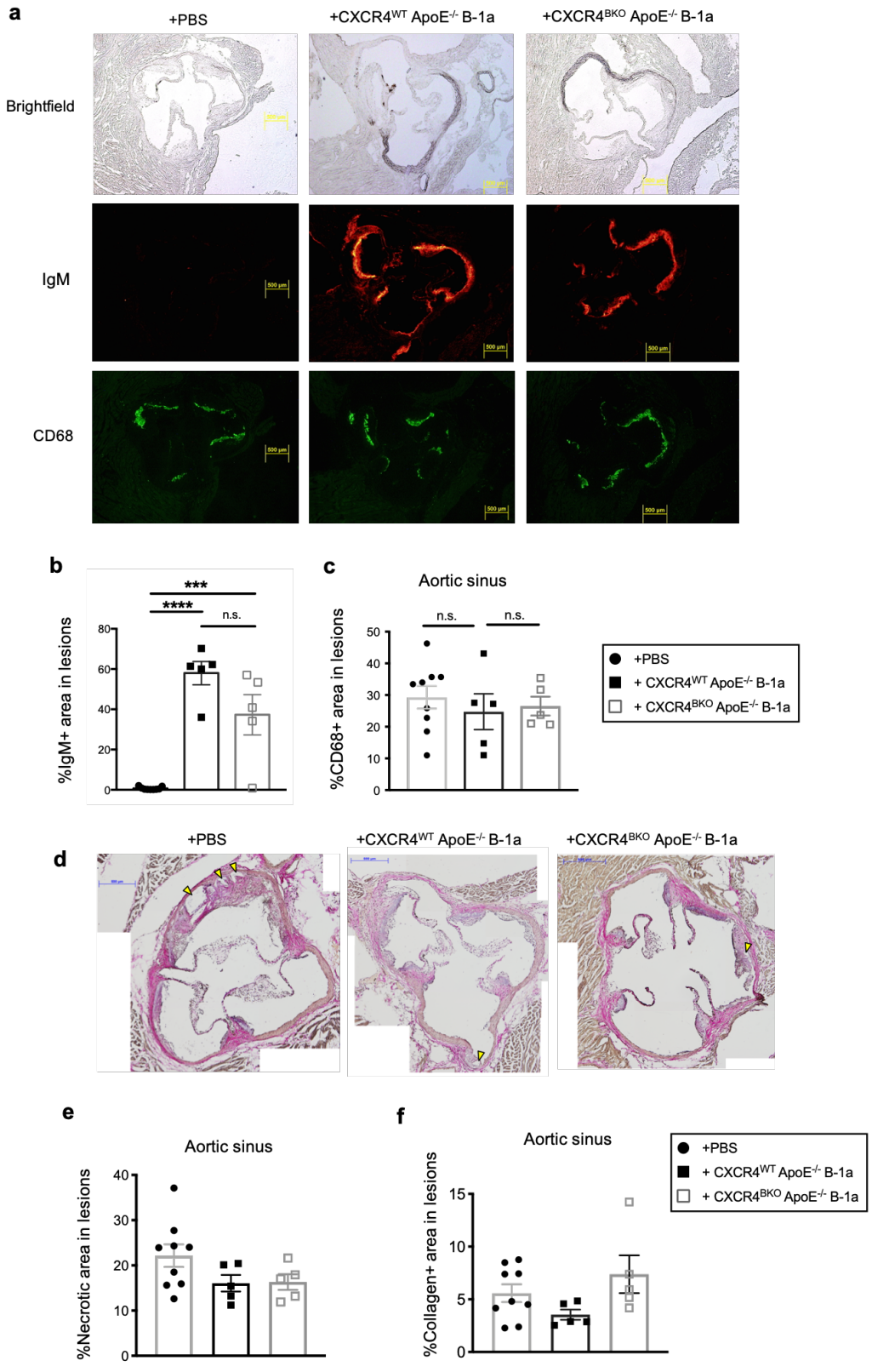
a
+PBS
+CXCR4WT ApoE-/- B-1a
+CXCR4BKO ApoE-/- B-1a
Brightfield
IgM
CD68
b
%IgM+ area in lesions
***
****
n.s.
c
Aortic sinus
%CD68+ area in lesions
n.s.
n.s.
+PBS
+ CXCR4WT ApoE-/- B-1a
+ CXCR4BKO ApoE-/- B-1a
d
+PBS
+CXCR4WT ApoE-/- B-1a
+CXCR4BKO ApoE-/- B-1a
e
Aortic sinus
%Necrotic area in lesions
f
Aortic sinus
%Collagen+ area in lesions
+PBS
+ CXCR4WT ApoE-/- B-1a
+ CXCR4BKO ApoE-/- B-1a

Figure 25. Reduced plasma cholesterol and total body weight after adoptive B-1a cell transfer into Rag1$^{-/-}$ ApoE$^{-/-}$ mice. Calculated concentration of total cholesterol (**a**), HDL cholesterol (**b**), triglycerides (**c**), and non-HDL cholesterol (**d**) in plasma of Western diet-fed Rag1$^{-/-}$ ApoE$^{-/-}$ mice adoptively transferred with 8x10^{4} CXCR4^{WT} ApoE$^{-/-}$ B-1a cells (n=12), CXCR4^{BKO} ApoE$^{-/-}$ B-1a cells (n=12), or PBS control (n=11). **P<0.01, ***P<0.001 using one-way ANOVA with Tukey's multiple comparisons test. Error bars represent mean ± s.e.m. (**e**) Average total body weights over the time course of Western diet feeding. *P<0.05 by 2-way ANOVA; F(2, 213)=4.65.

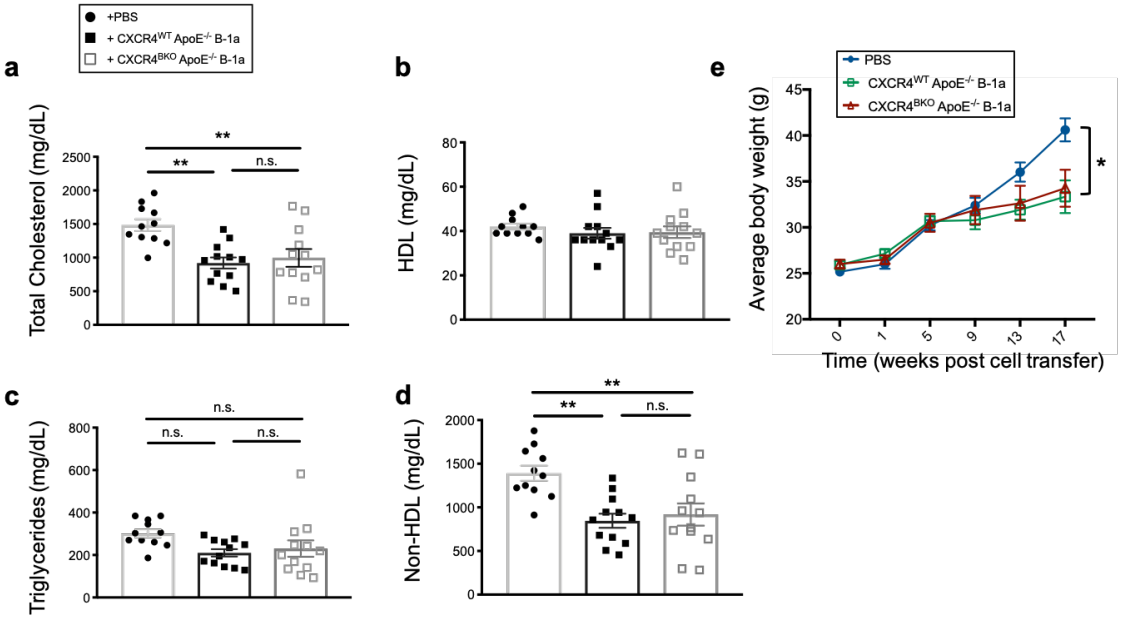

CXCR4 regulates bone marrow B-1a cell BrdU uptake, survival, and IL-5R expression

The fact that we saw fewer donor B-1a cells in the spleen, bone marrow, and PerC of Rag1$^{-/-}$ ApoE$^{-/-}$ recipients receiving CXCR4^{BKO}ApoE$^{-/-}$ B-1a cells (**Fig. 21c-e**), and the known role of CXCR4 in mediating cell survival led us to examine alternative mechanisms (besides migration) whereby CXCR4 regulates bone marrow B-1a number. We first examined whether loss of CXCR4 affected the bone marrow B-1a cell cycle by analyzing *in vivo* BrdU uptake in CXCR4^{WT} ApoE$^{-/-}$ and CXCR4^{BKO}ApoE$^{-/-}$ mice (**Fig. 26a**). Unexpectedly, despite overall lower B-1a cell numbers in CXCR4^{BKO}ApoE$^{-/-}$ bone marrow (**Chapter 3 Fig. 9b)**, B-1a cells from CXCR4^{BKO}ApoE$^{-/-}$ bone marrow demonstrated significantly greater BrdU uptake relative to CXCR4^{WT} ApoE$^{-/-}$ controls, indicating a greater frequency of cells in S-phase of the cell cycle (**Fig. 26b,c**). Splenic B-1a cells did not display differences in BrdU uptake between genotypes (**Fig. 26c**).

The greater frequency of BrdU+ B-1a cells, yet overall lower bone marrow B-1a cell number in CXCR4^{BKO}ApoE$^{-/-}$ mice led us to hypothesize that loss of CXCR4 may impair B-1a cell survival. Therefore, we quantified the frequency of dead B-1a cells by performing dead cell discrimination after gating on singlet, B-1a cells (**Fig. 26d,e**). The frequency of dead B-1a cells in the bone marrow of CXCR4^{BKO}ApoE$^{-/-}$ mice was >4-fold higher than that in CXCR4^{WT} ApoE$^{-/-}$ bone marrow (**Fig. 26f**). Splenic B-1a cells from CXCR4^{BKO}ApoE$^{-/-}$ mice also contained a significantly higher frequency of dead cells compared to CXCR4^{WT} ApoE$^{-/-}$ mice, although the fold increase (<2-fold) was much less robust than in the bone marrow (**Fig. 26f**).

To determine why absence of CXCR4 resulted in such drastic alterations in B-1a homeostasis in the bone marrow, we next turned to the cytokine IL-5, which has been demonstrated to have an important role in maintaining B-1a cell survival, proliferation, and antibody production [89,90,92,100]. To determine whether bone marrow B-1a cells from

CXCR4^{BKO}ApoE$^{-/-}$ mice are deficient in the capacity to sense IL-5, we quantified the frequency of IL-5R+ B-1a cells by flow cytometry (**Fig. 26g**). The overall frequency of IL-5R+ B-1a cells was low, and B cell-specific loss of CXCR4 resulted in further reduced IL-5R+ B-1a cells in the bone marrow (**Fig. 26h**). Splenic, peritoneal, and peripheral blood B-1a cells displayed no differences in IL-5R expression in the absence of CXCR4 (**Fig. 26h**). Taken together, these data indicate that the loss of B-1a cell number in bone marrow of CXCR4^{BKO}ApoE$^{-/-}$ mice is not only due to migration (as discussed in Chapter 3), but may also arise from BM-specific disruption in B-1a homeostasis. The underlying mechanisms responsible for reduced B-1a cell survival remain unanswered, but future strategies to further understand this phenotype are discussed below.

Figure 26. CXCR4 regulates bone marrow B-1a BrdU uptake, survival, and IL-5R expression. (**a**) Experimental schematic for *in vivo* cell cycle or cell survival analysis in $CXCR4^{WT}$ $ApoE^{-/-}$ and $CXCR4^{BKO}$ $ApoE^{-/-}$ mice. Representative gating strategy from one bone marrow sample per genotype (**b**) and quantification (**c**) of the frequency of S-phase BrdU+ B-1a cells in spleen and bone marrow of $CXCR4^{WT}$ $ApoE^{-/-}$ (n=4) or $CXCR4^{BKO}$ $ApoE^{-/-}$ (n=4) mice. *P<0.05 by Mann-Whitney test. Representative gating strategy from one bone marrow sample per genotype (**d,e**) and quantification (**f**) of the frequency of dead B-1a cells in spleen and bone marrow of $CXCR4^{WT}$ $ApoE^{-/-}$ (n=4) or $CXCR4^{BKO}$ $ApoE^{-/-}$ (n=4) mice. *P<0.05 by Mann-Whitney test. (**g**) Representative gating strategy from an FMO-IL5R control or one bone marrow sample per genotype and quantification (**h**) of the frequency of IL-5R+ B-1a cells in spleen, bone marrow, peritoneal cavity (PerC), and blood of $CXCR4^{WT}$ $ApoE^{-/-}$ (n=9) or $CXCR4^{BKO}$ $ApoE^{-/-}$ (n=10) mice. **P<0.01 by Mann-Whitney test.

Figure 26.

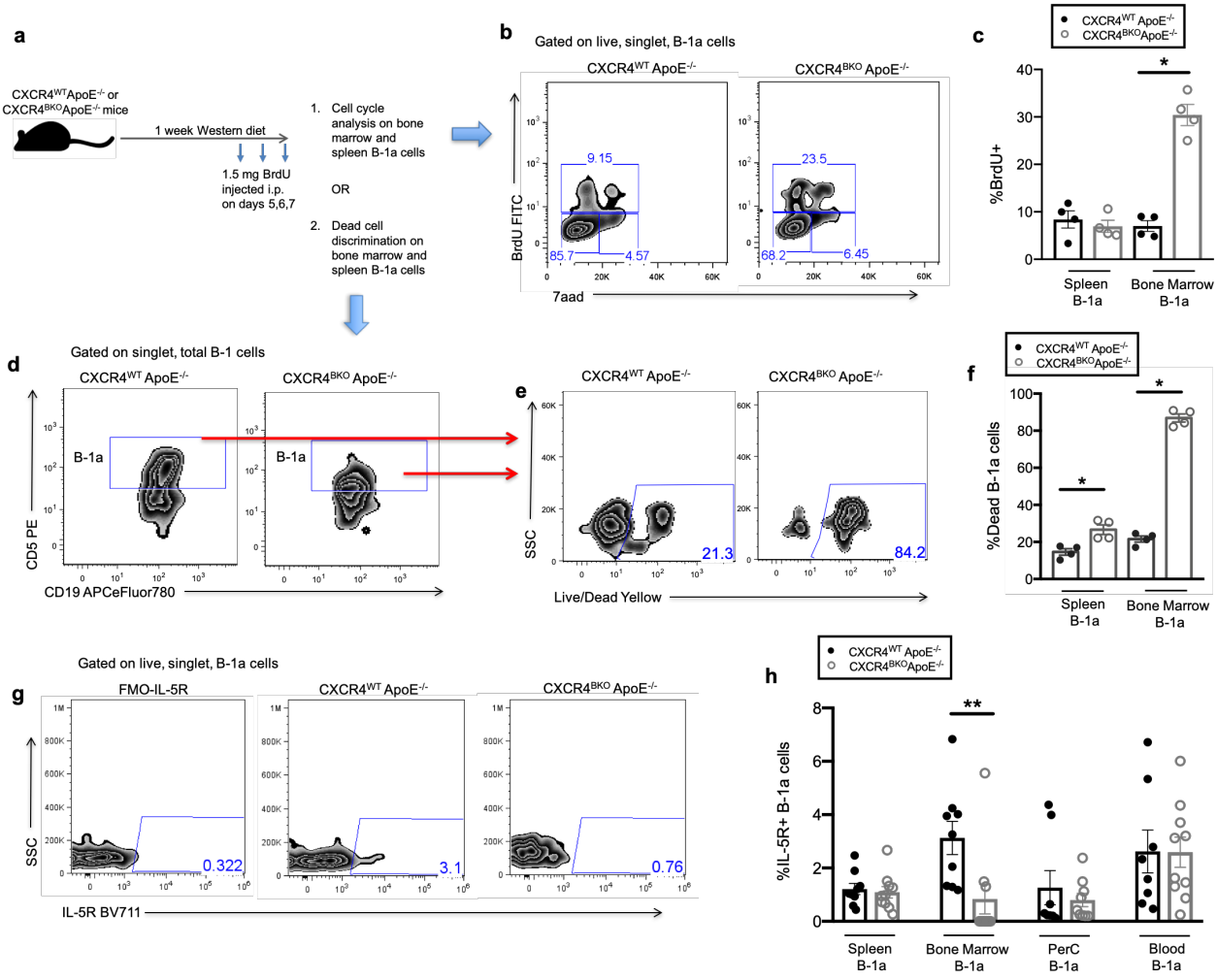
a
CXCR4WTApoE-/- or CXCR4BKOApoE-/- mice
1 week Western diet
1.5 mg BrdU injected i.p. on days 5,6,7
1. Cell cycle analysis on bone marrow and spleen B-1a cells
OR
2. Dead cell discrimination on bone marrow and spleen B-1a cells
b
Gated on live, singlet, B-1a cells
CXCR4WT ApoE-/-
CXCR4BKO ApoE-/-
BrdU FITC
7aad
9.15
85.7
4.57
23.5
68.2
6.45
c
CXCR4WT ApoE-/-
CXCR4BKOApoE-/-
%BrdU+
Spleen B-1a
Bone Marrow B-1a
d
Gated on singlet, total B-1 cells
B-1a
CD5 PE
CD19 APCeFluor780
e
SSC
Live/Dead Yellow
21.3
84.2
f
%Dead B-1a cells
g
Gated on live, singlet, B-1a cells
FMO-IL-5R
SSC
IL-5R BV711
0.322
3.1
0.76
h
%IL-5R+ B-1a cells
Spleen B-1a
Bone Marrow B-1a
PerC B-1a
Blood B-1a

DISCUSSION

The BM response to WD-induced hyperlipidemia

We began this chapter by examining the local bone marrow B-1a response to hyperlipidemia, and provided evidence that BM B-1a cells do not expand upon Western diet feeding. However, other B cell subsets, including B-1b and plasma cells could also produce atheroprotective IgM in the bone marrow. Yet, we demonstrate that the IgM ASC population in the bone marrow also does not expand in response to WD feeding. These data suggest that the BM is not a site for B-1a cell expansion or increased IgM production during hyperlipidemia. Because the BM is a site of constitutive atheroprotective IgM production, understanding the endogenous BM B-1a cell response is important because it could help to identify novel strategies for atheroprotection. We now know that the BM B-1a/IgM ASC population does not expand during hyperlipidemia, and that CXCR4 expression on B-1 cells also stays constant during hyperlipidemia (**Chapter 3, Figure 17**). This suggests that targeting CXCR4 on B-1a cells for increased BM localization may be an attractive option to effectively boost IgM production, since it is not already happening endogenously in mice. Our initial retroviral CXCR4 overexpression studies indicate that this is feasible (**Chapter 3, Figure 13**), though further studies are necessary to determine its effect on atheroprotection.

Alternatively, the relative IgM/B-1a homeostasis observed in the bone marrow in response to WD is itself an interesting finding, because it significantly differs from the spleen, where IgM ASC do increase during hyperlipidemia[188]. Whether there are immunoregulatory factors suppressing B-1a/IgM ASC expansion in the BM, or activating factors specific to the spleen might be an interesting avenue to pursue through analysis of secreted soluble factors within each niche. It may also be that the unique architecture

of the spleen, including specific B cell zones, enables a microenvironment favorable for IgM ASC expansion that is not present in the bone marrow. Many unanswered questions remain regarding the maintenance and differences between splenic and BM B-1 cells and IgM ASC, which are further explored in Chapter 5.

Previous studies have shown that the bone marrow B-1 population is critical for maintaining homeostatic levels of IgM[82]. This innate, natural IgM is an important first line of defense against exogenous pathogens[63,189], and for clearance of apoptotic cells[65,66,190]. Moreover, CD19 transgenic mice that contain an expanded B-1a compartment have increased titers of anti-PC natural IgM and reduced susceptibility to *S. pneumoniae* infection, while CD19$^{-/-}$ mice lacking B-1a cells have the opposite phenotype[50,51], indicating that B-1a cells are critical for generation of protective natural IgM. Our results align with this literature, as loss of BM B-1a cells in CXCR4^{BKO}ApoE$^{-/-}$ mice coincided with loss of PC-specific E06/T15 IgM. Interestingly, we found that plasma amount of E06/T15 IgM did not increase upon WD-feeding. This result also echoes previous studies demonstrating that B-1a-derived natural antibodies stay constant during influenza infection, while acquired antiviral IgM increases[40].

Notably, total plasma IgM levels increased in response to WD despite no increases in the BM B-1a/IgM ASC compartment. It appears that BM IgM production may not be necessary for generating the WD-induced increase in IgM, which could instead arise from splenic IgM ASC expansion, or IgM made in other niches such as the omental fat or PVAT. It is also important to consider the difference between innate natural IgM and antigen-induced/adaptive IgM, both of which can arise from B-1 cells[41]. For example, in contrast to E06/T15 IgM, we found that anti-MDA-LDL IgM was induced after WD. Several studies have shown that IgM specific for MDA epitopes is present in germ-free mice and expresses germline genes with limited N-additions, indicating that

MDA epitopes are targets of natural IgM antibodies[54,191]. However, several murine studies utilizing homologous MDA-LDL immunization demonstrate that MDA epitopes can also trigger adaptive immune responses. For example, MDA-LDL immunization induced MDA-specific T cell-dependent IgG antibodies and a T_H2 response[92,182]. In considering the sources for induced anti-MDA-LDL IgM in WD-fed mice, we note that the B-1b subset, especially, has been demonstrated to have adaptive immune capability and functions primarily through the TI-2 response that is BCR and antigen-specific[50,192]. Moreover, after adoptive transfer into lymphocyte-deficient Rag1$^{-/-}$ ApoE$^{-/-}$ mice, B-1b cells generate a greater amount of anti-MDA-LDL IgM compared to B-1a cells[38]. Thus, the fact that we see an induction in anti-MDA-LDL IgM after WD leads us to speculate that B-1b cells may contribute to this increase.

Overall, the observed differences between splenic and BM IgM ASC induction and between total and anti-MDA-LDL IgM versus E06/T15 IgM suggests that considerable heterogeneity exists within IgM-secreting B-1 populations. While B cell-specific loss of CXCR4 associated with loss of BM B-1a and reduced natural E06/T15 IgM, CXCR4-independent WD-induced IgM may have arisen from splenic IgM ASC expansion derived from B-1b or other B cell subsets. This heterogeneity aligns with a paradigm proposed by Baumgarth and colleagues, that distinct subsets of B-1 cells exist, some responsible for maintaining homeostatic IgM, and others that are primed responders responsible for generating antigen-induced IgM[41].

The B-1a cell-specific role of CXCR4 in IgM production

Next, to examine the B-1a-cell specific role of CXCR4, we turned to B-1a adoptive transfer into the B- and T-cell deficient Rag1$^{-/-}$ ApoE$^{-/-}$ model. We observed important differences in CXCR4-dependent regulation of total and anti-OSE IgM titers,

compared with the CXCR4^{BKO}ApoE$^{-/-}$ model. Specifically, while WD-fed CXCR4^{BKO}ApoE$^{-/-}$ mice did not have a deficiency in total and anti-MDA-LDL IgM compared to littermate controls (**Fig. 19e,g**), adoptive transfer of CXCR4^{BKO}ApoE$^{-/-}$ B-1a cells did result in reduced total and anti-MDA-LDL IgM titers compared to CXCR4^{WT}ApoE$^{-/-}$ B-1a cell transfer (**Fig. 21i,j**). Several differences between these models could account for these varying results. First, other B cell subsets that do not rely on CXCR4 for their maintenance could be responsible for IgM generation in CXCR4^{BKO}ApoE$^{-/-}$ mice, including splenic B-1b, as discussed above. Second, reduced B-1a number in multiple niches after adoptive transfer of CXCR4^{BKO}ApoE$^{-/-}$ B-1a cells (BM, spleen, and PerC; **Fig. 21c-e**), could have also contributed to the more marked reduction in IgM in the adoptive transfer model. Why absence of CXCR4 on B-1a cells results in this widespread reduction in B-1a number specifically after adoptive transfer, but not in the otherwise immunocompetent setting of the CXCR4^{BKO}ApoE$^{-/-}$ mouse is an interesting question for future study. It could be that other B cell subsets, T cells, or their secreted soluble factors, which are lacking in immunodeficient Rag1$^{-/-}$ ApoE$^{-/-}$ hosts, are important for maintaining long-term B-1a survival or localization in the spleen and PerC. Notably, we did not see marked differences in B-1a migration or number in the spleen after short-term 3-hour adoptive transfer of CXCR4^{BKO}ApoE$^{-/-}$ B-1a cells into Rag1$^{-/-}$ ApoE$^{-/-}$ hosts (**Chapter 3, Fig. 8**). This suggests that splenic B-1a loss observed after long-term transfer may be more indicative of impaired cell turnover or survival, as a consequence of increased age or hyperlipidemic conditions, rather than impaired migration.

Of note, the significant reduction in plasma IgM did not correlate with a marked defect in lesional IgM in Rag1$^{-/-}$ ApoE$^{-/-}$ mice given CXCR4^{BKO}ApoE$^{-/-}$ B-1a cells (**Fig. 21i vs Fig. 24b**). Whether lesional IgM accumulates from circulating IgM entering through leaky endothelium, or from vasa vasorum that brings in IgM generated in the PVAT and

adventitia remains an unanswered question. The contributions of PVAT B-1 cells versus peripheral B-1 cells to lesional IgM accumulation remains an area of open investigation. It is hard to answer these questions in our study, as lesional IgM likely accumulated over time, but we were only able to examine donor B-1a cell number at the time of sacrifice, post-16 weeks WD feeding. In the future, examining lesional IgM accumulation in mice with smooth muscle cell-specific deletion of PPAR-γ, which lack PVAT formation[193], could help determine the contribution of PVAT B-1 cells to lesional IgM and atheroprotection.

The role of B cell CXCR4 in atherosclerosis

We found that CXCR4 was not necessary for B-1a cell-mediated protection from WD-induced atherosclerosis, both in the $CXCR4^{BKO}ApoE^{-/-}$ model after 9 or 18 weeks WD, and in the adoptive transfer model into $Rag1^{-/-}$ $ApoE^{-/-}$ mice. However, the overall impact of loss of B-1a cells and IgM on atherosclerosis in the $CXCR4^{BKO}ApoE^{-/-}$ model was unclear, since perturbations were also seen in the B-2 cell subset (**Fig. 20c**), which has atherogenic functions. The $Rag1^{-/-}$ $ApoE^{-/-}$ model was also not ideal for assessment of atherosclerosis. These mice lack other B cell subsets and all T cells, which are known to influence atherosclerosis in both humans and mice. Moreover, the amount of IgM generated after B-1a adoptive transfer into $Rag1^{-/-}$ $ApoE^{-/-}$ mice was significantly lower than what was present in immunocompetent $ApoE^{-/-}$ mice after WD feeding. We have also attempted adoptive transfer into B cell deficient μMT mice, and mice deficient for secreted IgM. However, in these models, adoptively transferred B-1 cells do not survive and IgM titers generated by transferred B-1a cells are reduced to background levels by 3-6 weeks post-transfer[194, and data not shown].

Most significantly, we believe that standard murine models of atherosclerosis involving WD feeding are not ideal to answer whether CXCR4-mediated B-1a IgM production is atheroprotective, because of the excessive lipid burden present in these models. As shown in **Chapter 3 Figure 14**, we demonstrate that loss of secreted IgM enhances atherosclerosis in 80-weeks-aged ApoE$^{-/-}$ mice fed chow diet that have moderate cholesterol levels, but not in young ApoE$^{-/-}$ mice fed 8 weeks of Western diet that have excessive cholesterol levels. Because the primary mechanism whereby IgM is thought to protect against atherosclerosis development is through preventing oxidized LDL uptake by inflammatory cells and preventing downstream inflammatory processes, it may be that excessive cholesterol levels (and therefore excessive oxLDL) overwhelm this protective pathway. Alternative approaches to answering this question, and how we reconcile these results with our human findings from Chapter 3 are further discussed in Chapter 5.

Intriguingly, we also found that B-1a cell transfer reduced plasma non-HDL cholesterol in a manner independent of CXCR4 and circulating IgM. Previous studies also provide some support for B cell-mediated cholesterol reduction. For example, splenectomized ApoE$^{-/-}$ mice adoptively transferred with B cells from atherosclerotic ApoE$^{-/-}$ mice have reduced total cholesterol and reduced atherosclerosis[11]. Moreover, injection of apoptotic cells (which contain shared epitopes with oxLDL) reduced aortic root lesion area and total cholesterol in a B cell-dependent manner[72]. Our results are the first to show that B cell-mediated cholesterol reduction can be conferred by the B-1a subset, specifically. The mechanism by which B-1a cells reduce plasma cholesterol, if not through plasma IgM, is an interesting question for future study. One possible avenue to pursue is B-1 cell production of IL-10 [195], a cytokine which has previously been shown to alter circulating LDL levels[196] and cholesterol clearance by macrophages[197].

Alternatively, given the reduction in overall body weight after B-1a cell transfer, it could also be that B-1a cell recipients consumed less food or had other overall health differences from control PBS recipients, although triglyceride levels were no different and outward differences in mouse behavior characteristic of sickness were not visibly evident.

Another interesting finding was that B-1a cell transfer had region-specific effects on atherosclerosis, with significant attenuation of lesion area seen in the aortic arch and thoracic aorta, but no effect seen in the abdominal aorta. Of note, thoracic PVAT is phenotypically more similar to thermogenic brown adipose tissue while abdominal PVAT is more like white adipose tissue[198]. Whether this could impact on B-1a cell homing to these regions is unknown. Additionally, the aortic arch vascular smooth muscle cells (VSMCs) are from a different embryological origin than abdominal VSMC[199] and during lesion development, VSMC produce chemokines that attract B lymphocytes to the adventitia[87,200]. Further studies are needed to unravel these region-specific differences, which could inform strategies to enhance B-1a homing to PVAT.

The role of CXCR4 in B-1a cell homeostasis

Finally, we also provide evidence that CXCR4 regulates B-1a cell number by influencing B-1a cell survival. While CXCR4 has been linked to cell survival in hematopoietic progenitor cells and in cancer [134,135,138,201], niche-dependent regulation of B-1a cell homeostasis by CXCR4 has not previously been reported. We demonstrate a marked increase in BrdU+ B-1a cells and increased B-1a cell death in bone marrow, but not spleen, of $CXCR4^{BKO}ApoE^{-/-}$ mice compared to littermate control mice. Though increased BrdU may initially suggest increased cell proliferation, it has previously been shown that BrdU can be incorporated during apoptosis[202], or could be evidence for DNA

repair[203]. Intriguingly, CXCR4 antagonism has been shown to induce multinucleation, G2-M cell cycle arrest, and abnormal mitosis in ovarian cancer cells, coinciding with deregulated expression of DNA damage and spindle assembly checkpoint proteins, including Cdc2, Cdc25a, and Chk1, which are involved with progression from G2 to M phase [204]. CXCR4 has also been shown to regulate expression, localization, and phosphorylation of the cell cycle proteins Rb and E2F-1 in neurons[205]. In germinal center (GC) B cells, CXCR4 was demonstrated to increase in expression throughout the GC B cell cycle, with the highest relative expression on cells in G2/M phase, scaling with increased cell surface area [206]. These studies suggest that CXCR4 may be important for B-1a cell turnover as well, and lead us to hypothesize that our observations in $CXCR4^{BKO}ApoE^{-/-}$ mice could arise from an arrest in transition from G2 to M phase in BM B-1a cells. Several studies could be performed to test this hypothesis. First, analysis of cell cycle protein expression or phosphorylation status in sorted BM B-1a cells from $CXCR4^{WT}ApoE^{-/-}$ and $CXCR4^{BKO}ApoE^{-/-}$ mice could indicate whether proteins regulating the G2-M transition differ in the absence of CXCR4. Second, as CXCR4-mediated chemotaxis relies on actin polymerization, and rearrangement of the cytoskeleton is also involved in cell division, we could test for defects in actin polymerization and presence of multinucleated B-1a cells in $CXCR4^{BKO}ApoE^{-/-}$ BM using Imagestream. Another exciting possibility would be to utilize Fucci mice, in which dual-labeling of cells in G1 versus S/G2/M phases facilitates live cell imaging of cell cycle transitions. Isolation and transfection of Fucci B-1 cells with CXCR4 siRNA or overexpression with our previously generated CXCR4-GFP retrovirus and subsequent cell cycle visualization could pinpoint if and where a cell cycle block occurs.

Loss of CXCR4 on B-1a cells also resulted in a significant reduction in IL-5R expression on B-1a cells specifically in the bone marrow. IL-5/IL-5R signaling promotes

B-1a cell survival, proliferation, and IgM secretion [89,90,92,100], suggesting that loss of IL-5R may contribute to the homeostatic alterations we found in CXCR4^{BKO} ApoE$^{-/-}$ bone marrow B-1a cells, including increased cell death. It has previously been shown that IL-10 and CXCL12 act in synergy on peritoneal B-1 cells[93], suggesting that cytokines and chemokines can act cooperatively to modulate B-1 cell function. However, to our knowledge, our finding that loss of CXCR4 leads to reduced IL-5R expression is novel. How exactly B-1a expression of CXCR4 alters IL-5R expression remains unanswered and is an intriguing area for future study. First, to test whether reduced IL-5R expression is a consequence of B cell-intrinsic loss of CXCR4, and to see if this is functionally relevant, we could isolate CXCR4^{WT}ApoE$^{-/-}$ and CXCR4^{BKO}ApoE$^{-/-}$ B-1a cells and culture in the presence of IL-5, CXCL12, or both, and then measure IL-5R expression, cell proliferation, apoptosis, and IgM secretion. If CXCL12 stimulation induces increased IL-5R expression in CXCR4^{WT}ApoE$^{-/-}$ but not CXCR4^{BKO}ApoE$^{-/-}$ B-1a cells, this would indicate that CXCR4 signaling induces IL-5R expression in a B cell-intrinsic manner, and that our finding of reduced IL-5R expression on CXCR4-deficient BM B-1a cells was not a consequence of other factors in the bone marrow environment. Furthermore, if IL-5 stimulation led to cell proliferation, increased IgM secretion, or reduced apoptosis in a CXCR4-dependent manner, that would further establish a functional link between the two receptors. It was recently shown that CXCR4 colocalizes with the IgD-BCR and CD19 on the cell surface of splenic B cells, and that CXCR4-induced actin cytoskeleton remodeling depended on the IgD-BCR [207]. Whether IL-5R is also clustered close to CXCR4 on the cell surface could be tested using confocal microscopy or Imagestream, or more robust techniques like FRET or proximity ligation assay.

In sum, the data provided in this chapter raises many more questions about the role of CXCR4 in regulating B-1a cell homeostasis, and the role of BM B-1a cells and

BM IgM secretion in atherosclerosis. The implications of our findings and future approaches to address these questions are discussed further in Chapter 5.

Chapter 5

Discussion and Future Directions

Atherosclerosis is a complex, multi-factorial disease that has both genetic and environmental roots. Multiple contributors influence the development of atherosclerosis and the progression to cardiovascular events, including age, smoking, high blood pressure, lipid metabolism, deregulation of vascular wall cells, thrombotic factors, and the immune system. Much time, money, and research effort has been spent on understanding and treating atherosclerosis and heart disease, making it America's costliest disease according to the American Heart Association (AHA). The AHA has set a strategic goal to improve the cardiovascular health of all Americans by 20% while decreasing deaths from CVD and stroke by 20% by the year 2020[208]. To attain this goal, the AHA has recommended 7 lifestyle approaches to achieve better cardiovascular health, which include no smoking, regular physical activity, healthy diet, and maintenance of a healthy weight, blood pressure, cholesterol, and blood sugar level. Several of these lifestyle recommendations can also have a positive impact in improving immunity[209,210], and conversely, deregulated immune mechanisms are involved in obesity[211], hypertension[212], lipid metabolism[213], and diabetes[214] in turn. This suggests that some risk factors contributing to heart disease may converge on common immune pathways, and underscores the importance of efforts to identify key immune regulatory mechanisms in atherosclerosis. Evidence for the contribution of innate and adaptive immunity to atherosclerosis development has accumulated over the last few decades, and more recent advances have demonstrated complex, immune cell subset-specific roles that sustain or mitigate lesion advancement[4,215]. As our knowledge advances, deeper, more robust, and unbiased investigation into immune cell surface marker heterogeneity, functional diversity, and the associated impact on human disease becomes relevant for identifying disease biomarkers and developing targeted therapies.

In Chapters 3 and 4, we presented evidence that CXCR4 regulates B-1a number in the bone marrow, a population expressing a unique IgH V repertoire, and atheroprotective IgM production. We explore potential mechanisms by which CXCR4 regulates BM B-1a number, including migration and survival. Key differences between the BM and spleen IgM ASC response to WD-induced hyperlipidemia are demonstrated. Furthermore, we test whether B-1a CXCR4 expression facilitates atheroprotection in mice, and observe positive associations between human B-1 CXCR4 expression, anti-OSE IgM production, and protection in human CVD. Several new questions arise from this work, including: 1) What are the mechanisms facilitating IgH V repertoire diversification in BM B-1a cells? 2) Why are spleen and BM IgM ASC induced differently during WD? 3) Can B-1 cell heterogeneity be utilized for therapy? 4) Are WD-induced atherosclerosis models sufficient for studying B-1- or IgM-related mechanisms? 5) Could human B-1 CXCR4 expression be used as a therapeutic target? In this chapter, these remaining questions and future experiments to address them will be discussed.

The BM B-1a population expresses a unique IgH V repertoire

We demonstrate that the BM B-1a IgH V repertoire from 100-weeks-aged ApoE$^{-/-}$ mice is unique, diversified, and displays a shift away from germline sequences, compared to that of PerC B-1a cells. An important next question is what mechanisms facilitate this diversification in the BM. It is known that the enzyme Tdt, which facilitates N-additions, is not expressed during fetal life[103]. This suggests that niches where B-1a cells don't express many N-additions, like the PerC, may largely be derived from fetal liver precursors that self-renew throughout life. In contrast, the progenitor source seeding the BM B-1a population is not known. Montecino-Rodriguez et al identified a Lin^{-} CD19^{+}B220^{lo}CD93^{+} B-1 cell progenitor present at low frequency in adult bone marrow[104].

These adult BM B-1 progenitors express Tdt and their progeny acquire N-additions[103]. Therefore, the increased N-additions and repertoire diversity observed in BM B-1a cells in our experiment could be explained by their originating from the adult BM B-1 progenitor, rather than the fetal liver progenitors that give rise to body cavity B-1a cells. To test this, one could isolate and transfer either the $CD19^{+}B220^{lo}CD93^{+}$ adult BM B-1 progenitor or B-1 fetal liver progenitors into immunodeficient hosts, and examine the B-1a progeny generated in the bone marrow. If one of the progenitor populations is better able to regenerate wild-type numbers of BM B-1a cells that display a similar phenotype of increased N-additions, this may point to the progenitor source for the adult BM B-1a population. Alternatively, we may find that BM B-1a population is derived from multiple progenitor pools.

While a distinct B-1 progenitor could contribute to BM B-1a repertoire diversity, we also found commonalities between the PerC and BM B-1a repertoire. Indeed, certain VDJ and CDR-H3 sequences were common to both BM and PerC B-1a, and the most frequent CDR-H3 expressed by PerC and BM B-1a was the same: AGDYDGYWYFDV. This suggested to us that migration from PerC to BM could be possible, which we confirmed and demonstrated was CXCR4-dependent. Yet, we observed that B-1a migration to the BM was limited compared with B-1a migration to the spleen. As an alternative to migration, the presence of common IgH V sequences in BM and PerC B-1a could instead arise from separate and independent selection pressure in these niches driven by common antigens. For example, B-1a cells expressing AGDYDGYWYFDV, a CDR-H3 previously associated with recognizing phosphatidylcholine epitopes[49], could independently arise in PerC and BM due to heightened presence of PtC epitopes in aged $ApoE^{-/-}$ mice. The fact that 70% of PerC B-1a sequences expressed AGDYDGYWYFDV, compared with only 11.6% of BM B-1a sequences, could point to

reduced availability of PtC epitopes in the BM versus PerC. To differentiate between migration versus independent selection, one could analyze the BM IgH V repertoire after disrupting migration, for example using pertussis toxin, which inactivates chemokine receptor signaling, or specific chemokine receptor blockade or knockdown.

Importantly, more studies on the BM B-1a IgH V repertoire are needed to determine whether our results are a consequence of age or hyperlipidemic conditions in 100-weeks-aged ApoE$^{-/-}$ mice. Future IgH V repertoire analysis in younger mice, or mice without ApoE$^{-/-}$ deficiency may help to understand how the BM B-1a repertoire changes with time or with increased inflammation. While we did not see an expansion of BM B-1a cells in response to WD (**Chapter 4, Fig. 19a**), it could be that the IgM repertoire undergoes shifts instead. It is also important to note that while comparing the CDR-H3 of IgH V can provide some insight into BCR/antibody specificity, a major limitation of our approach is that the corresponding light chain regions were not sequenced or analyzed. The mature BCR consists of both heavy and light chains, and in order to determine antigen specificity, we would need to sequence the light chain variable region, amplify and express the light and heavy chains as single chain variable fragments via cloning methods, then test their specificities against an array of epitopes. These future experiments would be helpful to determine what BCR specificities are selected for during hyperlipidemia, and may facilitate discovery of new antigens to target against for atheroprotection.

<u>CXCR4 maintains BM B-1a number through regulating migration and survival</u>

Our data indicates that CXCR4 regulates BM B-1a number through regulating both B-1a migration to the BM and B-1a homeostasis. The circulatory patterns of B-1 cells remain incompletely understood and are a complex area of study. The methods we

used including adoptive transfer and flow cytometry are limited in that what we get is a snapshot image that is less informative about the kinetics of migration. Indeed, how frequently the BM B-1a population is replenished by migrating peripheral B-1a cells remains unknown. We found that the number of B-1a cells that migrated to the bone marrow was less than the number that migrated to the spleen both after short-term (**Chapter 3 Fig. 8c,d**) and long-term (**Chapter 4, Fig. 21c,d**) adoptive transfer. This could indicate that at least part of the BM B-1a population has more of a resident nature, maintaining itself through self-renewal, or replenishment through the aforementioned adult BM B-1 progenitor. Novel techniques like intravital imaging of intact bone marrow[216] could provide more information on whether and where B-1 cells organize in the bone marrow, how quickly they are replenished, and whether they interact with other cell types that could be important for their maintenance. While the BM localization of the B-1a subset, specifically is not known, previous studies have demonstrated that IgM+ B cells localize to both extravascular and intravascular regions of the bone marrow, often adjacent to sinusoid walls[217]. Some studies have suggested that their perisinusoidal location may increase their accessibility to encounter and respond to blood-borne pathogens[218].

We also demonstrated that absence of CXCR4 significantly impaired BM B-1a survival, and discussed potential next steps to examine the role of CXCR4 in cell cycle maintenance in Chapter 4. Studies by Nie et al[132] previously demonstrated that CXCR4 is important for B-2 progenitor cell retention and survival in the bone marrow, with B cell-specific loss of CXCR4 resulting in premature egress of B-2 cell progenitors into spleen and subsequent cell death. If CXCR4 is also important for regulating B-1a cell progenitors, then reduced progenitor cell survival could also contribute to the loss of mature BM B-1a cells we observe in $CXCR4^{BKO}ApoE^{-/-}$ mice. Near the start of this

project, we observed that CXCR4^{BKO}ApoE$^{-/-}$ mice had a defect selectively in BM B-1a cells, not spleen or PerC B-1a (**Chapter 3, Fig. 9b**). This led us to think that B-1a progenitor cell survival is likely not affected by loss of CXCR4, since B-1a cells are largely fetally-derived, and if loss of CXCR4 did impair B-1a progenitor survival, then we'd see global loss of B-1a number in all examined niches. However, since then, it has become clearer that separate B-1a progenitor pools exist, both in fetal liver and in adult BM, and that they can give rise to B-1a cells with distinct characteristics, including varying N-addition frequency[103]. Therefore, it is possible that the BM B-1a pool arises from adult BM B-1 progenitors in a CXCR4-dependent manner, while the PerC and/or spleen B-1a pool arises primarily from fetal liver progenitors in a CXCR4-independent manner. This hypothesis is supported by preliminary data demonstrating a loss of the CD19^{+}B220^{lo}CD93^{+} adult BM B-1 cell progenitor in CXCR4^{BKO}ApoE$^{-/-}$ mice (**Fig. 27**). Future studies on the CXCR4 dependency of adult BM B-1 progenitors could involve determining whether B-1a progenitors have disrupted localization in the BM microenvironment upon CXCR4 blockade using intravital imaging, or whether the B-1a progenitor cell cycle is impaired in the absence of CXCR4. Overall, our data suggest that a more complex heterogeneity in B-1a subsets exists than previously assumed, and that it is necessary for future studies to examine B-1a subsets not only in a surface marker-specific manner, but also in a niche-specific manner.

Figure 27. CXCR4^{BKO}ApoE$^{-/-}$ mice have reduced number of adult bone marrow B-1 progenitor cells. (**a**) Representative gating strategy for quantification of CD19+ B220lo IgM- CD93(AA4.1)+ BM B-1 progenitor cells from one CXCR4^{WT}ApoE$^{-/-}$ (top) and one CXCR4^{BKO}ApoE$^{-/-}$ (bottom) mouse. (**b**) Calculated number of CD19+ B220lo IgM- CD93(AA4.1)+ B-1 progenitor cells in CXCR4^{WT}ApoE$^{-/-}$ (n=3) and CXCR4^{BKO}ApoE$^{-/-}$ (n=2) mice.

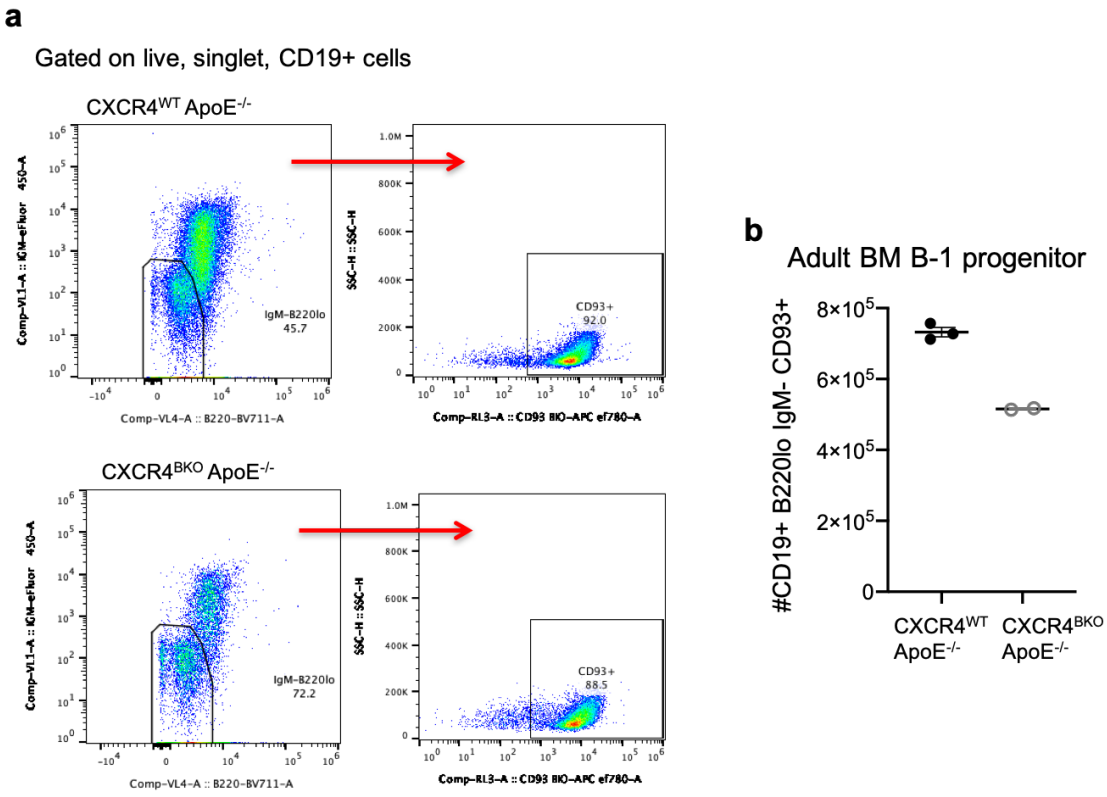

B-1 cell heterogeneity in mice

The data presented in chapters 3 and 4 indicate that the BM B-1a population is unique, and may be regulated by distinct mechanisms compared to PerC and splenic B-1a cells. These differences become functionally relevant in health and disease when considering the possibility that B-1a cells from different niches may have evolved for unique functions, or for IgM production against distinct antigens. Serosal peritoneal and pleural B-1 cells may have evolved to be rapid responders for exogenous antigens that enter through the gut and airways, while BM B-1 cells may have evolved to provide baseline homeostatic IgM production for sterile inflammatory processes like clearance of apoptotic cells. All of these B-1 populations may become important in the setting of atherosclerosis due to epitopes that are common to oxLDL, apoptotic cells, and exogenous pathogens, like PC and MDA.

Constitutive IgM production is lower in the PerC compared with the spleen and BM[78,82], and we have shown that BM IgM ASC do not expand in response to WD-induced hyperlipidemia in contrast to splenic IgM ASC (**Chapter 4, Fig. 19**). Therefore, important next questions include what maintains differential IgM production in these niches and what governs whether they can be induced or not? Previous studies have shown that in contrast to BM IgG ASC, the BM IgM ASC population does not rely on eosinophils or IL-6, but is sustained by IL-5 at least *in vitro*[91]. We also observed reduced IL-5R expression on BM B-1a cells from CXCR4^{BKO}ApoE$^{-/-}$ mice (**Chapter 4, Fig. 26**), coinciding with reduced B-1a number. IL-5-producing ILC2 cells have previously been shown to maintain peritoneal and fat-associated lymphoid cluster (FALC) B-1a number[99,100], and ILC2 are also found in the bone marrow[219]. Therefore, the dependence of BM IgM ASC/B-1a on IL-5/ILC2 production could be examined in the future using ILC2 knockout mice. Testing whether BM IgM ASC can be induced to increase IgM

production by exogenous IL-5 administration for atheroprotection might also be a potentially therapeutically relevant study. In these studies where BM IgM ASC are manipulated to increase IgM production, it would be important to develop targeted strategies and find an effective therapeutic window, to avoid IgM overproduction or autoimmunity.

Factors specific to the spleen could also maintain splenic IgM ASC or facilitate WD-induced IgM ASC expansion in the spleen. Our results demonstrating that the splenic B-1a population relies on CXCR4 after B-1a adoptive transfer into $Rag1^{-/-}$ $ApoE^{-/-}$ mice (**Chapter 4, Fig. 21d**), but does not require CXCR4 for its maintenance in $CXCR4^{BKO}ApoE^{-/-}$ mice (**Chapter 3, Fig. 9b**), suggests that splenic B-1a may rely on other cell types or secreted factors not present in $Rag1^{-/-}$ $ApoE^{-/-}$ mice. Interestingly, splenic B-1 cells have previously been shown to associate closely with the follicular dendritic cell (FDC) network, and splenic B cells support FDC development through production of lymphotoxin alpha[220,221]. Furthermore, B cells can serve as antigen transporters to FDC via complement or immune complexes, and conversely FDC can present antigen to cognate B cells to initiate the development of memory B cells or plasma cells[222]. This suggests a close link between splenic B cells and FDC that may be important for the maintenance of both populations. Therefore, a hypothesis to explain our differing results in $Rag1^{-/-}$ $ApoE^{-/-}$ versus $CXCR4^{BKO}ApoE^{-/-}$ mice could be: despite absence of CXCR4 on splenic B-1a, normal FDC development in $CXCR4^{BKO}ApoE^{-/-}$ mice supports or “rescues” splenic B-1a survival. In contrast, impaired FDC development in $Rag1^{-/-}$ $ApoE^{-/-}$ mice (due to lack of B cells) could result in impaired splenic B-1a survival in the absence of CXCR4. Co-culture experiments with FDC and CXCR4-deficient or –sufficient splenic or BM B-1a cells could help test this hypothesis, or examining splenic

IgM ASC and B-1a number in mice undergoing FDC ablation, which has previously been described[223].

In Chapter 4, we also discussed how the splenic B-1b population could contribute to the increase in IgM ASC and plasma IgM. Importantly, the report identifying increased anti-OSE IgM ASC in the spleen in response to hyperlipidemia found that there was no change in the frequency of splenic B-1a cells[72], similar to our results (**Fig. 19b**). Yet, they did find an increase in marginal zone B cells with hyperlipidemia, but splenic B-1b frequency was not examined. As MZ B cells and B-1b both participate in TI-2 responses, it is conceivable that splenic B-1b cells could also expand or secrete more IgM in response to hyperlipidemia. Given the possibility that B-1b cells could be induced during hyperlipidemia whereas B-1a cells may not be, understanding the differences between B-1a and B-1b cells also becomes important. Prior studies have demonstrated that B-1a cells primarily function in TI-1 responses activated through TLR or cytokine receptor signaling, while B-1b cells participate in TI-2 responses through the BCR and can generate B-1 cell memory[50,51]. CD5, which is used to distinguish B-1a from CD5- B-1b cells, functions as a negative regulator of BCR signaling[224]. An intriguing new study by Baumgarth and colleagues demonstrates that CD5+ peritoneal B-1a cells can lose expression of CD5 after TLR-mediated activation, which reorganizes the BCR signaling complex and leads to increased downstream BCR signaling[225]. This finding suggests that B-1a and B-1b cells may actually not be two separate populations, but varying activation states of the same population. Many questions remain, including 1) do B-1a cells from other locations like the spleen and BM also function similarly? 2) is loss of CD5 expression reversible, and can a B-1a cell that has differentiated into B-1b revert back to its CD5+ state? 3) do the antibodies made by CD5+ B-1 cells and activated CD5- B-1 cells differ? Future studies on isolated and TLR-stimulated BM/splenic B-1

subsets and subsequent analysis of CD5 expression and the IgH V repertoire could begin to answer these questions.

Overall, several different mechanisms could contribute to B-1 cell heterogeneity in mice, including niche-specific factors or antigens, development from distinct progenitor cells, or TLR- vs BCR-mediated signaling events. Given that B-1 cells have diverse immunoregulatory functions outside of IgM production, including cytokine production, antigen presentation, phagocytic capability, T cell modulation, and a newly discovered cholesterol-lowering capability, it is also important to examine functional differences in a niche-specific manner. Our data also suggests that B-1 heterogeneity could be taken advantage of for developing therapies for atheroprotection. For example, CXCR4 overexpression on B-1a cells selectively increased trafficking to the bone marrow and increased anti-OSE IgM production. Similar strategies could be developed to increase B-1 trafficking to other locations that are more conducive to IgM ASC expansion during hyperlipidemia, like the spleen, or for other niche-specific B-1 cell functions.

B-1 cell heterogeneity in humans

Previous reports by Rothstein's group[165-167] as well as ongoing studies in our lab demonstrate that the human CD20+ CD3- CD27+ CD43+ B-1 population is heterogeneous. The results provided in Chapter 3 demonstrate that functional heterogeneity in the B-1 subset can be separated by CXCR4 expression. While the overall frequency of circulating human B-1 cells did not associate with plasma anti-MDA-LDL IgM or reduced plaque burden, the addition of CXCR4 expression on B-1 cells did. Our analysis of PBMC has the caveat that B-1 cells are likely not secreting antibody within the blood itself, and may behave differently within tissues. Yet, because we are

examining a receptor that regulates trafficking, and because the peripheral blood is a highway for cells to get to their eventual destination, our associations point to the idea that CXCR4 guides human B-1 cells to niches where atheroprotective IgM is produced, like the bone marrow. Ongoing and future studies in our lab aim to examine human B-1 cell phenotype and function in other locations like the peritoneal fluid, spleen, or bone marrow to test whether this hypothesis stands. Notably, the CXCR4 antagonist plerixafor is used clinically for BM hematopoietic stem cell mobilization and autologous HSC transplantation in patients with non-Hodgkin's lymphoma and multiple myeloma[226]. Moreover, plerixafor can enhance the pro-apoptotic effects of anti-CD20 monoclonal antibody (rituximab) used to treat patients with diffuse large B cell lymphoma[227]. This is in line with studies in mice showing that CXCR4 is important for maintaining B cell survival. Examining the human B-1 cell population in patients undergoing plerixafor treatment might be useful for understanding whether CXCR4 impacts B-1 localization or functions, but it is also important to consider that patients receiving plerixafor likely don't represent healthy or normal conditions, and that plerixafor treatment targets all cells expressing CXCR4, not just the human B-1 subset.

It is likely that deeper heterogeneity exists in the human B-1 subset and that other surface markers also associate with distinct B-1 cell functions. Examining peripheral B-1 cells using techniques like CyTOF, which allow analysis of up to 40 surface or intracellular markers in a multidimensional, semi-unbiased way could identify new B-1 phenotypes that correlate with anti-OSE IgM production or atheroprotection. Novel studies in our lab have used CyTOF to examine B cell populations in patients with either high or low amount of plasma anti-MDA-LDL IgM (unpublished data). This analysis has identified 2 B cell clusters that display the typical Rothstein B-1 markers, CD27 and CD43, but that have differential IgM production *in vitro* and *in vivo*, and

differentially express CD24, a marker previously shown to inhibit CXCR4 function in a human pre-B cell line[228]. Whether these clusters also differ in signaling responses to TLR versus BCR-stimulation, cytokine production, antigen presentation and T cell stimulation, or other B-1 characteristics remain interesting unanswered questions for the future. Our lab is also interested in examining whether B cell populations differ in subjects with high or low amount of coronary artery disease. Future analysis in CAD subject cohorts of markers that regulate B cell checkpoints, chemokine receptor expression, signaling molecules, or markers involved in B cell regulation of other immune cells would increase understanding of how B cell populations change during CAD.

Limitations of WD-induced atherosclerosis models

As with any experimental disease model, it is important to consider how closely it recapitulates human disease and the human immune system. The data presented in preceding chapters indicates that WD-induced atherosclerosis models are significantly limited in representing human CVD, because of the extreme lipid burden present. Moreover, the use of immunodeficient $Rag1^{-/-}$ $ApoE^{-/-}$ mice is similarly flawed, as the absence of T and other B cells removes the contributions of these cells and their interactions, which are known to influence atherosclerosis development. Though this model provided a clean background to visualize adoptively transferred B-1a cells and IgM, sufficient IgM was not generated in $Rag1^{-/-}$ $ApoE^{-/-}$ mice to withstand the non-physiologic cholesterol burden created by 16 weeks WD. This does not diminish prior studies utilizing WD-fed models, which demonstrate that B-1a cell IgM production is atheroprotective, only that considering the balance between anti-OSE IgM and cholesterol in any given model may be important in designing future studies. Alternative

strategies utilizing immune-sufficient models, multiple B-1 cell injections to generate wild-type levels of IgM, or aged chow-fed ApoE$^{-/-}$ mice pose their own challenges and limitations, but may be useful for corroborating our findings.

B-1 CXCR4 expression as a therapeutic target

Overall, our studies suggest that strategies to increase B-1 CXCR4 expression may be protective against atherosclerosis. Intriguingly, the association between human B-1 CXCR4 expression and reduced plaque burden and stenosis was stronger than that between B-1 CXCR4 expression and amount of anti-MDA-LDL IgM (**Chapter 3 Fig. 15f vs Fig. 16d**). Moreover, multivariate analysis indicated that human B-1 CXCR4 expression associated with reduced plaque burden regardless of inclusion of anti-MDA-LDL IgM in the multivariate model. This suggests that B-1 CXCR4 expression may also regulate atheroprotective functions outside of IgM production. Does human B-1 CXCR4 expression also associate with B-1 ability to secrete cytokines, present antigen, or alter T cell function? Alternatively, does the IgM repertoire differ in B-1 subsets that have unique functions? Future *in vitro* studies addressing these questions would help understanding of this fascinating cell subset. Alternative strategies to overexpress B-1 CXCR4 *in vivo*, using lentiviral systems or liposomal delivery, or the discovery of a B-1 cell-specific surface receptor to use in targeted delivery of siRNA or CXCR4 antagonists, could aid future pre-clinical studies determining if B-1 CXCR4 expression is atheroprotective.

LITERATURE CITED

1 Global, regional, and national age–sex specific all-cause and cause-specific mortality for 240 causes of death, 1990–2013: a systematic analysis for the Global Burden of Disease Study 2013. *The Lancet* **385**, 117-171, doi:10.1016/S0140-6736(14)61682-2 (2015).

2 Benjamin, E. J. *et al.* Heart Disease and Stroke Statistics-2018 Update: A Report From the American Heart Association. *Circulation* **137**, e67-e492, doi:10.1161/CIR.0000000000000558 (2018).

3 Hansson, G. K. Regulation of immune mechanisms in atherosclerosis. *Annals of the New York Academy of Sciences* **947**, 157-165; discussion 165-156 (2001).

4 Libby, P., Lichtman, A. H. & Hansson, G. K. Immune effector mechanisms implicated in atherosclerosis: from mice to humans. *Immunity* **38**, 1092-1104, doi:10.1016/j.immuni.2013.06.009 (2013).

5 Libby, P., Ridker, P. M. & Hansson, G. K. Progress and challenges in translating the biology of atherosclerosis. *Nature* **473**, 317-325, doi:10.1038/nature10146 (2011).

6 Ridker, P. M. *et al.* Antiinflammatory Therapy with Canakinumab for Atherosclerotic Disease. *N Engl J Med*, doi:10.1056/NEJMoa1707914 (2017).

7 Perry, H. M., Bender, T. P. & McNamara, C. A. B cell subsets in atherosclerosis. *Frontiers in Immunology* **3**, doi:10.3389/fimmu.2012.00373 (2012).

8 Tsiantoulas, D., Diehl, C. J., Witztum, J. L. & Binder, C. J. B Cells and Humoral Immunity in Atherosclerosis. *Circulation Research* **114**, 1743-1756, doi:10.1161/circresaha.113.301145 (2014).

9 Srikakulapu, P. & McNamara, C. A. B cells and atherosclerosis. *Am J Physiol Heart Circ Physiol* **312**, H1060-H1067, doi:10.1152/ajpheart.00859.2016 (2017).

10 Montecino-Rodriguez, E. & Dorshkind, K. B-1 B cell development in the fetus and adult. *Immunity* **36**, 13-21, doi:10.1016/j.immuni.2011.11.017 (2012).

11 Caligiuri, G., Nicoletti, A., Poirier, B. & Hansson, G. K. Protective immunity against atherosclerosis carried by B cells of hypercholesterolemic mice. *The Journal of clinical investigation* **109**, 745-753, doi:10.1172/JCI7272 (2002).

12 Major, A. S., Fazio, S. & Linton, M. F. B-lymphocyte deficiency increases atherosclerosis in LDL receptor-null mice. *Arterioscler Thromb Vasc Biol* **22**, 1892-1898 (2002).

13 Ait-Oufella, H. *et al.* B cell depletion reduces the development of atherosclerosis in mice. *The Journal of Experimental Medicine* **207**, 1579-1587, doi:10.1084/jem.20100155 (2010).

14 Kyaw, T. *et al.* Depletion of B2 but not B1a B cells in BAFF receptor-deficient ApoE mice attenuates atherosclerosis by potently ameliorating arterial inflammation. *PloS one* **7**, e29371, doi:10.1371/journal.pone.0029371 (2012).

15 Kyaw, T. *et al.* Conventional B2 B cell depletion ameliorates whereas its adoptive transfer aggravates atherosclerosis. *Journal of immunology* **185**, 4410-4419, doi:10.4049/jimmunol.1000033 (2010).

16 Sage, A. P. *et al.* BAFF Receptor Deficiency Reduces the Development of Atherosclerosis in Mice—Brief Report. *Arteriosclerosis, Thrombosis, and Vascular Biology* **32**, 1573-1576, doi:10.1161/ATVBAHA.111.244731 (2012).

17 George, J. *et al.* Hyperimmunization of apo-E-deficient mice with homologous malondialdehyde low-density lipoprotein suppresses early atherogenesis. *Atherosclerosis* **138**, 147-152 (1998).

18 Zhou, X., Caligiuri, G., Hamsten, A., Lefvert, A. K. & Hansson, G. K. LDL immunization induces T-cell-dependent antibody formation and protection against atherosclerosis. *Arterioscler Thromb Vasc Biol* **21**, 108-114 (2001).

19 Gistera, A. *et al.* Low-Density Lipoprotein-Reactive T Cells Regulate Plasma Cholesterol Levels and Development of Atherosclerosis in Humanized Hypercholesterolemic Mice. *Circulation* **138**, 2513-2526, doi:10.1161/CIRCULATIONAHA.118.034076 (2018).

20 Schiopu, A. *et al.* Recombinant human antibodies against aldehyde-modified apolipoprotein B-100 peptide sequences inhibit atherosclerosis. *Circulation* **110**, 2047-2052, doi:10.1161/01.CIR.0000143162.56057.B5 (2004).

21 Tsimikas, S. *et al.* Relationship of IgG and IgM autoantibodies to oxidized low density lipoprotein with coronary artery disease and cardiovascular events. *Journal of Lipid Research* **48**, 425-433, doi:10.1194/jlr.M600361-JLR200 (2007).

22 Tsimikas, S. *et al.* Oxidation-specific biomarkers, prospective 15-year cardiovascular and stroke outcomes, and net reclassification of cardiovascular events. *Journal of the American College of Cardiology* **60**, 2218-2229, doi:10.1016/j.jacc.2012.08.979 (2012).

23 Bagchi-Chakraborty, J. *et al.* B Cell Fcgamma Receptor IIb Modulates Atherosclerosis in Male and Female Mice by Controlling Adaptive Germinal Center and Innate B-1-Cell Responses. *Arterioscler Thromb Vasc Biol* **39**, 1379-1389, doi:10.1161/ATVBAHA.118.312272 (2019).

24 Bot, I. *et al.* Perivascular mast cells promote atherogenesis and induce plaque destabilization in apolipoprotein E-deficient mice. *Circulation* **115**, 2516-2525, doi:10.1161/CIRCULATIONAHA.106.660472 (2007).

25 Sun, J. *et al.* Mast cells promote atherosclerosis by releasing proinflammatory cytokines. *Nat Med* **13**, 719-724, doi:10.1038/nm1601 (2007).

26 Wang, K. Y. *et al.* Histamine deficiency decreases atherosclerosis and inflammatory response in apolipoprotein E knockout mice independently of serum cholesterol level. *Arterioscler Thromb Vasc Biol* **31**, 800-807, doi:10.1161/ATVBAHA.110.215228 (2011).

27 Tsiantoulas, D. *et al.* Increased Plasma IgE Accelerate Atherosclerosis in Secreted IgM Deficiency. *Circ Res* **120**, 78-84, doi:10.1161/CIRCRESAHA.116.309606 (2017).

28 Wang, J. *et al.* IgE stimulates human and mouse arterial cell apoptosis and cytokine expression and promotes atherogenesis in Apoe(–/–) mice. *The Journal of Clinical Investigation* **121**, 3564-3577, doi:10.1172/JCI46028 (2011).

29 Lippi, G., Cervellin, G. & Sanchis-Gomar, F. Immunoglobulin E (IgE) and ischemic heart disease. Which came first, the chicken or the egg? *Annals of Medicine* **46**, 456-463, doi:10.3109/07853890.2014.927714 (2014).

30 Tsiantoulas, D., Diehl Cody, J., Witztum Joseph, L. & Binder Christoph, J. B Cells and Humoral Immunity in Atherosclerosis. *Circulation research* **114**, 1743-1756, doi:10.1161/CIRCRESAHA.113.301145 (2014).

31 Wilson, J. M., McNamara, C. A. & Platts-Mills, T. A. E. IgE, α-Gal and atherosclerosis. *Aging* **11**, 1900-1902, doi:10.18632/aging.101894 (2019).

32 Wilson, J. M. *et al.* IgE to the Mammalian Oligosaccharide Galactose-α-1,3-Galactose Is Associated With Increased Atheroma Volume and Plaques With Unstable Characteristics—Brief Report. *Arteriosclerosis, Thrombosis, and Vascular Biology* **38**, 1665-1669, doi:10.1161/ATVBAHA.118.311222 (2018).

33 Nus, M. *et al.* Marginal zone B cells control the response of follicular helper T cells to a high-cholesterol diet. *Nat Med* **23**, 601-610, doi:10.1038/nm.4315 (2017).

34 Strom, A. C. *et al.* B regulatory cells are increased in hypercholesterolaemic mice and protect from lesion development via IL-10. *Thromb Haemost* **114**, 835-847, doi:10.1160/TH14-12-1084 (2015).

35 Gjurich, B. N., Taghavie-Moghadam, P. L., Ley, K. & Galkina, E. V. L-selectin deficiency decreases aortic B1a and B(reg) subsets and promotes atherosclerosis. *Thrombosis and haemostasis* **112**, 803-811, doi:10.1160/TH13-10-0865 (2014).

36 Sage, A. P. *et al.* Regulatory B cell-specific interleukin-10 is dispensable for atherosclerosis development in mice. *Arterioscler Thromb Vasc Biol* **35**, 1770-1773, doi:10.1161/ATVBAHA.115.305568 (2015).

37 Kyaw, T. *et al.* B1a B Lymphocytes Are Atheroprotective by Secreting Natural IgM That Increases IgM Deposits and Reduces Necrotic Cores in Atherosclerotic Lesions. *Circulation Research* **109**, 830-840, doi:10.1161/CIRCRESAHA.111.248542 (2011).

38 Rosenfeld, S. M. *et al.* B-1b Cells Secrete Atheroprotective IgM and Attenuate Atherosclerosis. *Circ Res*, doi:10.1161/CIRCRESAHA.117.306044 (2015).

39 Hilgendorf, I. *et al.* Innate response activator B cells aggravate atherosclerosis by stimulating T helper-1 adaptive immunity. *Circulation* **129**, 1677-1687, doi:10.1161/CIRCULATIONAHA.113.006381 (2014).

40 Baumgarth, N. *et al.* Innate and acquired humoral immunities to influenza virus are mediated by distinct arms of the immune system. *Proceedings of the National Academy of Sciences of the United States of America* **96**, 2250-2255 (1999).

41 Baumgarth, N. B-1 Cell Heterogeneity and the Regulation of Natural and Antigen-Induced IgM Production. *Front Immunol* **7**, 324, doi:10.3389/fimmu.2016.00324 (2016).

42 Baumgarth, N., Tung, J. W. & Herzenberg, L. A. Inherent specificities in natural antibodies: a key to immune defense against pathogen invasion. *Springer seminars in immunopathology* **26**, 347-362, doi:10.1007/s00281-004-0182-2 (2005).

43 Grönwall, C., Vas, J. & Silverman, G. J. Protective roles of natural IgM antibodies. *Frontiers in Immunology* **3**, doi:10.3389/fimmu.2012.00066 (2012).

44 Holodick, N. E., Rodriguez-Zhurbenko, N. & Hernandez, A. M. Defining Natural Antibodies. *Front Immunol* **8**, 872, doi:10.3389/fimmu.2017.00872 (2017).

45 Panda, S. & Ding, J. L. Natural antibodies bridge innate and adaptive immunity. *Journal of immunology* **194**, 13-20, doi:10.4049/jimmunol.1400844 (2015).

46 Hooijkaas, H., Benner, R., Pleasants, J. R. & Wostmann, B. S. Isotypes and specificities of immunoglobulins produced by germ-free mice fed chemically defined ultrafiltered "antigen-free" diet. *Eur J Immunol* **14**, 1127-1130, doi:10.1002/eji.1830141212 (1984).

47 Baumgarth, N. The double life of a B-1 cell: self-reactivity selects for protective effector functions. *Nat Rev Immunol* **11**, 34-46 (2011).

48 Prohaska, T. A. *et al.* Massively Parallel Sequencing of Peritoneal and Splenic B Cell Repertoires Highlights Unique Properties of B-1 Cell Antibodies. *Journal of immunology* **200**, 1702-1717, doi:10.4049/jimmunol.1700568 (2018).

49 Yang, Y. *et al.* Distinct mechanisms define murine B cell lineage immunoglobulin heavy chain (IgH) repertoires. *Elife* **4**, e09083, doi:10.7554/eLife.09083 (2015).

50 Alugupalli, K. R. & Gerstein, R. M. Divide and conquer: division of labor by B-1 B cells. *Immunity* **23**, 1-2, doi:10.1016/j.immuni.2005.07.001 (2005).

51 Haas, K. M., Poe, J. C., Steeber, D. A. & Tedder, T. F. B-1a and B-1b cells exhibit distinct developmental requirements and have unique functional roles in innate and adaptive immunity to S. pneumoniae. *Immunity* **23**, 7-18, doi:10.1016/j.immuni.2005.04.011 (2005).

52 Cole, L. E. *et al.* Antigen-specific B-1a antibodies induced by Francisella tularensis LPS provide long-term protection against F. tularensis LVS challenge. *Proceedings of the National Academy of Sciences of the United States of America* **106**, 4343-4348, doi:10.1073/pnas.0813411106 (2009).

53 Yang, Y. *et al.* Antigen-specific antibody responses in B-1a and their relationship to natural immunity. *Proceedings of the National Academy of Sciences of the United States of America* **109**, 5382-5387, doi:10.1073/pnas.1121631109 (2012).

54 Chou, M. Y. *et al.* Oxidation-specific epitopes are dominant targets of innate natural antibodies in mice and humans. *The Journal of clinical investigation* **119**, 1335-1349, doi:10.1172/JCI36800 (2009).

55 Tsiantoulas, D., Gruber, S. & Binder, C. J. B-1 cell immunoglobulin directed against oxidation-specific epitopes. *Front Immunol* **3**, 415, doi:10.3389/fimmu.2012.00415 (2012).

56 Palinski, W. *et al.* Cloning of monoclonal autoantibodies to epitopes of oxidized lipoproteins from apolipoprotein E-deficient mice. Demonstration of epitopes of oxidized low density lipoprotein in human plasma. *Journal of Clinical Investigation* **98**, 800-814 (1996).

57 Shaw, P. X. *et al.* Human-derived anti-oxidized LDL autoantibody blocks uptake of oxidized LDL by macrophages and localizes to atherosclerotic lesions in vivo. *Arterioscler Thromb Vasc Biol* **21**, 1333-1339, doi:10.1161/hq0801.093587 (2001).

58 Shaw, P. X. *et al.* Natural antibodies with the T15 idiotype may act in atherosclerosis, apoptotic clearance, and protective immunity. *The Journal of clinical investigation* **105**, 1731-1740, doi:10.1172/JCI8472 (2000).

59 Hayakawa, K. *et al.* Positive selection of natural autoreactive B cells. *Science* **285**, 113-116 (1999).

60 Kreslavsky, T., Wong, J. B., Fischer, M., Skok, J. A. & Busslinger, M. Control of B-1a cell development by instructive BCR signaling. *Current opinion in immunology* **51**, 24-31, doi:https://doi.org/10.1016/j.coi.2018.01.001 (2018).

61 Alugupalli, K. R. *et al.* The resolution of relapsing fever borreliosis requires IgM and is concurrent with expansion of B1b lymphocytes. *Journal of immunology* **170**, 3819-3827 (2003).

62 Baumgarth, N. *et al.* B-1 and B-2 cell-derived immunoglobulin M antibodies are nonredundant components of the protective response to influenza virus infection. *J Exp Med* **192**, 271-280 (2000).

63 Boes, M., Prodeus, A. P., Schmidt, T., Carroll, M. C. & Chen, J. A critical role of natural immunoglobulin M in immediate defense against systemic bacterial infection. *J Exp Med* **188**, 2381-2386 (1998).

64 Chen, Y. *et al.* Regulation of dendritic cells and macrophages by an anti-apoptotic cell natural antibody that suppresses TLR responses and inhibits inflammatory arthritis. *Journal of immunology* **183**, 1346-1359, doi:10.4049/jimmunol.0900948 (2009).

65 Chen, Y., Park, Y.-B., Patel, E. & Silverman, G. J. IgM Antibodies to Apoptosis-Associated Determinants Recruit C1q and Enhance Dendritic Cell Phagocytosis of Apoptotic Cells(). *Journal of immunology (Baltimore, Md. : 1950)* **182**, 6031-6043, doi:10.4049/jimmunol.0804191 (2009).

66 Ogden, C. A., Kowalewski, R., Peng, Y., Montenegro, V. & Elkon, K. B. IGM is required for efficient complement mediated phagocytosis of apoptotic cells in vivo. *Autoimmunity* **38**, 259-264 (2005).

67 Harmon, D. B. *et al.* Protective Role for B-1b B Cells and IgM in Obesity-Associated Inflammation, Glucose Intolerance, and Insulin Resistance. *Arteriosclerosis, Thrombosis, and Vascular Biology*, doi:10.1161/atvbaha.116.307166 (2016).

68 Hörkkö, S. *et al.* Monoclonal autoantibodies specific for oxidized phospholipids or oxidized phospholipid–protein adducts inhibit macrophage uptake of oxidized low-density lipoproteins. *Journal of Clinical Investigation* **103**, 117-128 (1999).

69 Lewis, M. J. *et al.* Immunoglobulin M Is Required for Protection Against Atherosclerosis in Low-Density Lipoprotein Receptor–Deficient Mice. *Circulation* **120**, 417-426, doi:10.1161/circulationaha.109.868158 (2009).

70 Cesena, F. H. Y. *et al.* Immune-modulation by polyclonal IgM treatment reduces atherosclerosis in hypercholesterolemic apoE−/− mice. *Atherosclerosis* **220**, 59-65, doi:http://dx.doi.org/10.1016/j.atherosclerosis.2011.10.002 (2012).

71 Binder, C. J. *et al.* Pneumococcal vaccination decreases atherosclerotic lesion formation: molecular mimicry between Streptococcus pneumoniae and oxidized LDL. *Nat Med* **9**, 736-743, doi:10.1038/nm876 (2003).

72 Grasset, E. K. *et al.* Sterile inflammation in the spleen during atherosclerosis provides oxidation-specific epitopes that induce a protective B-cell response. *Proceedings of the National Academy of Sciences of the United States of America* **112**, E2030-2038, doi:10.1073/pnas.1421227112 (2015).

73 Hosseini, H. *et al.* Phosphatidylserine liposomes mimic apoptotic cells to attenuate atherosclerosis by expanding polyreactive IgM producing B1a lymphocytes. *Cardiovasc Res* **106**, 443-452, doi:10.1093/cvr/cvv037 (2015).

74 Que, X. *et al.* Oxidized phospholipids are proinflammatory and proatherogenic in hypercholesterolaemic mice. *Nature* **558**, 301-306, doi:10.1038/s41586-018-0198-8 (2018).

75 Tsimikas, S. *et al.* Human oxidation-specific antibodies reduce foam cell formation and atherosclerosis progression. *Journal of the American College of Cardiology* **58**, 1715-1727, doi:10.1016/j.jacc.2011.07.017 (2011).

76 Jones, D. D. *et al.* The omentum is a site of protective IgM production during intracellular bacterial infection. *Infect Immun* **83**, 2139-2147, doi:10.1128/IAI.00295-15 (2015).

77 Srikakulapu, P. *et al.* Perivascular Adipose Tissue Harbors Atheroprotective IgM-Producing B Cells. *Frontiers in physiology* **8**, 719, doi:10.3389/fphys.2017.00719 (2017).

78 Holodick, N. E., Tumang, J. R. & Rothstein, T. L. Immunoglobulin secretion by B1 cells: Differential intensity and IRF4-dependence of spontaneous IgM secretion by peritoneal and splenic B1 cells. *European Journal of Immunology* **40**, 3007-3016, doi:10.1002/eji.201040545 (2010).

79 Ansel, K. M., Harris, R. B. & Cyster, J. G. CXCL13 is required for B1 cell homing, natural antibody production, and body cavity immunity. *Immunity* **16**, 67-76 (2002).

80 Ha, S. A. *et al.* Regulation of B1 cell migration by signals through Toll-like receptors. *J Exp Med* **203**, 2541-2550, doi:10.1084/jem.20061041 (2006).

81 Yang, Y., Tung, J. W., Ghosn, E. E., Herzenberg, L. A. & Herzenberg, L. A. Division and differentiation of natural antibody-producing cells in mouse spleen. *Proceedings of the National Academy of Sciences of the United States of America* **104**, 4542-4546, doi:10.1073/pnas.0700001104 (2007).

82 Choi, Y. S., Dieter, J. A., Rothaeusler, K., Luo, Z. & Baumgarth, N. B-1 cells in the bone marrow are a significant source of natural IgM. *European journal of immunology* **42**, 120-129, doi:10.1002/eji.201141890 (2012).

83 Holodick, N. E., Vizconde, T. & Rothstein, T. L. Splenic B-1a Cells Expressing CD138 Spontaneously Secrete Large Amounts of Immunoglobulin in Naive Mice. *Front Immunol* **5**, 129, doi:10.3389/fimmu.2014.00129 (2014).

84 Savage, H. P. *et al.* Blimp-1-dependent and -independent natural antibody production by B-1 and B-1-derived plasma cells. *J Exp Med* **214**, 2777-2794, doi:10.1084/jem.20161122 (2017).

85 Srikakulapu, P. *et al.* Artery Tertiary Lymphoid Organs Control Multilayered Territorialized Atherosclerosis B-Cell Responses in Aged ApoE-/- Mice. *Arterioscler Thromb Vasc Biol* **36**, 1174-1185, doi:10.1161/ATVBAHA.115.306983 (2016).

86 Yin, C., Mohanta, S. K., Srikakulapu, P., Weber, C. & Habenicht, A. J. Artery Tertiary Lymphoid Organs: Powerhouses of Atherosclerosis Immunity. *Front Immunol* **7**, 387, doi:10.3389/fimmu.2016.00387 (2016).

87 Grabner, R. *et al.* Lymphotoxin beta receptor signaling promotes tertiary lymphoid organogenesis in the aorta adventitia of aged ApoE-/- mice. *J Exp Med* **206**, 233-248, doi:10.1084/jem.20080752 (2009).

88 Chace, J. H., Fleming, A. L., Gordon, J. A., Perandones, C. E. & Cowdery, J. S. Regulation of differentiation of peritoneal B-1a (CD5+) B cells. Activated peritoneal macrophages release prostaglandin E2, which inhibits IgM secretion by peritoneal B-1a cells. *Journal of immunology* **154**, 5630-5636 (1995).

89 Moon, B. G., Takaki, S., Miyake, K. & Takatsu, K. The role of IL-5 for mature B-1 cells in homeostatic proliferation, cell survival, and Ig production. *Journal of immunology* **172**, 6020-6029 (2004).

90 Takatsu, K., Kouro, T. & Nagai, Y. Interleukin 5 in the link between the innate and acquired immune response. *Adv Immunol* **101**, 191-236, doi:10.1016/S0065-2776(08)01006-7 (2009).

91 Reynolds, A. E., Kuraoka, M. & Kelsoe, G. Natural IgM is produced by CD5- plasma cells that occupy a distinct survival niche in bone marrow. *Journal of immunology* **194**, 231-242, doi:10.4049/jimmunol.1401203 (2015).

92 Binder, C. J. *et al.* IL-5 links adaptive and natural immunity specific for epitopes of oxidized LDL and protects from atherosclerosis. *Journal of Clinical Investigation* **114**, 427-437, doi:10.1172/JCI200420479 (2004).

93 Balabanian, K. *et al.* Interleukin-10 modulates the sensitivity of peritoneal B lymphocytes to chemokines with opposite effects on stromal cell-derived factor-1 and B-lymphocyte chemoattractant. *Blood* **99**, 427-436 (2002).

94 Balabanian, K. *et al.* Role of the chemokine stromal cell-derived factor 1 in autoantibody production and nephritis in murine lupus. *Journal of immunology* **170**, 3392-3400 (2003).

95 Weber, G. F. *et al.* Pleural innate response activator B cells protect against pneumonia via a GM-CSF-IgM axis. *J Exp Med* **211**, 1243-1256, doi:10.1084/jem.20131471 (2014).

96 Jackson-Jones, L. H. & Benezech, C. Control of innate-like B cell location for compartmentalised IgM production. *Current opinion in immunology* **50**, 9-13, doi:10.1016/j.coi.2017.10.006 (2018).

97 Benezech, C. *et al.* Inflammation-induced formation of fat-associated lymphoid clusters. *Nature immunology* **16**, 819-828, doi:10.1038/ni.3215 http://www.nature.com/ni/journal/v16/n8/abs/ni.3215.html - supplementary-information (2015).

98 Moro, K. *et al.* Innate production of T(H)2 cytokines by adipose tissue-associated c-Kit(+)Sca-1(+) lymphoid cells. *Nature* **463**, 540-544, doi:10.1038/nature08636 (2010).

99 Jackson-Jones, L. H. *et al.* Fat-associated lymphoid clusters control local IgM secretion during pleural infection and lung inflammation. *Nat Commun* **7**, 12651, doi:10.1038/ncomms12651 (2016).

100 Perry, H. M. *et al.* Helix-loop-helix factor inhibitor of differentiation 3 regulates interleukin-5 expression and B-1a B cell proliferation. *Arterioscler Thromb Vasc Biol* **33**, 2771-2779, doi:10.1161/ATVBAHA.113.302571 (2013).

101 Duber, S. *et al.* Induction of B-cell development in adult mice reveals the ability of bone marrow to produce B-1a cells. *Blood* **114**, 4960-4967, doi:10.1182/blood-2009-04-218156 (2009).

102 Holodick, N. E., Repetny, K., Zhong, X. & Rothstein, T. L. Adult BM generates CD5+ B1 cells containing abundant N-region additions. *Eur J Immunol* **39**, 2383-2394, doi:10.1002/eji.200838920 (2009).

103 Holodick, N. E., Vizconde, T. & Rothstein, T. L. B-1a cell diversity: nontemplated addition in B-1a cell Ig is determined by progenitor population and developmental location. *Journal of immunology* **192**, 2432-2441, doi:10.4049/jimmunol.1300247 (2014).

104 Montecino-Rodriguez, E., Leathers, H. & Dorshkind, K. Identification of a B-1 B cell-specified progenitor. *Nature immunology* **7**, 293-301, doi:10.1038/ni1301 (2006).

105 Ghosn, E. E., Sadate-Ngatchou, P., Yang, Y., Herzenberg, L. A. & Herzenberg, L. A. Distinct progenitors for B-1 and B-2 cells are present in adult mouse spleen. *Proceedings of the National Academy of Sciences of the United States of America* **108**, 2879-2884, doi:10.1073/pnas.1019764108 (2011).

106 Kretschmer, K., Stopkowicz, J., Scheffer, S., Greten, T. F. & Weiss, S. Maintenance of peritoneal B-1a lymphocytes in the absence of the spleen. *Journal of immunology* **173**, 197-204 (2004).

107 Wardemann, H., Boehm, T., Dear, N. & Carsetti, R. B-1a B cells that link the innate and adaptive immune responses are lacking in the absence of the spleen. *J Exp Med* **195**, 771-780, doi:10.1084/jem.20011140 (2002).

108 Forster, I. & Rajewsky, K. Expansion and functional activity of Ly-1+ B cells upon transfer of peritoneal cells into allotype-congenic, newborn mice. *Eur J Immunol* **17**, 521-528, doi:10.1002/eji.1830170414 (1987).

109 Lalor, P. A., Herzenberg, L. A., Adams, S. & Stall, A. M. Feedback regulation of murine Ly-1 B cell development. *Eur J Immunol* **19**, 507-513, doi:10.1002/eji.1830190315 (1989).

110 Holodick, N. E., Vizconde, T., Hopkins, T. J. & Rothstein, T. L. Age-Related Decline in Natural IgM Function: Diversification and Selection of the B-1a Cell Pool with Age. *The Journal of Immunology*, 1600073, doi:10.4049/jimmunol.1600073 (2016).

111 Dal Porto, J. M., Burke, K. & Cambier, J. C. Regulation of BCR signal transduction in B-1 cells requires the expression of the Src family kinase Lck. *Immunity* **21**, 443-453, doi:10.1016/j.immuni.2004.07.018 (2004).

112 Wang, H. *et al.* Expression of plasma cell alloantigen 1 defines layered development of B-1a B-cell subsets with distinct innate-like functions. *Proceedings of the National Academy of Sciences of the United States of America* **109**, 20077-20082, doi:10.1073/pnas.1212428109 (2012).

113 Yuan, J., Nguyen, C. K., Liu, X., Kanellopoulou, C. & Muljo, S. A. Lin28b reprograms adult bone marrow hematopoietic progenitors to mediate fetal-like lymphopoiesis. *Science* **335**, 1195-1200, doi:10.1126/science.1216557 (2012).

114 Wray-Dutra, M. N. *et al.* Activated PIK3CD drives innate B cell expansion yet limits B cell-intrinsic immune responses. *J Exp Med* **215**, 2485-2496, doi:10.1084/jem.20180617 (2018).

115 Choi, S. C. *et al.* Mouse IgM Fc receptor, FCMR, promotes B cell development and modulates antigen-driven immune responses. *Journal of immunology* **190**, 987-996, doi:10.4049/jimmunol.1202227 (2013).

116 Guo, B. & Rothstein, T. L. RasGRP1 Is an Essential Signaling Molecule for Development of B1a Cells with Autoantigen Receptors. *Journal of immunology* **196**, 2583-2590, doi:10.4049/jimmunol.1502132 (2016).

117 Enyindah-Asonye, G. *et al.* CD6 Receptor Regulates Intestinal Ischemia/Reperfusion-induced Injury by Modulating Natural IgM-producing B1a Cell Self-renewal. *The Journal of biological chemistry* **292**, 661-671, doi:10.1074/jbc.M116.749804 (2017).

118 Doran, A. C. *et al.* B-Cell Aortic Homing and Atheroprotection Depend on Id3. *Circulation Research* **110**, e1-e12, doi:10.1161/CIRCRESAHA.111.256438 (2012).

119 Srikakulapu, P., McSkimming, C. & McNamara, C. Abstract 464: Chemokine Receptor CCR6 Expression on B Cells Augments Local IgM Production and Atheroprotection. *Arteriosclerosis, Thrombosis, and Vascular Biology* **36**, A464-A464, doi:10.1161/atvb.36.suppl_1.464 (2016).

120 Foussat, A. *et al.* Production of stromal cell-derived factor 1 by mesothelial cells and effects of this chemokine on peritoneal B lymphocytes. *Eur J Immunol* **31**,

350-359, doi:10.1002/1521-4141(200102)31:2<350::AID-IMMU350>3.0.CO;2-0 (2001).

121 Berberich, S., Forster, R. & Pabst, O. The peritoneal micromilieu commits B cells to home to body cavities and the small intestine. *Blood* **109**, 4627-4634, doi:10.1182/blood-2006-12-064345 (2007).

122 Kunisawa, J. *et al.* Sphingosine 1-phosphate regulates peritoneal B-cell trafficking for subsequent intestinal IgA production. *Blood* **109**, 3749-3756, doi:10.1182/blood-2006-08-041582 (2007).

123 Kawahara, T., Ohdan, H., Zhao, G., Yang, Y. G. & Sykes, M. Peritoneal cavity B cells are precursors of splenic IgM natural antibody-producing cells. *Journal of immunology* **171**, 5406-5414 (2003).

124 Murakami, M. *et al.* Oral administration of lipopolysaccharides activates B-1 cells in the peritoneal cavity and lamina propria of the gut and induces autoimmune symptoms in an autoantibody transgenic mouse. *J Exp Med* **180**, 111-121 (1994).

125 Waffarn, E. E. *et al.* Infection-induced type I interferons activate CD11b on B-1 cells for subsequent lymph node accumulation. *Nat Commun* **6**, 8991, doi:10.1038/ncomms9991 (2015).

126 Moon, H., Lee, J. G., Shin, S. H. & Kim, T. J. LPS-induced migration of peritoneal B-1 cells is associated with upregulation of CXCR4 and increased migratory sensitivity to CXCL12. *Journal of Korean medical science* **27**, 27-35, doi:10.3346/jkms.2012.27.1.27 (2012).

127 Hansell, C. A. *et al.* Universal expression and dual function of the atypical chemokine receptor D6 on innate-like B cells in mice. *Blood* **117**, 5413-5424, doi:10.1182/blood-2010-11-317115 (2011).

128 Colombo, M. J., Sun, G. & Alugupalli, K. R. T-Cell-Independent Immune Responses Do Not Require Cxc Ligand 13-Mediated B1 Cell Migration. *Infection and Immunity* **78**, 3950-3956, doi:10.1128/IAI.00371-10 (2010).

129 Zou, Y. R., Kottmann, A. H., Kuroda, M., Taniuchi, I. & Littman, D. R. Function of the chemokine receptor CXCR4 in haematopoiesis and in cerebellar development. *Nature* **393**, 595-599, doi:10.1038/31269 (1998).

130 Ma, Q., Jones, D. & Springer, T. A. The chemokine receptor CXCR4 is required for the retention of B lineage and granulocytic precursors within the bone marrow microenvironment. *Immunity* **10**, 463-471 (1999).

131 Luker, K. E., Steele, J. M., Mihalko, L. A., Ray, P. & Luker, G. D. Constitutive and chemokine-dependent internalization and recycling of CXCR7 in breast cancer cells to degrade chemokine ligands. *Oncogene* **29**, 4599-4610, doi:10.1038/onc.2010.212 (2010).

132 Nie, Y. *et al.* The Role of CXCR4 in Maintaining Peripheral B Cell Compartments and Humoral Immunity. *The Journal of Experimental Medicine* **200**, 1145-1156, doi:10.1084/jem.20041185 (2004).

133 Balabanian, K. *et al.* Proper desensitization of CXCR4 is required for lymphocyte development and peripheral compartmentalization in mice. *Blood* **119**, 5722-5730, doi:10.1182/blood-2012-01-403378 (2012).

134 Guo, Y., Hangoc, G., Bian, H., Pelus, L. M. & Broxmeyer, H. E. SDF-1/CXCL12 enhances survival and chemotaxis of murine embryonic stem cells and production of primitive and definitive hematopoietic progenitor cells. *Stem Cells* **23**, 1324-1332, doi:10.1634/stemcells.2005-0085 (2005).

135 Kayali, A. G. *et al.* The stromal cell–derived factor-1α/CXCR4 ligand–receptor axis is critical for progenitor survival and migration in the pancreas. *The Journal of Cell Biology* **163**, 859-869, doi:10.1083/jcb.200304153 (2003).

136 Chatterjee, S., Behnam Azad, B. & Nimmagadda, S. The intricate role of CXCR4 in cancer. *Adv Cancer Res* **124**, 31-82, doi:10.1016/B978-0-12-411638-2.00002-1 (2014).

137 Mo, W. *et al.* CXCR4/CXCL12 Mediate Autocrine Cell- Cycle Progression in NF1-Associated Malignant Peripheral Nerve Sheath Tumors. *Cell* **152**, 1077-1090, doi:10.1016/j.cell.2013.01.053.

138 Liao, A. *et al.* SDF-1/CXCR4 Axis Regulates Cell Cycle Progression and Epithelial-Mesenchymal Transition via Up-regulation of Survivin in Glioblastoma. *Molecular Neurobiology* **53**, 210-215, doi:10.1007/s12035-014-9006-0 (2016).

139 Doring, Y., Pawig, L., Weber, C. & Noels, H. The CXCL12/CXCR4 chemokine ligand/receptor axis in cardiovascular disease. *Frontiers in physiology* **5**, 212, doi:10.3389/fphys.2014.00212 (2014).

140 de Gaetano, M., Dempsey, E., Marcone, S., James, W. G. & Belton, O. Conjugated linoleic acid targets beta2 integrin expression to suppress monocyte adhesion. *Journal of immunology* **191**, 4326-4336, doi:10.4049/jimmunol.1300990 (2013).

141 Liu, Z. *et al.* The hydrogen sulfide donor, GYY4137, exhibits anti-atherosclerotic activity in high fat fed apolipoprotein E(-/-) mice. *Br J Pharmacol* **169**, 1795-1809, doi:10.1111/bph.12246 (2013).

142 Doring, Y. *et al.* Vascular CXCR4 Limits Atherosclerosis by Maintaining Arterial Integrity: Evidence From Mouse and Human Studies. *Circulation* **136**, 388-403, doi:10.1161/CIRCULATIONAHA.117.027646 (2017).

143 Zernecke, A. *et al.* Protective Role of CXC Receptor 4/CXC Ligand 12 Unveils the Importance of Neutrophils in Atherosclerosis. *Circulation Research* **102**, 209-217, doi:10.1161/CIRCRESAHA.107.160697 (2008).

144 Kiechl, S. *et al.* Coronary artery disease-related genetic variant on chromosome 10q11 is associated with carotid intima-media thickness and atherosclerosis. *Arterioscler Thromb Vasc Biol* **30**, 2678-2683, doi:10.1161/ATVBAHA.110.213785 (2010).

145 LeBlanc, M. *et al.* Identifying Novel Gene Variants in Coronary Artery Disease and Shared Genes With Several Cardiovascular Risk Factors. *Circ Res* **118**, 83-94, doi:10.1161/CIRCRESAHA.115.306629 (2016).

146 Mehta, N. N. *et al.* The novel atherosclerosis locus at 10q11 regulates plasma CXCL12 levels. *Eur Heart J* **32**, 963-971, doi:10.1093/eurheartj/ehr091 (2011).

147 Runmin, G. *et al.* Genetic variation of CXCR4 and risk of coronary artery disease: epidemiological study and functional validation of CRISPR/Cas9 system. *Oncotarget* **9**, 14077-14083, doi:10.18632/oncotarget.23491 (2018).

148 Schunkert, H. *et al.* Large-scale association analysis identifies 13 new susceptibility loci for coronary artery disease. *Nat Genet* **43**, 333-338, doi:10.1038/ng.784 (2011).

149 Shendre, A. *et al.* Local Ancestry and Clinical Cardiovascular Events Among African Americans From the Atherosclerosis Risk in Communities Study. *J Am Heart Assoc* **6**, doi:10.1161/JAHA.116.004739 (2017).

150 Jackson, S. M., Wilson, P. C., James, J. A. & Capra, J. D. in *Advances in Immunology* Vol. 98 151-224 (Academic Press, 2008).

151 Liu, Y. J. *et al.* Sequential triggering of apoptosis, somatic mutation and isotype switch during germinal center development. *Seminars in immunology* **8**, 169-177, doi:10.1006/smim.1996.0021 (1996).

152 Liu, Y. J. & Arpin, C. Germinal center development. *Immunol Rev* **156**, 111-126, doi:10.1111/j.1600-065x.1997.tb00963.x (1997).

153 Klein, U., Rajewsky, K. & Kuppers, R. Human immunoglobulin (Ig)M+IgD+ peripheral blood B cells expressing the CD27 cell surface antigen carry somatically mutated variable region genes: CD27 as a general marker for somatically mutated (memory) B cells. *J Exp Med* **188**, 1679-1689, doi:10.1084/jem.188.9.1679 (1998).

154 Tangye, S. G., Liu, Y. J., Aversa, G., Phillips, J. H. & de Vries, J. E. Identification of functional human splenic memory B cells by expression of CD148 and CD27. *J Exp Med* **188**, 1691-1703, doi:10.1084/jem.188.9.1691 (1998).

155 Macallan, D. C. *et al.* B-cell kinetics in humans: rapid turnover of peripheral blood memory cells. *Blood* **105**, 3633-3640, doi:10.1182/blood-2004-09-3740 (2005).

156 Fecteau, J. F. & Neron, S. CD40 stimulation of human peripheral B lymphocytes: distinct response from naive and memory cells. *Journal of immunology* **171**, 4621-4629, doi:10.4049/jimmunol.171.9.4621 (2003).

157 Fecteau, J. F., Cote, G. & Neron, S. A new memory CD27-IgG+ B cell population in peripheral blood expressing VH genes with low frequency of somatic mutation. *Journal of immunology* **177**, 3728-3736, doi:10.4049/jimmunol.177.6.3728 (2006).

158 Griffin, D. O., Holodick, N. E. & Rothstein, T. L. Human B1 cells in umbilical cord and adult peripheral blood express the novel phenotype CD20(+)CD27(+)CD43(+)CD70(−). *The Journal of Experimental Medicine* **208**, 67-80, doi:10.1084/jem.20101499 (2011).

159 Rothstein, T. L., Griffin, D. O., Holodick, N. E., Quach, T. D. & Kaku, H. Human B-1 cells take the stage. *Annals of the New York Academy of Sciences* **1285**, 97-114, doi:10.1111/nyas.12137 (2013).

160 Rothstein, T. L. & Quach, T. D. The human counterpart of mouse B-1 cells. *Annals of the New York Academy of Sciences* **1362**, 143-152, doi:10.1111/nyas.12790 (2015).

161 Covens, K. *et al.* Characterization of proposed human B-1 cells reveals pre-plasmablast phenotype. *Blood* **121**, 5176-5183, doi:10.1182/blood-2012-12-471953 (2013).

162 Descatoire, M., Weill, J. C., Reynaud, C. A. & Weller, S. A human equivalent of mouse B-1 cells? *J Exp Med* **208**, 2563-2564, doi:10.1084/jem.20112232 (2011).

163 Perez-Andres, M. *et al.* The nature of circulating CD27+CD43+ B cells. *J Exp Med* **208**, 2565-2566, doi:10.1084/jem.20112203 (2011).

164 Griffin, D. O. & Rothstein, T. L. Human b1 cell frequency: isolation and analysis of human b1 cells. *Front Immunol* **3**, 122, doi:10.3389/fimmu.2012.00122 (2012).

165 Quach, T. D. *et al.* Distinctions among Circulating Antibody-Secreting Cell Populations, Including B-1 Cells, in Human Adult Peripheral Blood. *Journal of immunology* **196**, 1060-1069, doi:10.4049/jimmunol.1501843 (2016).

166 Griffin, D. O. & Rothstein, T. L. A small CD11b(+) human B1 cell subpopulation stimulates T cells and is expanded in lupus. *J Exp Med* **208**, 2591-2598, doi:10.1084/jem.20110978 (2011).

167 Griffin, D. O. & Rothstein, T. L. Human "orchestrator" CD11b(+) B1 cells spontaneously secrete interleukin-10 and regulate T-cell activity. *Mol Med* **18**, 1003-1008, doi:10.2119/molmed.2012.00203 (2012).

168 Huan, T. *et al.* A Systems Biology Framework Identifies Molecular Underpinnings of Coronary Heart Disease. *Arteriosclerosis, Thrombosis, and Vascular Biology* **33**, 1427-1434, doi:10.1161/ATVBAHA.112.300112 (2013).

169 Rodriguez-Zhurbenko, N., Quach, T. D., Hopkins, T. J., Rothstein, T. L. & Hernandez, A. M. Human B-1 Cells and B-1 Cell Antibodies Change With Advancing Age. *Front Immunol* **10**, 483, doi:10.3389/fimmu.2019.00483 (2019).

170 Rothstein, T. L. Natural Antibodies as Rheostats for Susceptibility to Chronic Diseases in the Aged. *Front Immunol* **7**, 127, doi:10.3389/fimmu.2016.00127 (2016).

171 Ravandi, A. *et al.* Relationship of IgG and IgM autoantibodies and immune complexes to oxidized LDL with markers of oxidation and inflammation and cardiovascular events: results from the EPIC-Norfolk Study. *Journal of Lipid Research* **52**, 1829-1836, doi:10.1194/jlr.M015776 (2011).

172 Iseme, R. A. *et al.* A role for autoantibodies in atherogenesis. *Cardiovasc Res* **113**, 1102-1112, doi:10.1093/cvr/cvx112 (2017).

173 Porsch, F. & Binder, C. J. Impact of B-Cell-Targeted Therapies on Cardiovascular Disease. *Arterioscler Thromb Vasc Biol* **39**, 1705-1714, doi:10.1161/ATVBAHA.119.311996 (2019).

174 Skaggs, B. J., Hahn, B. H. & McMahon, M. Accelerated atherosclerosis in patients with SLE--mechanisms and management. *Nat Rev Rheumatol* **8**, 214-223, doi:10.1038/nrrheum.2012.14 (2012).

175 Novikova, D. S. *et al.* The Effects of Rituximab on Lipids, Arterial Stiffness and Carotid Intima-Media Thickness in Rheumatoid Arthritis. *Journal of Korean medical science* **31**, 202-207, doi:10.3346/jkms.2016.31.2.202 (2016).

176 Sage, A. P., Tsiantoulas, D., Binder, C. J. & Mallat, Z. The role of B cells in atherosclerosis. *Nature Reviews Cardiology* **16**, 180-196, doi:10.1038/s41569-018-0106-9 (2019).

177 Hegab, Z., Gibbons, S., Neyses, L. & Mamas, M. A. Role of advanced glycation end products in cardiovascular disease. *World J Cardiol* **4**, 90-102, doi:10.4330/wjc.v4.i4.90 (2012).

178 Engelbertsen, D. *et al.* Low Levels of IgM Antibodies against an Advanced Glycation Endproduct-Modified Apolipoprotein B100 Peptide Predict Cardiovascular Events in Nondiabetic Subjects. *Journal of immunology* **195**, 3020-3025, doi:10.4049/jimmunol.1402869 (2015).

179 Kothari, H. *et al.* Association of D-dimer with Plaque Characteristics and Plasma Biomarkers of Oxidation-Specific Epitopes in Stable Subjects with Coronary Artery Disease. *J Cardiovasc Transl Res*, doi:10.1007/s12265-018-9790-4 (2018).

180 Kantor, A. B., Merrill, C. E., Herzenberg, L. A. & Hillson, J. L. An unbiased analysis of V(H)-D-J(H) sequences from B-1a, B-1b, and conventional B cells. *Journal of immunology* **158**, 1175-1186 (1997).

181 Lefranc, M.-P. *et al.* IMGT®, the international ImMunoGeneTics information system® 25 years on. *Nucleic Acids Res* **43**, D413-D422, doi:10.1093/nar/gku1056 (2015).

182 Gonen, A. *et al.* Atheroprotective immunization with malondialdehyde-modified LDL is hapten specific and dependent on advanced MDA adducts: implications for development of an atheroprotective vaccine. *Journal of Lipid Research* **55**, 2137-2155, doi:10.1194/jlr.M053256 (2014).

183 Vale, A. M. *et al.* The peritoneal cavity B-2 antibody repertoire appears to reflect many of the same selective pressures that shape the B-1a and B-1b repertoires. *Journal of immunology* **185**, 6085-6095, doi:10.4049/jimmunol.1001423 (2010).

184 Bleul, C. C., Fuhlbrigge, R. C., Casasnovas, J. M., Aiuti, A. & Springer, T. A. A highly efficacious lymphocyte chemoattractant, stromal cell-derived factor 1 (SDF-1). *The Journal of Experimental Medicine* **184**, 1101-1109, doi:10.1084/jem.184.3.1101 (1996).

185 Wang, J. C. & Bennett, M. Aging and atherosclerosis: mechanisms, functional consequences, and potential therapeutics for cellular senescence. *Circ Res* **111**, 245-259, doi:10.1161/CIRCRESAHA.111.261388 (2012).

186 Karshovska, E., Zagorac, D., Zernecke, A., Weber, C. & Schober, A. A small molecule CXCR4 antagonist inhibits neointima formation and smooth muscle progenitor cell mobilization after arterial injury. *J Thromb Haemost* **6**, 1812-1815, doi:10.1111/j.1538-7836.2008.03086.x (2008).

187 Zernecke, A. *et al.* SDF-1alpha/CXCR4 axis is instrumental in neointimal hyperplasia and recruitment of smooth muscle progenitor cells. *Circ Res* **96**, 784-791, doi:10.1161/01.RES.0000162100.52009.38 (2005).

188 Grasset, E. K. *et al.* Sterile inflammation in the spleen during atherosclerosis provides oxidation-specific epitopes that induce a protective B-cell response. *Proceedings of the National Academy of Sciences* **112**, E2030-E2038, doi:10.1073/pnas.1421227112 (2015).

189 Mi, Q.-S. *et al.* Highly reduced protection against Streptococcus pneumoniae after deletion of a single heavy chain gene in mouse. *Proceedings of the National Academy of Sciences of the United States of America* **97**, 6031-6036 (2000).

190 Gronwall, C., Vas, J. & Silverman, G. J. Protective Roles of Natural IgM Antibodies. *Front Immunol* **3**, 66, doi:10.3389/fimmu.2012.00066 (2012).

191 Papac-Milicevic, N., Busch, C. J. L. & Binder, C. J. Malondialdehyde Epitopes as Targets of Immunity and the Implications for Atherosclerosis. *Advances in immunology* **131**, 1-59, doi:10.1016/bs.ai.2016.02.001 (2016).

192 Alugupalli, K. R. *et al.* B1b lymphocytes confer T cell-independent long-lasting immunity. *Immunity* **21**, 379-390, doi:10.1016/j.immuni.2004.06.019 (2004).

193 Chang, L. *et al.* Loss of perivascular adipose tissue on peroxisome proliferator-activated receptor-gamma deletion in smooth muscle cells impairs intravascular thermoregulation and enhances atherosclerosis. *Circulation* **126**, 1067-1078, doi:10.1161/CIRCULATIONAHA.112.104489 (2012).

194 Baumgarth, N., Jager, G. C., Herman, O. C. & Herzenberg, L. A. CD4+ T cells derived from B cell-deficient mice inhibit the establishment of peripheral B cell pools. *Proceedings of the National Academy of Sciences of the United States of America* **97**, 4766-4771, doi:10.1073/pnas.97.9.4766 (2000).

195 O'Garra, A. *et al.* Ly-1 B (B-1) cells are the main source of B cell-derived interleukin 10. *Eur J Immunol* **22**, 711-717, doi:10.1002/eji.1830220314 (1992).

196 Caligiuri, G. *et al.* Interleukin-10 Deficiency Increases Atherosclerosis, Thrombosis, and Low-density Lipoproteins in Apolipoprotein E Knockout Mice. *Molecular Medicine* **9**, 10-17 (2003).

197 Han, X., Kitamoto, S., Wang, H. & Boisvert, W. A. Interleukin-10 overexpression in macrophages suppresses atherosclerosis in hyperlipidemic mice. *The FASEB Journal* **24**, 2869-2880, doi:10.1096/fj.09-148155 (2010).

198 van Dam, A. D., Boon, M. R., Berbee, J. F. P., Rensen, P. C. N. & van Harmelen, V. Targeting white, brown and perivascular adipose tissue in atherosclerosis development. *Eur J Pharmacol* **816**, 82-92, doi:10.1016/j.ejphar.2017.03.051 (2017).

199 Majesky, M. W. Developmental basis of vascular smooth muscle diversity. *Arterioscler Thromb Vasc Biol* **27**, 1248-1258, doi:10.1161/ATVBAHA.107.141069 (2007).

200 Hu, D. *et al.* Artery Tertiary Lymphoid Organs Control Aorta Immunity and Protect against Atherosclerosis via Vascular Smooth Muscle Cell Lymphotoxin beta Receptors. *Immunity* **42**, 1100-1115, doi:10.1016/j.immuni.2015.05.015 (2015).

201 Cheng, Q. *et al.* CXCR4-CXCL12 interaction is important for plasma cell homing and survival in NZB/W mice. *Eur J Immunol* **48**, 1020-1029, doi:10.1002/eji.201747023 (2018).

202 Herrup, K., Neve, R., Ackerman, S. L. & Copani, A. Divide and die: cell cycle events as triggers of nerve cell death. *The Journal of neuroscience : the official journal of the Society for Neuroscience* **24**, 9232-9239, doi:10.1523/JNEUROSCI.3347-04.2004 (2004).

203 Cooper-Kuhn, C. M. & Kuhn, H. G. Is it all DNA repair? Methodological considerations for detecting neurogenesis in the adult brain. *Brain Res Dev Brain Res* **134**, 13-21, doi:10.1016/s0165-3806(01)00243-7 (2002).

204 Kwong, J., Kulbe, H., Wong, D., Chakravarty, P. & Balkwill, F. An antagonist of the chemokine receptor CXCR4 induces mitotic catastrophe in ovarian cancer cells. *Mol Cancer Ther* **8**, 1893-1905, doi:10.1158/1535-7163.MCT-08-0966 (2009).

205 Khan, M. Z. *et al.* The chemokine receptor CXCR4 regulates cell-cycle proteins in neurons. *J Neurovirol* **9**, 300-314, doi:10.1080/13550280390201010 (2003).

206 Weber, T. S. Cell Cycle-Associated CXCR4 Expression in Germinal Center B Cells and Its Implications on Affinity Maturation. *Front Immunol* **9**, 1313, doi:10.3389/fimmu.2018.01313 (2018).

207 Becker, M., Hobeika, E., Jumaa, H., Reth, M. & Maity, P. C. CXCR4 signaling and function require the expression of the IgD-class B-cell antigen receptor. *Proceedings of the National Academy of Sciences of the United States of America* **114**, 5231-5236, doi:10.1073/pnas.1621512114 (2017).

208 Sacco, R. L. The new American Heart Association 2020 goal: achieving ideal cardiovascular health. *J Cardiovasc Med (Hagerstown)* **12**, 255-257, doi:10.2459/JCM.0b013e328343e986 (2011).

209 Davison, G., Kehaya, C. & Wyn Jones, A. Nutritional and Physical Activity Interventions to Improve Immunity. *Am J Lifestyle Med* **10**, 152-169, doi:10.1177/1559827614557773 (2016).

210 Qiu, F. *et al.* Impacts of cigarette smoking on immune responsiveness: Up and down or upside down? *Oncotarget* **8**, 268-284, doi:10.18632/oncotarget.13613 (2017).

211 Francisco, V. *et al.* Obesity, Fat Mass and Immune System: Role for Leptin. *Frontiers in physiology* **9**, 640, doi:10.3389/fphys.2018.00640 (2018).

212 Norlander, A. E., Madhur, M. S. & Harrison, D. G. The immunology of hypertension. *J Exp Med* **215**, 21-33, doi:10.1084/jem.20171773 (2018).

213 Getz, G. S. & Reardon, C. A. The mutual interplay of lipid metabolism and the cells of the immune system in relation to atherosclerosis. *Clin Lipidol* **9**, 657-671, doi:10.2217/clp.14.50 (2014).

214 Zhou, T. *et al.* Role of Adaptive and Innate Immunity in Type 2 Diabetes Mellitus. *J Diabetes Res* **2018**, 7457269, doi:10.1155/2018/7457269 (2018).

215 Gistera, A. & Hansson, G. K. The immunology of atherosclerosis. *Nat Rev Nephrol* **13**, 368-380, doi:10.1038/nrneph.2017.51 (2017).

216 Lee, S. H. *et al.* Real-Time Monitoring of Cancer Cells in Live Mouse Bone Marrow. *Front Immunol* **9**, 1681, doi:10.3389/fimmu.2018.01681 (2018).

217 Osmond, D. G. & Batten, S. J. Genesis of B lymphocytes in the bone marrow: extravascular and intravascular localization of surface IgM-bearing cells in mouse bone marrow detected by electron-microscope radioautography after in vivo perfusion of 125I anti-IgM antibody. *Am J Anat* **170**, 349-365, doi:10.1002/aja.1001700310 (1984).

218 Cariappa, A. *et al.* Perisinusoidal B cells in the bone marrow participate in T-independent responses to blood-borne microbes. *Immunity* **23**, 397-407, doi:10.1016/j.immuni.2005.09.004 (2005).

219 Omata, Y. *et al.* Group 2 Innate Lymphoid Cells Attenuate Inflammatory Arthritis and Protect from Bone Destruction in Mice. *Cell Rep* **24**, 169-180, doi:10.1016/j.celrep.2018.06.005 (2018).

220 Wen, L., Shinton, S. A., Hardy, R. R. & Hayakawa, K. Association of B-1 B cells with follicular dendritic cells in spleen. *Journal of immunology* **174**, 6918-6926, doi:10.4049/jimmunol.174.11.6918 (2005).

221 Fu, Y. X., Huang, G., Wang, Y. & Chaplin, D. D. B lymphocytes induce the formation of follicular dendritic cell clusters in a lymphotoxin alpha-dependent fashion. *J Exp Med* **187**, 1009-1018, doi:10.1084/jem.187.7.1009 (1998).

222 Rezk, S. A., Nathwani, B. N., Zhao, X. & Weiss, L. M. Follicular dendritic cells: origin, function, and different disease-associated patterns. *Hum Pathol* **44**, 937-950, doi:10.1016/j.humpath.2012.10.005 (2013).

223 Wang, X. *et al.* Follicular dendritic cells help establish follicle identity and promote B cell retention in germinal centers. *J Exp Med* **208**, 2497-2510, doi:10.1084/jem.20111449 (2011).

224 Hippen, K. L., Tze, L. E. & Behrens, T. W. CD5 maintains tolerance in anergic B cells. *J Exp Med* **191**, 883-890, doi:10.1084/jem.191.5.883 (2000).

225 Savage, H. P. *et al.* TLR induces reorganization of the IgM-BCR complex regulating murine B-1 cell responses to infections. *Elife* **8**, doi:10.7554/eLife.46997 (2019).

226 Keating, G. M. Plerixafor: a review of its use in stem-cell mobilization in patients with lymphoma or multiple myeloma. *Drugs* **71**, 1623-1647, doi:10.2165/11206040-000000000-00000 (2011).

227 Reinholdt, L. *et al.* The CXCR4 antagonist plerixafor enhances the effect of rituximab in diffuse large B-cell lymphoma cell lines. *Biomark Res* **4**, 12, doi:10.1186/s40364-016-0067-2 (2016).

228 Schabath, H., Runz, S., Joumaa, S. & Altevogt, P. CD24 affects CXCR4 function in pre-B lymphocytes and breast carcinoma cells. *J Cell Sci* **119**, 314-325, doi:10.1242/jcs.02741 (2006).